Simulation-Based Virtual Driver Fatigue Prediction and Determination of Optimal Vehicle Seat Dynamic Parameters

By

Prasad Bhagwan Kumbhar, B.E., M.E.

A Thesis

In

MECHANICAL ENGINEERING

Submitted to the Graduate Faculty
of Texas Tech University in
Partial Fulfillment of
the Requirements for
the Degree of

MASTER OF SCIENCE

IN

MECHANICAL ENGINEERING

Approved

James Yang, Ph.D.
Chair of Committee

Peijun Xu, Ph.D.

Stephen Ekwaro-Osire, Ph.D.

Dominick Casadonte
Interim Dean of the Graduate School

August, 2013

ACKNOWLEDGEMENTS

Along with my efforts, this thesis work is the result of help and support from many people. At this stage of my academic life, I want to take this opportunity to express my deepest gratitude to those people.

First and foremost, I express my deepest gratitude to my advisor Dr. James Yang for his support, encouragement and timely guidance. His guidance helped me in all the stages of research counting from literature review to writing my thesis. I also want to thank my co-advisor Dr. Peijun Xu (Ebco Inc., Elgin, Illinois), for helping me at each level of our research. I really appreciate his continuous help, patience and immense knowledge in this field. This research work would not have been possible without his help and knowledge. Besides my advisor Dr. Yang, co-advisor Dr. Xu, I am thankful to the rest of my thesis committee, Dr. Stephen Ekwaro for his valuable time in evaluating my research work and giving me valuable suggestions. I greatly appreciate the assistance provided by all the students in Human Centric Design Research Lab.

The unconditional love and support that I received from my family members and friends is a continuous source of energy for me. I want to express sincere gratitude with love to my parents Mr. Bhagwan Kumbhar and Mrs. Sushila Kumbhar for their help and being with me. Last but not the least, I want to thank the mechanical engineering department of Texas Tech University for giving me the excellent opportunity of working with them.

TABLE OF CONTENTS

ACKNOWLEDGEMENTS ..... **ii**

ABSTRACT ..... **vi**

LIST OF TABLES ..... **viii**

LIST OF FIGURES ..... **ix**

I. INTRODUCTION **1**

1.1 Motivation 1

1.2 Objective 2

1.3 Vibration evaluation methods 2

1.3.1 Weighted root mean square (rms) Acceleration 3

1.3.2 Vibration dose value (VDV) 4

1.3.3 Maximum transient vibration value (MTVV) 5

1.4 Biodynamic response functions 5

1.4.1 Mechanical impedance (DPMI) 5

1.4.2 Apparent mass (APMS) 6

1.4.3 Seat to head transmissibility (STHT) 6

1.5 Vibration frequency and human body resonance 7

1.6 International standard ISO 2631-1 9

1.7 Vehicle seat 12

1.8 Contact pressure at seat-body interface 13

1.9 Literature review of biodynamic models for whole body vibration 13

1.10 Experimental methods of assessing ride comfort 33

1.11 Thesis overview 35

II. HUMAN BIODYNAMIC MODEL AND SEAT MODEL 36

2.1 Introduction 36

2.2 Human model development 36

2.3 Human biodynamic model and its properties..... 38

2.4 Vehicle seats models 43

2.4.1 Case 1 - Hard seat model..... 44

2.4.2 Case 2 - Seat model with cushion but no seat suspension..... 46

2.4.3 Case 3 - Seat model with both cushion and seat suspension (Isolated Seat).... 47

2.5 Equations of motion 49

2.6 Summary 66

III. TRANSFER FUNCTION AND TRANSMISSIBILITY 68

3.1 Introduction 68

3.2 Derivation of transfer function and transmissibility 69

3.3 Transmissibility..... 72

3.3.1 Seat model with backrest angle $\alpha = 21^{\circ}$..... 74

3.3.2 Seat model with backrest angle $\alpha = 0^{\circ}$..... 81

3.3.3 Comparison of two backrest angles..... 88

3.4 Summary 88

IV. ABSORBED POWER AND FATIGUE PREDICTION 89

4.1 Introduction 89

4.2 Power calculation in mechanical system..... 90

4.3 Derivation for the absorbed power..... 92

4.4 Derivation for Case 1 - Hard seat model..... 96

4.5 Derivation for Case 2 and Case 3..... 103

4.6 Plots of absorbed power under sinusoidal displacement excitation 106

4.7 Absorbed power under constant amplitude of acceleration excitation 110

4.8 Plots of absorbed power under constant amplitude of acceleration excitation 116

4.9 Summary 120

V. SEAT DYNAMIC PARAMETERS DETERMINATION 122

5.1 Introduction 122

5.2 Optimization problem formulation..... 122

5.2.1 Case 2 seat model 124

5.2.2 Case 3 seat model 126

5.3 Discussion 128

5.4 Summary 130

VI. CONCLUSION AND FUTURE WORK.....131

6.1 Conclusion..... 131

6.2 Future work 132

BIBLIOGRAPHY 133

ABSTRACT

Vehicle ride comfort plays an important role in vehicle selection and customer satisfaction. It depends upon various factors including road irregularities, vehicle suspension, vehicle dynamics, tires, seat design and the human body's properties. For a given chassis, the seat design is one of the important aspects in vehicle interior design. Vehicle seat design is a special example of the product design process which takes multiple iterations. It is essential to reduce the total number of iterations in the early design stage to save time and money. How do the designers know the optimal seat parameters such as cushion, seat suspension, and etc. in the early design stage? What's the fatigue level for drivers to drive this newly designed vehicle? To answer these questions, a simulation based biodynamic human model is the best choice to assess the designed seat instead of physical prototypes. This research work focuses on developing a simulation method to predict virtual driver fatigue and determine optimal seat dynamic parameters for cushion and seat suspension. These dynamic properties include the stiffness and damping values of the cushion and seat suspension. A 14-degree of freedom (DOF) multibody biodynamic human model in 2D is selected from literature to assess three types of seat. The human model has total mass of 71.32 kg with 5 body segments. Backrest support and feet contact with the ground are included in this model. Three types of seat models are used in this research. The first seat has neither cushion nor seat suspension and is called a hard seat. The second type of seat has a seat and backrest cushion but does not have seat suspension. Last seat model, which is known as an isolated seat, has seat suspension and a seat and backrest cushion. Transmissibility and absorbed power are derived and plotted in vertical and horizontal directions for all three types of seats. For the given three types of seats, the seat with the backrest and seat pan cushion and seat suspension has the best performance compared to the hard seat or the seat without seat suspension based on transmissibility and absorbed power. It was shown that human body response depends on the dynamic properties of seat suspension and cushion. Furthermore, an optimization based method is used to determine the optimal dynamic seat parameters for seat suspension, and cushion. It was shown that the

biodynamic human simulation model is a useful tool to virtually assess the designed seats or design seats.

LIST OF TABLES

1.1 Human body complaints according to change in vibration frequency 8
1.2 Resonance frequencies of different human body parts 8
1.3 Weighting factors for one-third octave band (ISO 2631-1) 9
1.4 Parameter values for Wan and Schimmel's model 19
1.5 Parameter values for Boileau and Rakheja's model 20
1.6 Parameter values for Liu's model 20
1.7 Parameter values for Muksian and Nash's model 22
2.1 Human body mass, inertial properties and geometry parameters 41
2.2 Biomechanical properties of human body model 42
2.3 Seat and cushion material properties 49
4.1 Total unweighted and weighted absorbed power for 3 cases (Displacement) 110
4.2 Total unweighted and weighted absorbed power for 3 cases (Acceleration) 120
5.1 Optimal values of seat dynamic parameters for Case 2 124
5.2 Optimal values of seat dynamic parameters for Case 3 126
5.3 Original and optimal total weighted absorbed power for Case 2 and 3 128

LIST OF FIGURES

1.1 Coermann's one-DOF model 15
1.2 Wei and Griffin's one-DOF model 15
1.3 Muksian and Nash's two-DOF nonlinear model 16
1.4 Allen's two-DOF linear model 17
1.5 Wei and Griffin's two-DOF linear model 17
1.6 Suggs three-DOF linear model 18
1.7 Wan and Schimmel's four-DOF linear model 19
1.8 Boileau and Rakheja's four-DOF linear model 20
1.9 Liu's four-DOF nonlinear model 21
1.10 Muksian and Nash's seven-DOF model 22
1.11 Nigam and Malik's fifteen-DOF model 25
1.12 Ippili's nonlinear MB model 30
1.13 Cho and Yoon's nine-DOF model 31
1.14 Liang and Chiang's fourteen-DOF model 33
2.1 Human biodynamic model 39
2.2 Angle made by Body 5 39
2.3 Seat model for Case 1 – Hard Seat 45
2.4 Seat model with cushion but no seat suspension – Case 2 46
2.5 Seat model for Case 3 - Isolated Seat 48
3.1 Human body vertical and horizontal frequency weighting 69
3.2 Schematic representation of transfer function 71
3.3 Transmissibility of Body 1 in the horizontal direction (α =21º) 74
3.4 Transmissibility of Body 2 in the horizontal direction (α =21º) 75
3.5 Transmissibility of Body 3 in the horizontal direction (α =21º) 75
3.6 Transmissibility of Body 4 in the horizontal direction (α =21º) 76
3.7 Transmissibility of Body 5 in the horizontal direction (α =21º) 76
3.8 Transmissibility of Body 1 in the vertical direction (α =21º) 78
3.9 Transmissibility of Body 2 in the vertical direction (α =21º) 78

3.10 Transmissibility of Body 3 in the vertical direction (α =21º) 79
3.11 Transmissibility of Body 4 in the vertical direction (α =21º) 79
3.12 Transmissibility of Body 5 in the vertical direction (α =21º) 80
3.13 Transmissibility of Body 1 in the horizontal direction (α =0º) 82
3.14 Transmissibility of Body 2 in the horizontal direction (α =0º) 82
3.15 Transmissibility of Body 3 in the horizontal direction (α =0º) 83
3.16 Transmissibility of Body 4 in the horizontal direction (α =0º) 83
3.17 Transmissibility of Body 5 in the horizontal direction (α =0º) 84
3.18 Transmissibility of Body 1 in the vertical direction (α =0º) 85
3.19 Transmissibility of Body 2 in the vertical direction (α =0º) 85
3.20 Transmissibility of Body 3 in the vertical direction (α =0º) 86
3.21 Transmissibility of Body 4 in the vertical direction (α =0º) 86
3.22 Transmissibility of Body 5 in the vertical direction (α =0º) 87
4.1 Simple dynamic system 93
4.2 Frequency verses unweighted absorbed power (Displacement Input) 106
4.3 Frequency verses weighted absorbed power (Displacement Input) 107
4.4 Total unweighted absorbed power for 3 cases (Displacement Input)..... 109
4.5 Total weighted absorbed power for 3 cases (Displacement Input)..... 109
4.6 Frequency verses unweighted absorbed power (Acceleration Input)..... 117
4.7 Frequency verses unweighted absorbed power (Acceleration Input)..... 117
4.8 Total unweighted absorbed power for 3 cases (Acceleration Input) 119
4.9 Total weighted absorbed power for 3 cases (Acceleration Input) 119
5.1 Original and optimized weighted absorbed power for Case 2..... 125
5.2 Original and optimized weighted absorbed power for Case 3..... 127
5.3 Total absorbed powers with original and optimal seat dynamic parameters for sinusoidal displacement input..... 129
5.4 Total absorbed powers with original and optimal seat dynamic parameters for constant magnitude acceleration input..... 129

CHAPTER 1

INTRODUCTION

1.1 Motivation

The human body is exposed to vibrations in all types of vehicle environments like in on-road vehicle transport in the car, buses, off-road transport in the tractors, mining machines, rail transport in trains, monorails and marine transport in ships and boats. In each of these environments, the human body gets vibrations through the contact area and it causes discomfort and some health issues. About 8 million workers in United States are working in the area where they are exposed to occupational vibrations. Many experiential evidence have shown that a human body can potentially be injured by vibrations. These vibrations have adverse effects on the human body. This vibration includes vibration having low frequency to higher intensity vibration. The effect of vibration on the human body depends upon the intensity of vibration, exposure time, body sitting posture, human body type etc. Some of these adverse effects are summarized as below (Griffin, 1990).

- Most common result of vibration on human body is low back pain when human body is continuously exposed to low frequency vibrations.
- Vibration causes various physiological problems which include cardiovascular issues like sudden change in heart beats, pain induced hyperventilation.
- Vibration may cause involuntary muscular contraction and suppression of motor reflexes which causes fatigue in the human body.
- The visual, vestibular and auditory system gets affected by the vibrations. This will affect human vision, talk and movement during driving.
- The vibrations with frequency below 1 Hz (specifically from 0.1 to 0.5 Hz) results in feeling of motion sickness.
- Whole body vibration causes disorders in digestive, genital, urinary and reproductive system.

- Some people experience nervous and musculoskeletal disorders like spline fracture, insensitivity to some body parts during driving.
- Vibration shows slow detriment to human health.

This shows that whole body vibration is harmful to the health of the human body. Whole body vibration is a very important factor in vehicle ride comfort. Different experimental methods are used in automobile industries to measure vibration exposure in vehicles. But this method is not that effective because each human body's sensitivity to vibrations is different. But over the past few years, different artificial models were developed by various researchers through varying test conditions involving vibration excitations, human postural constraints and subject populations. It is critical to predict driver fatigue and determine the optimal seat dynamic parameters in the early design stage of the seat and subsequently vehicle design to save time and money. These dynamic parameters of the seat include stiffness and damping coefficients of seat suspension and cushion. Digital human modeling has gained momentum in the past decade due to advanced computing techniques. It would be a great idea to develop an accurate digital human model to assess seat or vehicle performance instead of physical mockups.

1.2 Objective

The research objectives are listed as follows:

1) Have a comprehensive literature review about methods of assessing ride comfort.
2) Select an advanced biodynamic human model to study the performance of different seats.
3) Derive equations of motion for the human biodynamic model and seat system.
4) Evaluate human body response using transfer function and absorbed power.
5) Investigate the virtual driver fatigue.
6) Determine the optimal seat dynamic parameters.

1.3 Vibration evaluation methods

Various vibration evaluation methods are found in the literature. There are some international standards that define how to evaluate whole body vibration and comfort. For

evaluation purposes output quantities of signals like acceleration or force are measured. Three important aspects of the signal that need to be consider for vibrational inputs are the duration of exposure, amplitude, and its frequency. Three methods are found in the literature. They are weighted root mean square acceleration, vibration dose value and maximum transient vibration value.

1.3.1 Weighted root mean square (rms) Acceleration

According to ISO 2631-1 in time domain, the weighted root mean square acceleration can be calculated using equation 1.1.

$$a_{w,rms} = \left[\frac{1}{T} \int_0^T a_w{}^2(t)dt \right]^{\frac{1}{2}} \tag{1.1}$$

Where $a_w(t)$ is instantaneous frequency weighted acceleration and T is the duration of measurement. For translational vibration, the weighted rms acceleration is expressed in meters per second squared and for rotational vibrations it is expressed in radians per second squared.

In the frequency domain, it can be determined by appropriately adding the attaching weights to the narrow band or one-third octave band data in one specific direction as shown in equation 1.2. ISO 2631-1 defines this frequency weightings developed based on human body sensitivity to different frequencies. There are six frequency weighting factors developed for vibration evaluation with respect to health, comfort, perception and motion sickness. These weighting factors are explained in this chapter in section 1.8. The frequency weighted rms acceleration is calculated as shown in equation 1.2.

$$a^f_{w,rms} = \left[\sum_{i=1}^{N} (W_i \left(a_{w,rms} \right)_i)^2 \right]^{\frac{1}{2}} \tag{1.2}$$

Where, $\left(a_{w,rms}\right)_i$ is the rms acceleration and W_i is the respective weighting factor for the i^{th} one-third octave band and *N* is the number of one-third octave bands in the frequency range.

For random vibrations, the frequency weighted rms acceleration for a frequency band can be calculated by considering power spectrum density as shown in equation 1.3.

$$a_{w,rms}^{random} = \left[\int_{f1}^{f2} |W(f)|^2 \, S(f) df \right]^{\frac{1}{2}} \tag{1.3}$$

Where, f_1 and f_2 are the lower and upper frequency limits of a frequency band, $S(f)$ is the power spectral density of acceleration and $W(f)$ is the frequency weighting factor.

1.3.2 Vibration dose value (VDV)

On-road vehicle vibrational inputs are from the road profile irregularities. The transmitted path is from the tire to chassis, to vehicle body, to seat, and finally to human body. The fourth power vibration dose method is more sensitive to peaks (road irregularities) as it considers fourth power of accelerations (Griffin, 1986; 1990). This method is also called as vibration dose method as it gives value of vibration dose value. This method is explained in British Standard 6841 (1987) for the assessment of vibrational exposure. VDV is a fourth root of integral sum of the fourth power of the frequency weighted acceleration with respect to time and defined in equation 1.4.

$$\text{VDV} = \left[\int_0^T \left[a_w(t) \right]^4 dt \right]^{\frac{1}{4}} \tag{1.4}$$

These standards also focus on different locations of body for this acceleration measurement which are feet, seat and back. The comfort value (vibrational) is assessed by checking the value of VDV does not reach to a critical boundary value.

1.3.3 Maximum transient vibration value (MTVV)

This weighted rms value does not consider occasional shocks and transient vibration. For this purpose, running rms evaluation method is used. The running rms evaluation method considers occasional shocks and transient vibration by the use of a short integration time constant. According to ISO 2631-1, the equation 1.5 is used to calculate running rms acceleration.

$$a_w(t_0) = \left[\frac{1}{T} \int_{(t_0 - T)}^{t_0} [a_w(t)]^2 dt \right]^{\frac{1}{2}} \tag{1.5}$$

Where, $a_w(t)$ is instantaneous frequency weighted acceleration, T is the integration time, and t_0 is the observation time.

The maximum value out of these running rms acceleration values is selected as MTVV. This is shown in the equation 1.6. This value will represents vibration exposure under high magnitude of shocks.

$$\text{MTVV} = \max[a_w(t_0)] \tag{1.6}$$

1.4 Biodynamic response functions

The human body subjected to vibration is widely assessed in terms of biodynamic response function. There are three biodynamic response functions. These are driving point mechanical impedance, apparent mass, and seat to head transmissibility. Out of it, first two are used to describe “to the body” transfer function and last is “through the body” transfer function.

1.4.1 Mechanical impedance (DPMI)

According to ISO/DIS 5982 (2001), the mechanical impedance is a complex ratio of applied periodic excitation force at frequency *f,* $F(f)$ to the resulting vibration velocity

$v(f)$ measured at the same point and in the same direction of applied force. This ratio is expressed numerically in equation 1.7.

$$Z(f) = \frac{F(f)}{v(f)} \tag{1.7}$$

Mechanical Impedance is also known as DPMI and it gives information about external force necessary to produce the specific response in the system.

1.4.2 Apparent mass (APMS)

Apparent mass (effective mass) is defined in ISO/DIS 5982 (2001) as a complex ratio of applied periodic excitation force at frequency *f,* $F(f)$ to the resulting vibration acceleration at the frequency $a(f)$ measured at the same point and in the same direction of applied force. The equation 1.8 is used to calculate the apparent mass.

$$AP(f) = \frac{F(f)}{a(f)} \tag{1.8}$$

The APMS is to the body biodynamic response function it gives information about the force applied to a body that accelerates body by an amount proportional to force in direct proportional with body mass. The apparent mass is having the advantage that it can be directly obtained from the signals provided by force transducers and accelerometers.

1.4.3 Seat to head transmissibility (STHT)

The STHT is a complex ratio of response motion of the head to the forced vibration motion at the seat-body interface.

$$H(f) = \frac{Head\ output(f)}{Seat\ input(f)} \tag{1.9}$$

STHT is ‘through the body’ biodynamic function which signifies the extent to which the input vibration input to the body is transmitted to the parts of body.

1.5 Vibration frequency and human body resonance

The human body is not a rigid body but it is a complex mechanical system having elastic properties. The human body response to whole body vibration is not only related to magnitude and duration but it also depends upon the frequency of the vibration. Human body will responds differently for different frequencies of applied vibrations (Griffin, 2001). At the low frequencies below 1 Hz, vertical vibrations of seat and the body parts are very similar as there is very small relative motion. The motion of the body increases with increasing frequencies and reaches to resonance frequency. So Resonance frequency occurs when transmissibility reaches to its peak value. At resonance frequency, the body part will vibrate at a magnitude greater than applied vibratory force. This can affect physiological functions of human body including muscle function, respiratory and circulatory functions.

For studying physiological reaction of human body, Magid and Coermann (1960) did experiment on seated human subjects exposed to the vibrations of increasing frequency. These subjects are exposed to the vibration of increasing frequencies from 1 to 20 Hz. After the test, subjects are asked to explain their experience and complaints about body pain or reactions. These reactions are summarized in Table 1.1.

In practical life, human body is not exposed to pure, simple vibrations but the exposures include complex waves of different frequencies, magnitude and direction. When human body frequency matches with excitation frequency, resonance occurs. At the resonance frequency, the maximum amount of vibration gets transmitted to that body parts. Different body parts have different resonance frequencies. These resonance frequencies of different human body parts for various body postures are summarized in Table 1.2 (Dupuis and Zerlett, 1986). Same human body has different resonance frequency for vibrations in different directions. For this following coordinate system is defined: X as front side of body, Y as left side of body and Z as upper side of body.

Table 1.1 Human body complaints according to change in vibration frequency

Complaint	Vibration Frequency(Hz)
Headache	4-9
Speech disturbance	13 - 20
Jaw resonance	6 - 8
Pharynx disturbances	12 - 16
Respiration complaints	4 - 8
Chest pain	5 - 7
Back pain	8 - 12
Abdominal pain	4 -10
Constant urge to urinate and defecate	10 -18
Increased muscle tension	13 -20

Table 1.2 Resonance frequencies of different human body parts

Body Posture	Body Part	Vibration Direction	Resonance Frequency (Hz)
Sitting	Trunk	Z	3 - 6
	Chest		4 - 6
	Spinal column		3 - 5
	Shoulder		2 - 6
	Stomach		4 - 5(7)
	Eyes		20 - 25
Standing	Knee	X	1 - 3
	Shoulder		1 - 2
	Head		1 - 2
	Whole Body	Z	4 - 7
Reclining	Foot	X	16 - 31
	Knee		4 - 8
	Abdomen		4 - 8
	Chest		6 -12
	Skull		50 - 70
	Foot	Y	0.8 - 3
	Abdomen		0.8 - 4
	Head		0.6 - 4
	Foot	Z	1 - 3
	Abdomen		1.5 - 6
	Head		1 - 4

Today, a guideline in defining human tolerance to whole body vibration has been adopted as an International Standard ISO 2631-1 (1997). For evaluating exposure for high level of

vibration and shocks, ISO 2631-5 (2004) has been used. The ISO 2631-4 (2001) is used to define different methods for the measurement of periodic, random and transient vibration. For health, comfort and perception, frequency range from 0.5 to 80 Hz is considered while for motion sickness, it is in between 0.1 to 0.5 Hz.

1.6 International standard ISO 2631-1

ISO 2631-1 is developed by International Standard Organization (ISO). This standard gives the general information required for evaluating human body exposure to whole body vibrations. This includes different vibration measurement methods, vibration evaluation methods like rms acceleration, VDV value, MMTV value. This standard also defines different frequency weighting factors useful in calculations with respects to health, comfort, perception and motion sickness.

In this section these frequency weighting factors given in ISO 2631-1 are explained. Human body sensitivity is not fixed but it is depends upon variation in frequency. Frequency weighting functions accounts for this variation in the sensitivity with frequency. Therefore frequency weighting factors are used to compensate and to normalize the differences in human susceptibility and sensitivity at different frequencies.

Table 1.3 summarizes frequency weighting factors for one-third octave band frequencies. In this standard frequency weighting factors are given in the frequency range from 0.1 to 400 Hz in one-third octave band frequency range. Frequency weighting factors are not calculated below 0.1 Hz because frequency below 0.1 Hz is not important in calculation of weighted acceleration. This standard also focuses on possible tolerance for these weighting factors.

Table 1.3 Weighting factors for one-third octave band (ISO 2631-1)

Frequency	Weighting Factors					
f (Hz)	W_k	W_d	W_f	W_c	W_e	W_j
0.1	0.0312	0.0624	0.6950	0.0624	0.0625	0.0310
0.125	0.0486	0.0973	0.8950	0.0972	0.0975	0.0483

Table 1.3 Continued

Frequency	Weighting Factors					
f (Hz)	W_k	W_d	W_f	W_c	W_e	W_j
0.16	0.0790	0.1580	1.0060	0.1580	0.1590	0.0785
0.2	0.1210	0.2430	0.9920	0.2430	0.2450	0.1200
0.25	0.1820	0.3650	0.8540	0.3640	0.3680	0.1810
0.315	0.2630	0.5300	0.6190	0.5270	0.5360	0.2620
0.4	0.3520	0.7130	0.3840	0.7080	0.7230	0.3510
0.5	0.4180	0.8530	0.2240	0.8430	0.8620	0.4170
0.63	0.4590	0.9440	0.1160	0.9290	0.9390	0.4580
0.8	0.4770	0.9920	0.0630	0.9720	0.9410	0.4780
1	0.4820	1.0110	0.0235	0.9910	0.8800	0.4840
1.25	0.4840	1.0080	0.0100	1.0000	0.7720	0.4850
1.6	0.4940	0.9680	0.0038	1.0070	0.6320	0.4830
2	0.5310	0.8900	0.0016	1.0120	0.5120	0.4820
2.5	0.6310	0.7760	0.0006	1.0170	0.4090	0.4890
3.15	0.8040	0.6420	0.0003	1.0220	0.3230	0.5240
4	0.9670	0.5120	0.0001	1.0240	0.2530	0.6280
5	1.0390	0.4090		1.0130	0.2020	0.7930
6.3	1.0540	0.3230		0.9740	0.1600	0.9460
8	1.0360	0.2530		0.8910	0.1250	1.0170
10	0.9880	0.2120		0.7760	0.1000	1.0300
12.5	0.9020	0.1610		0.6470	0.0801	1.0260
16	0.7680	0.1250		0.5120	0.0625	1.0180
20	0.6360	0.1000		0.4090	0.0500	1.0120
25	0.5130	0.0800		0.3250	0.0399	1.0070
31.5	0.4050	0.0632		0.2560	0.0316	1.0010

Table 1.3 Continued

Frequency	Weighting Factors					
f (Hz)	W_k	W_d	W_f	W_c	W_e	W_j
40	0.3140	0.0494		0.1990	0.0247	0.9910
50	0.2460	0.0388		0.1560	0.0194	0.9720
63	0.1860	0.0205		0.1180	0.0148	0.9310
80	0.1320	0.0211		0.0844	0.0105	0.8430
100	0.0807	0.0141		0.0567	0.0071	0.7080
125	0.0540	0.0086		0.0345	0.0043	0.5390
160	0.0205	0.0046		0.0182	0.0023	0.3640
200	0.0152	0.0024		0.0097	0.0012	0.2430
250	0.0079	0.0013		0.0051	0.0006	0.1580
315	0.0040	0.0006		0.0026	0.0003	0.1000
400	0.0020	0.0003		0.0013	0.0002	0.0624

The Table 1.3 summarizes principal and additional frequency weighting factors. The effect of vibration on health, comfort, perception and motion sickness are depends on the vibration frequency content. Different frequency weighting factors are given for different axes of vibration, different purpose like comfort, motion sickness. There are total 6 weighting factors in Table 1.3 with respects to health, comfort, perception and motion sickness. These are divided into two types:

1) Principal weighting factor

   W_k – For vibrations in Z-direction and vertical recumbent direction

   W_d – For vibrations in X and Y-directions and horizontal recumbent direction

   W_f – For motion sickness study

2) Additional weighing factor

   W_c – For vibrations at seat-back interface

   W_e – For measurement of rotational vibration

   W_j – For vibrations of the head of recumbent person

These weighting factors are used for calculation of the weighted absorbed power in the Chapter 4. Different weighting factors are used for different vibration direction.

1.7 Vehicle seat

A vehicle travelling on roads vibrates due to the road irregularities. These vibrations are transferred to the vehicle chassis through the tires. From the chassis, these vibrations are transferred to the vehicle body parts, including the seat. As the human body is in direct contact with the seat cushion, it is very important that the seat should provide a good vibration isolator so that a minimum amount of vibrations can be transferred to the human body. Sitting posture is the most common scenario in running vehicles. The maximum vibration inputs in human body are through the seats. As human body is in direct contact with seat, its analysis and design is very important in study of ride comfort. Approximately 70% of the human mass is supported by the seat with the reminder supported by the feet support (Gouw et al., 1990). Therefore the analysis of vehicle seat is important in the study of ride comfort.

In vehicle suspension and dynamics research with quarter, half or full vehicle modeling, seat, driver or passenger and cab are commonly treated as combined sprung mass (Gouw et al., 1990; Wong, 2008; Ma, et al., 2008; ISO 2631-4, 2001; ISO 2631-5, 2004). In the full vehicle chassis and body durability testing, the driver and passenger are replaced with sandbag or water dummy to match the vehicle corner weight (Xu et al., 2005; Xu et al., 2006; Soliman, 2011). In road load analysis for vehicle chassis, the driver or passenger and seat are also normally to be combined with cab (Xu et al., 2005) as sprung mass. In the cab's rubber mount design and analysis, a cab, a seat and an occupant can be taken as a single combined body (Xu et al., 2008; 2011). In this case, the effect of seat and occupant's motion and force relative to the cab is neglected.

In the testing and analysis of seat cushion, seat suspension, cab suspension and vehicle ride comfort, the seated driver/passenger can be replaced with rigid mass (Ma et al., 2008; Mayton et al., 2006; Montazeri et al., 2008; Shurpali and Mullinix, 2011) sandbag (Pang et al., 2004), water dummy, or anthropodynamic dummy (Lewis and Griffin,

2002). In the mathematical analysis, the seated human body can be modeled as a different number of DOF mass-spring-damping mechanical systems including the one-DOF (Kordestani et al., 2010), two-DOF (Pang and Qatu, 2005), three-DOF (Amirouche et al., 1997), and higher number degree of freedoms such as seven-DOF (Deb and Joshi, 2012).

1.8 Contact pressure at seat-body interface

In the study of postural comfort, the contact pressure at the interface of seat and driver is a very important parameter. When this contact pressure is uniform, the seating posture is comfortable and the driver will get good riding experience.

Brook et al. (2009) studied particular factors affecting the driving postural comfort for lower parts of human body. A customized pressure pad subsystem was used to monitor pressure distribution between the driver and vehicle seat. This study indicates significant differences between pressure distributions in car in terms of fore-aft seat position for three drivers. Tang et al. (2010) investigated the effects of varying the frequencies of vertical vibration on seat-interface contact pressure of human body on three different seat cushions by using finite element analysis. Finally they showed that SAF 6060 seat cushion can be used to reduce the amplitude of varying maximum contact pressure in the frequency range of 10-20 Hz. This seat cushion is made from SAF 6060 polymer foam having rate-independent hyper elastic and viscoelastic behavior.

1.9 Literature review of biodynamic models for whole body vibration

In literature, many mathematical models for the study of biodynamic responses of seated human body have been developed. Biodynamic model development can be traced back to 1900's (Hamilton, 1918). Since then, various models have been developed. These models can be divided into three groups as lumped parameter model, finite element model and multibody model (Kumbhar et al., 2012). In each of this type of models, several models are proposed in literature.

- ***Lumped parameter models (LP models)***

A human body is not just a mass but has various physically distant parts like legs, hand, torso, neck, head, etc. The lumped parameter model considers human body as several concentrated masses (representing body parts) which are connected by the springs and dampers. Thus it is made from lumped masses, springs and dampers. It is a most popular analytical method for the study of response of seated body. This is a simple, easy method of analysis and is easy to validate the results. But it has some disadvantages as it is only used for 1-D vibrational analysis only.

According to Nigam and Malik (1987), the following are the important steps in development of lumped parameter model.

i) The segmentation of body – Human body is made from various organs. In LP model, these body parts are segmented into various mass segments. To connect these masses together and to represent the flexibility of body parts, springs and dampers are used.

ii) Mass and stiffness values of segments – In this step, values of mass and stiffness for each mass segment is evaluated.

iii) Connection between segments – These different segments are lumped at discrete points and connected by springs and damper sets.

iv) Stiffness values of springs and dampers – The stiffness values of springs and dampers are evaluated.

Lumped parameter models are subdivided based on number of degrees of freedom (DOF) they have.

- ***One- DOF model***

Among all the models, this is a simplest model used to predict the response of human body to vibration. But as this model represents human body as only one mass segment, it is not able to properly simulate body responses.

Coermann (1962) presented a one-DOF model which considers human body as a single mass (m_1=56.8 kg) and contact between seat and human body is

represented by a spring (k_1=75000 ± 28300 N/m) and damper (C_1=3840 ± 1007 N-s/m). This model is represented in Figure 1.1.

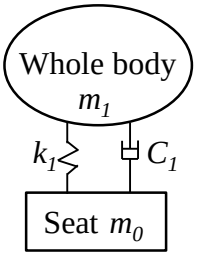

Figure 1.1 Coermann's one-DOF model

Wei and Griffin (1998) presented a similar model but it has two separate masses of total mass equal to 51.2 kg for the human body. This model is represented in Figure 1.2. In this figure, mass marked as mass of buttocks and legs (m_0=7.8 kg) is in rigid contact with seat and the mass of seat is neglected. The upper body mass (m_1=43.4 Kg) is connected to the buttocks and legs using a linear spring (k_1=44130 N/m) and damper (C_1=1485.0 N-s/m).

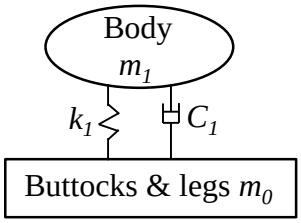

Figure 1.2 Wei and Griffin's one-DOF model

This model is very similar to Fairley and Griffin's model (Fairley and Griffin, 1989). In this model mass marked as mass of buttocks and legs (m_0) is 6.0 kg and the upper body mass (m_1) is 45.6 kg. These are interconnected by using a linear spring (k_1=45000 N/m) and damper (C_1=1360 N-s/m).

- ***Two-DOF model***

Two-DOF models consist of two separate masses each representing head and body of human body which are connected by springs and damper to represents physical properties of body.

Muksian and Nash (1976) introduced a nonlinear two-DOF model having total mass 79.83 kg shown in Figure 1.3. This model is separated into three mass segments. The top one is the head (m_2=5.44 kg), middle is the body (m_1=47.17 kg), and bottom is the pelvis (m_0=27.22 kg). The springs and dampers are used to connect between these three separated segments and all springs and dampers are linear except the body spring and damper used to connect to the body and pelvis (k_1=63318 N/m, k_2=0, C_1=467 N-s/m, C_2=686 N-s/m). The damper (C_1) used to connect body and pelvis is having linear and nonlinear parts. The pelvis is rigidly connected to the seat as physical properties of pelvis are included in spring and damper connecting them.

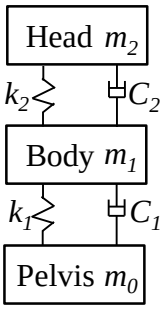

Figure 1.3 Muksian and Nash's two-DOF nonlinear model

Allen (1978) presented a linear two-DOF model having total mass of 56.8 kg as shown in Figure 1.4. This model is made from two separate mass elements one is head (m_2=5.5 kg) and other is body (m_1=51.3 kg) which is seated on third element, seat (m_0). All springs (k_1=74300 ± 17400 and k_2=41000 ± 24100 N/m) and dampers (C_1=2807 ± 1007 N-s/m and C_2=318 ± 161 N-s/m) are linear in this model.

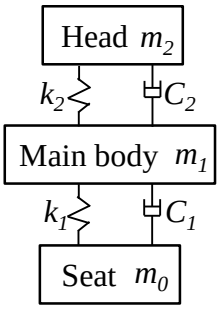

Figure 1.4 Allen's two-DOF linear model

Wei and Griffin (1998) presented a linear two-DOF model which is modified from their one-DOF model. This model has total mass 50.8 kg divided into three separate mass elements as shown in Figure 1.5. These three elements are head (m_2=10.7 kg), body (m_1=33.4 kg), buttocks and legs (m_0=6.7 kg). Similar to their one-DOF model, the mass of buttocks and legs is in rigid contact with seat and the mass of seat is neglected. All springs (k_1=35776 N/m *and* k_2=38374 N/m) and dampers (C_1=761N-s/m and C_2=458N-s/m) are linear for this model.

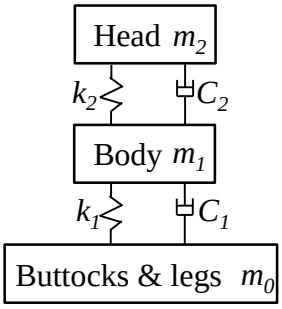

Figure 1.5 Wei and Griffin's two-DOF linear model

Lewis and Griffin (2002) used Wei & Griffin's one and two-DOF models and did experiment for testing seats with five foam cushions. Anthropodynamic dummies were developed having suitable apparent mass for testing these seats. In the frequency range 2-4 Hz, larger difference was found between measured cushion transmissibility's using two-DOF model than with one-

DOF. This indicates need of increasing more degree of freedom for getting more accurate results.

- ***Three-DOF model***

  Three-DOF models consist of three separate masses each representing human body parts which are connected by springs and damper to represents physical properties of body.

  Suggs et al. (1969) reported a linear three-DOF model having total mass 56.8 kg. As shown in Figure 1.6, this model has four separate mass elements as head (m_3=5.5 kg), upper torso (m_2=36kg), lower torso (m_1=15.3kg), and seat (m_0). Upper torso and lower torso are connected rigidly with spring and damper set (k_2 & C_2) whose properties (stiffness and damping coefficient) are selected infinite. Other springs and dampers are linear (k_1=40900 ± 22700 N/m, k_3=74300 ± 17400 N/m, C_1=2806 N-s/m, C_1=318 ± 42 N-s/m).

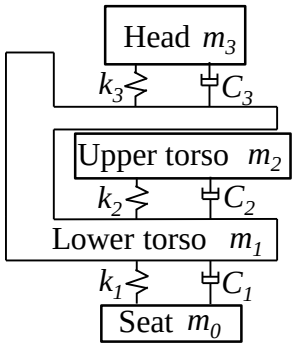

Figure 1.6 Suggs three-DOF linear model

- ***Four-DOF model***

  Four-DOF models consist of four separate masses each representing head, upper torso, viscera, lower torso parts which are connected by springs and damper to represents physical properties of body.

  Wan and Schimmel (1995) introduced a four-DOF linear having total mass of 60.67 kg as shown in Figure 1.7. This model has 4 separate body elements

head (m_4), upper torso (m_3), viscera (m_2) and lower torso (m_1) which is rigidly connected to seat (m_0). These segments are connected by five sets of linear springs and dampers (k_i & C_i). The values for these parameters are summarized in Table 1.4.

Table 1.4 Parameter values for Wan and Schimmel's model

Mass (kg)	Stiffness Coefficient (N/m)	Damping Coefficient (N-s/m)
m_1=36	k_1=49340	C_1=2475
m_2=5.5	k_2=20000	C_2=330
m_3=15	k_3=10000	C_3=200
m_4=4.17	k_4=134400	C_4=250
	k_5=192000	C_5=909.1

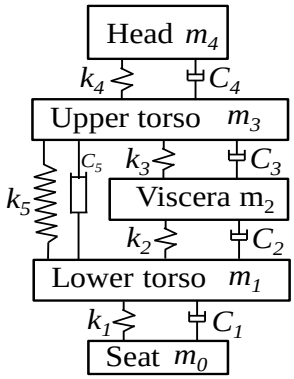

Figure 1.7 Wan and Schimmel's four-DOF linear model

Wagner and Liu (2000) integrated this model with a full vehicle for ride quality assessment.

Boileau and Rakheja (1998) introduced a four-DOF linear model having total mass of 55.2 kg. As shown in Figure 1.8, this model consists of four mass segments representing head (m_4), upper torso with chest (m_3), lower torso (m_2) and thigh and pelvis (m_1) which is rested on seat (m_0). These segments are interconnected by four sets of linear springs and dampers (k_i & C_i). All the values of masses and properties of springs and dampers listed in Table 1.5 are obtained by optimization procedure of data.

Table 1.5 Parameter values for Boileau and Rakheja's model

Mass (kg)	Stiffness Coefficient (N/m)	Damping Coefficient (N-s/m)
m_1=12.78	k_1=90000	C_1=2064
m_2=8.62	k_2=162800	C_2=4585
m_3=28.49	k_3=183000	C_3=4750
m_4=5.31	k_4=310000	C_4=400

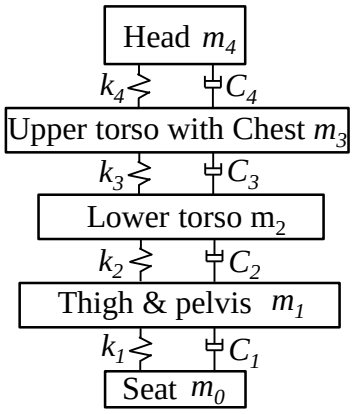

Figure 1.8 Boileau and Rakheja's four-DOF linear model

Liu at al. (1998) also proposed a four-DOF nonlinear model having total mass of 55.2 kg. The model shown in Figure 1.9 consists of four mass elements each representing head (m_4), upper torso (m_3), viscera (m_2) and pelvis (m_1). They are kept on seat (m_0). They are interconnected by four sets of nonlinear springs and dampers (k_i & C_i) whose values are listed in Table 1.6. The viscera are not connected to upper torso but it is hanging on it. Therefore this model considers gravitational effect.

Table 1.6 Parameter values for Liu's model

Mass (kg)	Stiffness Coefficient (N/m)	Damping Coefficient (N-s/m)
m_1=29	k_1=0	C_1=0.50
m_2=6.8	k_2=2931.8	C_2=138.77
m_3=21.8	k_3=0	C_3=0.22
m_4=5.5	k_4=202290	C_4=210.96

This model was also validated on live human drop tests by Zong and Lam (2002).

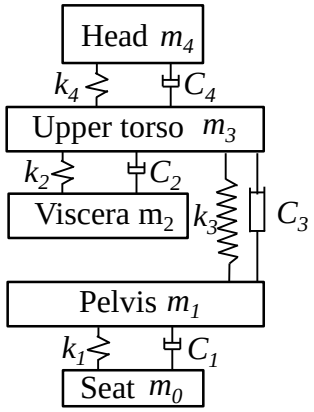

Figure 1.9 Liu's four-DOF nonlinear model

- ***Seven-DOF model***

  Muksian and Nash (1974) developed a seven-DOF nonlinear model with total seven elements having total mass of 80 kg as shown in Figure 1.10. Each element represents head (m_7), back (m_6), torso (m_5), thorax (m_4), diaphragm (m_3), abdomen (m_2) and pelvis (m_1). These are interconnected by nonlinear spring and damper sets except two sets of springs (k_6 and k_7) and dampers (C_6 and C_7) which are linear used to connect neck and back. Pelvis mass is rigidly connected to seat (m_0). New phenomenon introduced in this model is coulomb damping forces to represent sliding surface between torso and back and related muscle contraction and diaphragm muscle forces. The whole body vibration was studied in vertical direction. Table 1.7 represents the values of various parameters in this system.

Table 1.7 Parameter values for Muksian and Nash's model

Mass (kg)	Stiffness Coefficient (N/m)	Damping Coefficient (N-s/m)
m_1=27.230	k_1=0	C_1=0
m_2=5.921	k_2=877	C_2=292
m_3=0.455	k_3=877	C_3=292
m_4=1.362	k_4=877	C_4=292
m_5=37.762	k_5=877	C_5=292
m_6=6.820	k_6=52600	C_6=3580
m_7=5.450	k_7=52600	C_7=3580
-	k_{56}=52600	C_{56}=3580

Patil et al. (1977; 1988) modified above seven-DOF model by adding one set of spring and damper between the pelvis and seat. Therefore this eight-DOF nonlinear model was further extended to include seat suspension system and the tractor model.

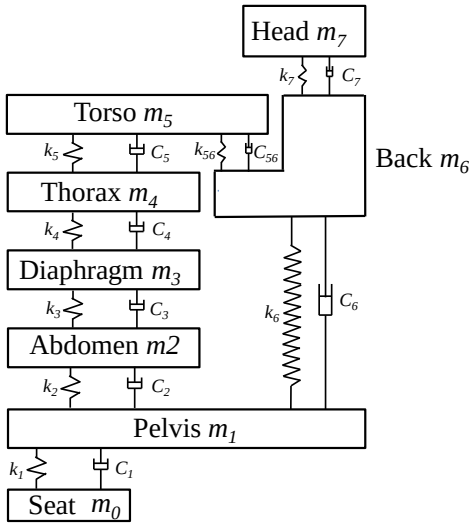

Figure 1.10 Muksian and Nash's seven-DOF model

- ***Eleven-DOF model***

Qassem et al. (1994) and Qassem and Othman (1996) reported an eleven-DOF linear model. It is based on the seven-DOF model with some modification and has total mass of 91.7 kg. The important difference between Patil's seven-

DOF model (Patil et al, 1977) and this model is that all spring-damper sets in this model are linear. Human back is again divided into cervical, thoracic, and lumber spines. This model was used to study hand arm system a mass of 10.35-12.15 kg in the thorax and abdomen for pregnant female subjects.

- ***Fifteen-DOF model***

Nigam and Malik (1987) proposed a fifteen-DOF model shown in figure 1.11. This human body is represented by lumped parameter model consisting masses and springs. The LP model was made from 15 body segments (having elliptical shapes) and 14 joints. In this model, the mass of individual segment is proportional to its volume and it can be expressed as a fraction of total body mass.

According to this, the mass of any segment is given by equation 1.10.

$$M_{si} = \frac{M_b a_i b_i c_i}{\sum_{j=1}^{n} a_j b_j c_j} \tag{1.10}$$

Where, M_b - Total mass of the body

M_{si} - Mass of any i^{th} segment

a_i, b_i and c_i – Semi axes of any i^{th} ellipsoid

i – Subscript for segment.

n – Number of segments.

Similarly the stiffness of the segment can be calculated by considering the mechanical properties and axial tension in truncated ellipsoid. The axial stiffness *(S_i)* is derived as shown in equation 1.11.

$$S_i = \frac{\pi E a_i b_i}{C_i I_i} \tag{1.11}$$

Where, $E = \sqrt{E_b E_t}$ (Axial elastic modulus)

$$I_i = c_i \int_{-d_i}^{d_i} dz / (c_i^2 - z^2)$$

E_b - Elastic modulus of bone

E_t - Elastic modulus of tissue

Here they ignored damping of body and standing posture of body is considered. After evaluating these values these segments with rigid masses are connected with massless springs in series.

For free vibration, equation of motion for this model is represented in equation 1.12.

$$\mathbf{M\ddot{X} + KX = 0} \tag{1.12}$$

Where, $\mathbf{M}$ – Mass matrix (Dimension 15x15)

$\mathbf{K}$ – Stiffness matrix (Dimension 15x15)

$\mathbf{\ddot{X}, X}$ – Acceleration and displacement vector of body (Dimension 15x1)

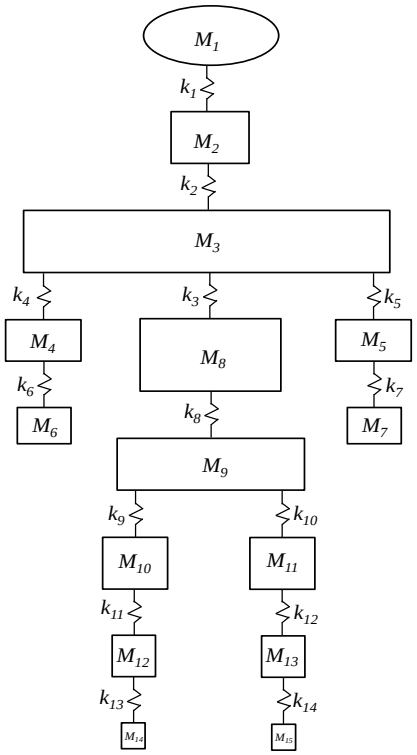

Figure 1.11 Nigam and Malik's fifteen-DOF model

They did the experiment and found that natural frequencies of the model are within the range of available range.

- ***Finite element models (FE models)***

Finite element model considers human body consists of numerous finite elements whose properties are obtained from various experiments on human corpses. With the help of powerful finite element software, this model can be used to study biodynamic response of human body and used in predicting injuries in occupants. According to Liang and Chiang (2006; 2008), in some FE models the spine is a layered structure of rigid elements. In the FE method, beam spring and masses are used to model spine, viscera, head, pelvis, and buttock tissues. Linder (2000) studied the influence of head motion on the responses of rear impact. Also to investigate human responses on side impact, Low and Prasad (1990) verified MADYMO side impact model.

Pennestri et al. (2005) developed a numerical model based on finite element model. They validated this model by means of static and dynamic tests on actual vehicle. This approach allows to study all three dimensional behaviors on dummy human body and simulate it with different poses such as seating, standing, changing different parameters such as seat inclination, seat height. So this model consists of 6 body elements for occupant and 2 bodies for car environment. Occupant bodies include head, arm, forearm, thigh, leg and foot while car environment is represented by seat and steering wheel. For the contact between the thigh and seat, the mesh generation is optimized. For meshing of the nonlinear material property it is discretized with hexahedral solid elements. This is to reproduce the polyurethane form characteristic. As human body thigh is made from two parts that is bone and tissues with muscles, it is modeled with two materials. The inner part (bone) is considered as a rigid bar and external part (tissues with muscles) is considered deformable. Remaining body parts are modeled with coarse mesh. For experiential tests, ten people were seated on a seat which is equipped with pressure mats with many transducers. Relevant parameters such as peak location, maximum pressure value in pressure field are measured in pressure field and found very close. This pressure field depends on anthropometrical feature of the seated occupant. Therefore the shape of pressure field varies from one occupant to other. But it will not going to affect because here pressure concentration is more important than shape of pressure field. Accelerometers are mounted at measuring points on chassis to measure acceleration values. At the interface of body with seat cushion and with backrest, the two three-axial SAE plate accelerometers are placed. To measure vibrational input to occupant's body, the other accelerometers are located at the steering wheel, at pedal and at the anchor points of the seat. Then using BS 6841 standard (1987), vibration dose value (VDV) is computed and compared with result from FE model.

Tang et al. (2010) used finite element modeling approach to investigate the effects of varying the frequencies of vertical vibration on contact pressure between seat cushion and buttock tissues of human body on three different seat cushions. They developed a simple two-dimensional human buttock-thigh model to simulate the response of the muscles of buttock and thigh. Finally they shown SAF 6060 seat cushion can be used to reduce the amplitude of varying maximum contact pressure in the frequency range of 10-20 Hz. This seat cushion is made from SAF 6060 polymer foam having rate-independent hyper elastic and viscoelastic behavior.

- ***Multibody models (MB model)***

Lumped Parameter models explained above used to accurately predict human response to vibration but the analysis is limited to vertical direction. The human body is very complex dynamic system whose properties vary from one part to other and from individual to individual. Hence to study this complex behavior, more comprehensive mathematical model is needed. Here came need of multibody human model which are made from several rigid bodies connected by pin or ball and socket joints (called as bushing elements). This model is similar to several rigid bodies connected by bushing element. Bushing elements are used to represent rotational and translational motion.

Various MB models are proposed in the literature. Amirouche and Ider (1988) developed a MB model having 13 rigid and flexible segments interconnected by spherical, revolute and free joints. This model is in seating position having origin of coordinate system at the center of each joints of rotation. For free joints six degrees of freedom are allowed, three for translations and three for rotations. Using Kane's equation, the equation of motion is developed. The governing equation was developed by allowing small oscillations as this simulation involves study for human responses to low accelerations. These input excitation forces were applied simultaneously in different parts in different directions. To represent

human body tissues, muscles, ligaments and disc vertebrae, they were modeled by linear and nonlinear stiffness and damping matrices. For analysis, they used human body system dynamics which is automated three-dimensional program used to predict human body responses to vibration. By proper selection of stiffness and damping coefficients, this model was capable of predicting human responses by trial and error procedure.

Pennestri et al. (2005) developed a numerical model based on multibody dynamics model. They validated this model by means of static and dynamic tests on actual vehicle. This approach allows studying all the three-dimensional behavior of dummy human body with different poses such as seating, standing, changing different parameters such as seat inclination, seat height. This model is made from 15 rigid elements. Out of these elements, twelve were used to define human model and 3 described car environment. Hence this is equivalent to occupant having two feet with legs, two thighs, two arms, two forearms, head, neck, shoulders and chest which are rigidly connected. Remaining elements are seat, pedals and steering wheel. For representing body joints and connecting each other, kinematics constraints and spring-damper are used. There are two spherical joints in between pelvis and thighs, two revolute joints in between thighs and legs, two revolute joints in between legs and feet, one prismatic joint in between pelvis and upper part, two spherical joints in between upper part and arms, two revolute joints with transverse axes in between arms and forearms. Spring and damper elements used in the model are as follows: the first one is translational to represent the stiffness of torso in between pelvis and the upper part and the second to reproduce the muscular elasticity of the elbow, and a rotational spring-damper elements is used in between arm and forearm. This human model needs to fix in car environment. For the car environment, seat, pedal and steering wheel contact are simulated by nonlinear spring damper elements. These elements are selected from the results of compression test on cushions. And with the help of four very stiff springs, the contact between hand steering wheel and feet platform are

simulated. For controlling of this model an anthropometrical database was used which automatically adjust geometry, mass properties and spring locations by changing only weight percentile and height percentile. It is also possible to modify the backrest inclination.

Ippili et al. (2008) developed a nonlinear integro-differential planer multi-degree model of seat occupant system as shown in Fig. 14. This model was modified from Kim and Yoon's model (Kim et al., 2005). Human body was modeled by three interconnected rigid bodies as shown in Figure 1.12. Each AB, BC and CD represents torso, femur and shin of human body respectively. In this model, head is not modeled. These three links has center of mass at G_1, G_2 and G_3. In this structure, point B represents hip joint. Four sets of nonlinear viscoelastic springs-damper sets were used to model seat foam. First two represents the back support part of seat. They are represented by k_1, C_1 for upper back and k_2, C_2 for lower back. These sets were assumed to be attached to human body and constrained to remain perpendicular with human body. The seating part of cushion of seat was represented by springs-damper sets k_3, C_3 and k_4, C_4. Constrained Lagrangian formulation was used to derive equation of motion. This model was used to determine static equilibrium position of seated occupant.

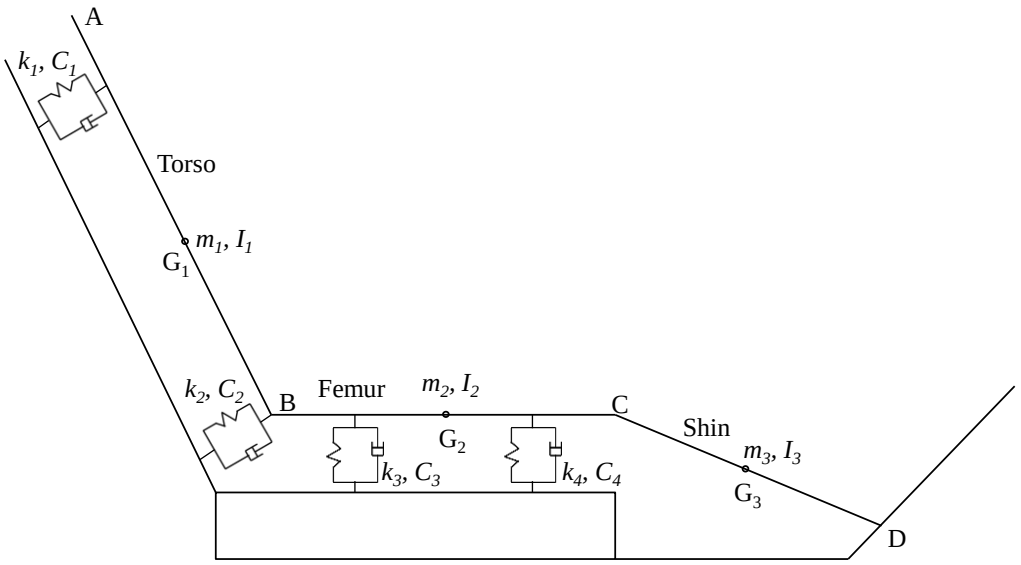

Figure 1.12 Ippili's nonlinear MB model

Cho and Yoon (2001) developed a two-dimensional model to study vehicle ride comfort. This is a nine-DOF model having total mass of 56.8 kg. As shown is Figure 1.13, this model is made from 3 rigid segments in which each segment representing a group of body parts. The lower body (m_1) represents sacrum and legs, the upper body parts (m_2) represents trunk plus the arms and last mass (m_3) represents head of human body. These elements are interconnected by bushing elements to represent properties of vertebral column. The vertical and horizontal springs and dampers between two masses are used to characterize both the deformable properties of the pelvis and thighs and the contacting properties of the back with a rigid seat. To exactly simulate car environment, three vertical and horizontal spring-damper units representing the mechanical properties of seat and backrest cushions are connected in series. For this model, the foot support is ignored by assuming the vibration input through foot is small.

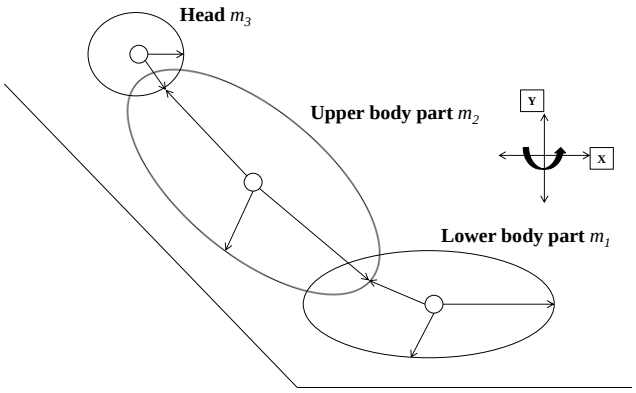

Figure 1.13 Cho and Yoon's nine-DOF model

Kim and Yoon (2005) worked on the development of a biomechanical model of human body which can be used to analyze human body's response to the vertical vibration. According to them, the apparent mass and the seat to head transmissibility are related with human body response and the comfort feeling. They worked on developing an appropriate structure of human body in seated position based on results of apparent mass and head transmissibility. Based on the experiments on human subjects, they proposed different models and best model is finalized. They used seat to head transmissibility and apparent mass doe analyzing human body response. They made eight human mechanical models based on different body structure. For each model, the seat to head transmissibility's and apparent masses are measured. These results of eight different models are compared with recorded results of five subjects and best human body structure is proposed. Human body parameters are finalized based on literature and parameter search using dynamic analysis and genetic optimization. Proposed human body model is having 5 mass elements each representing legs with feet, pelvis, torso, head and viscera of the human body. The body masses are interconnected by bushing elements which consists sets of linear translational and rotational spring damper. This bushing element represents body joints which are allowed to move in horizontal, vertical and rotational direction. This shows that the human model is a multibody model in a seated position with feet support is included in this

model. This model does not consider any backrest support. Therefore this model is limited to analysis with an erect sitting posture without backrest support.

Liang and Chiang (2008) proposed a multibody model to study the biodynamic response for different postures along with and without backrest support. They considered three cases. One without backrest support and other two are with backrest support with 12º and 21º as backrest angles. Their main intension of study was the effect of back support on the response of human body. They studied two MB models, one proposed by Cho and Yoon (2001) having 9-DOFs and other proposed by Kim and Yoon (2005) having fourteen DOFs. These models were modified so as to best fitted to results from experiments of seated human body in various automobile postures. The proposed biodynamic is shown in the Figure 1.14. This model in a seated position and human body response is assessed in terms of STH transmissibility, DPM impedance and AP mass. They showed that the back support condition and the body mass affect the results of apparent mass and overall response of human body. This study also showed that minimum vibration get transferred with a seat having backrest support at angle 21º in comparison with no backrest support and with 12º backrest support.

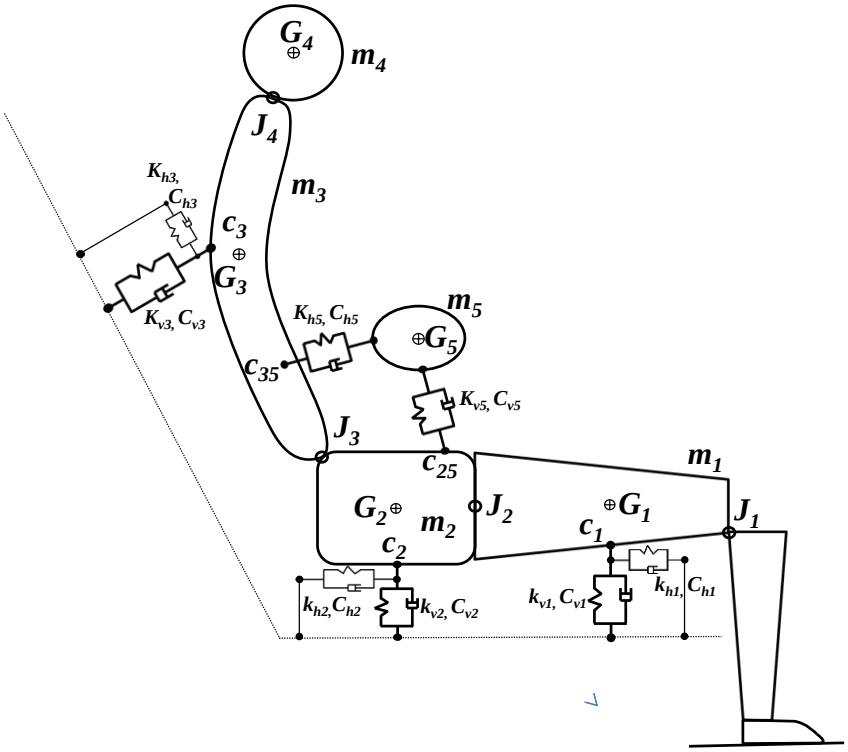

Figure 1.14 Liang and Chiang's fourteen-DOF model

1.10 Experimental methods of assessing ride comfort

For minimizing the discomfort, first it needs to be measured directly or indirectly. The vibration intensity is measured by the amplitude ratio, acceleration level, relative amplitude between adjacent body parts and vehicle pitch. Conventionally vehicle ride performance is measured using experimental approach. Now in this modern era of technology, other methods like simulation and dummy testing are used for this purpose. Human body is a dynamic system whose mechanical properties vary from moment to moment and from one organ to other. And also there is variation in the individual sensitivity to vibration. Therefore the most difficult problem of all ride comfort studies is considered to be the actual human subject who is seated in a vehicle. This is because of the human body's variability, adaptability, sensitivity and absence of a fixed scale of values render study in the simpler engineering senses is difficult. Hence it is very difficult to determine the ride comfort.

The exact value of ride comfort is difficult to determine because it depends on various factors such as vibration amplitude, frequency, direction, posture, input position etc. But various researchers attempted to define the ride comfort. They are summarized as following (El-Gindy et al., 2001):

- ***Ride measurement in vehicles***

  In this method, the occupants are travelled on a road in real vehicle environment and their responses such as 'unpleasant' or 'intolerable' are recorded. Then these results are studied for that specific test location. This method considers random inputs which characterize the actual road regularities. Other methods like shake table and ride simulator test uses sinusoidal inputs which may result in simplifying the problem but the results are somewhat unrealistic. Thus ride measurement method is more efficient. At the same time its drawback is that this method is more based on judgment of jury results in assessment may vary from one jury to other.

- ***Ride simulator test***

  In this method, the actual vehicle body is mounted on the hydraulic actuators which is resembles vehicle motion with pitch, roll and bounce. An analog computer is used for simulation of vehicle suspension system. In analog computers, the actual road inputs are feed using recorded analog signals. This helps in changing suspension system parameters very easily (Deusen, 1967). Using this apparatus with well-trained jury, it is possible to obtain subjective impression of vibrations. However, this method also fails in establishing meaningful objective measure. The advantage of this method is that it reproduces vehicle vibration in three dimensions. Ride simulator test is accurate one, at the same time it is very expensive.

- ***Shaker table test***

  This test is done in laboratory not on road conditions. In shaker table test with the help of hydraulic actuators, the sinusoidal forces inputs are generated and displacements (amplitude, velocity) are measured. As shaker table test uses sinusoidal input, it does not produce real vibration. Also it considers only vertical vibration and not longitudinal and lateral vibration.

- ***Subjective ride measurement***

  This is a traditional technique used for comparing ride quality of vehicles on given road section with well-trained ride jury. A well-designed evaluation scheme having 10 point rating is used for determination. According to this rating, vehicle test having minimum 5 (midpoint) is acceptable level. This method gives a meaningful comparison of ride quality of different vehicles but this difference cannot be quantitatively determined. Thus for an individual vehicle, this rating is meaningless. The accuracy of this experiment depends on set of experiment and jury. Therefore it can be increased by well-designed experiments and a large enough jury.

1.11 Thesis overview

This thesis is organized into six chapters. As seen, the first Chapter introduces research objective and summarizes compressive literature review of human biodynamic models. Chapter 2 will present details about selected human biodynamic model and seat models. After that equations of motion are derived for the human body model with seat model. In Chapter 3, expressions for transfer function are derived and transmissibility plots are obtained for three types of seat models and results are compared. Chapter 4 derives expressions for the unweighted and weighted absorbed power for three types of seat models with human model. The absorbed power is calculated and human body fatigue is predicted based on it. In Chapter 5, seat dynamic parameters are optimized to minimize fatigue. At the end in Chapter 6, the conclusion and future work is summarized.

CHAPTER 2

HUMAN BIODYNAMIC MODEL AND SEAT MODEL

2.1 Introduction

In this chapter, one human biodynamic model from the literature is explained in detail. Then three types of seat models are explained. Based on Newtonian method, the equations of motion are derived for coupled system of human model with seat model.

A valid human biodynamic model is very useful for studying the human body response to whole body vibration. In literature various models were proposed which are essential for studying behavior of human body subjected to certain excitations. In literature, three types of biodynamic models were proposed. They are lumped parameter models, finite elements models and multibody models. The multibody dynamic models have various advantages like it can be used to predict body response in different directions like horizontal, vertical and rotational directions. They accurately represent human body postures in 2-D or 3-D. Therefore, in this research one multibody human model is used and it is coupled with three types of seats. For this coupled system, equations of motion are derived and presented.

2.2 Human model development

Kim and Yoon (2005) reported a biomechanical model of human body which can be used to analyze human body's response to the vertical vibration. The apparent mass and the seat to head transmissibility are related with human body response and the comfort feeling. Kim and Yoon (2005) performed experiment on human subjects and the results were compared on different proposed models and finally developed an appropriate structure of human body in seated position based on results of apparent mass and head transmissibility. . Five subjects were collected to perform the excitation experiments. They were exposed to random vibration of 1 m/s^2 rms acceleration in the vertical direction within the frequency range of 1 Hz to 50 Hz. These subjects were asked to sit in a normal posture, keeping their body in upright comfortable position. The feet were

rested on the foot-plate and the hands were put on lap. Based on experimental data (seat to head transmissibility and apparent mass of each subject), eight human mechanical models were proposed based on different body structure. These eight models had different body structure including different torso structure, different pelvis-thigh structure. For each model, the seat to head transmissibility's and apparent masses were calculated. These results of eight different models were compared with experimental data from the five subjects and a best human body structure was proposed. Human body parameters were finalized based on literature and parameter search using dynamic analysis and genetic optimization. The human model had 5 mass elements each representing legs with feet, pelvis, torso, head and viscera of the human body. The body masses were interconnected by bushing elements which consists sets of linear translational and rotational spring damper. This bushing element represented body joints which are allowed to move in horizontal, vertical and rotational direction. So this human model is a multibody model in a seated position where the feet support was included in this model. However, this model did not consider any backrest support. Therefore, it limited to analysis with an erect sitting posture without backrest support. Based on the comparison results, this developed model showed about 1% least square error in apparent mass and head transmissibility.

Liang and Chiang (2008) stated that for studying human body response in seated position to the vibrations, the model should be at least two-dimensional in the sagittal plane. Liang and Chiang selected two models from literature, one proposed by Kim and Yoon (2005) and other developed by Cho and Yoon (2001). Cho and Yoon's model is 9-DOF model with backrest support and it does not consider feet support. Model developed by Kim and Yoon is 14-DOF and considers feet support but it does not consider seat backrest support. So certain modification needs to be done to match the model with actual vehicle seating environment. So Kim's model was modified and backrest support was included as in Cho's model. This modified model measured with the seat to head transmissibility, driving point mechanical impedance, and apparent mass for following three automotive postures:

1. Model without backrest support.
2. Model with backrest support with backrest an angle 21º.
3. Model with backrest support with backrest an angle 12º.

They did experiments on actual human subjects with these three automotive postures. For validation purpose these experimental results were compared with simulation results obtained from the modified model. They found that human model by considering backrest support at an angle 21º gives better results as compared with other two models. Because the reason is that backrest support in automotive seating environment works on maintaining sitting posture and decreasing muscle tension in human torso. This proposed model was analyzed and validated in terms of seat to head transmissibility, driving point mechanical impedance and apparent mass with similar model published in literature. Therefore, this proposed model by Liang and Chiang can be recommended for studying human body response exposed to the vertical vibrations in seated position.

2.3 Human biodynamic model and its properties

In this study, a model proposed by Liang and Chiang (2008) is adapted for analyzing human body response. This is a linear 14-DOF model in the 2D sagittal plane. Note that this human body model was originally derived from experimental measurements from the hip contact point to head vertical transmissibility and apparent mass. The calculated responses using this model for Body 2 to 5 are more reliable than those for Body 1. This model is shown in Figure 2.1.

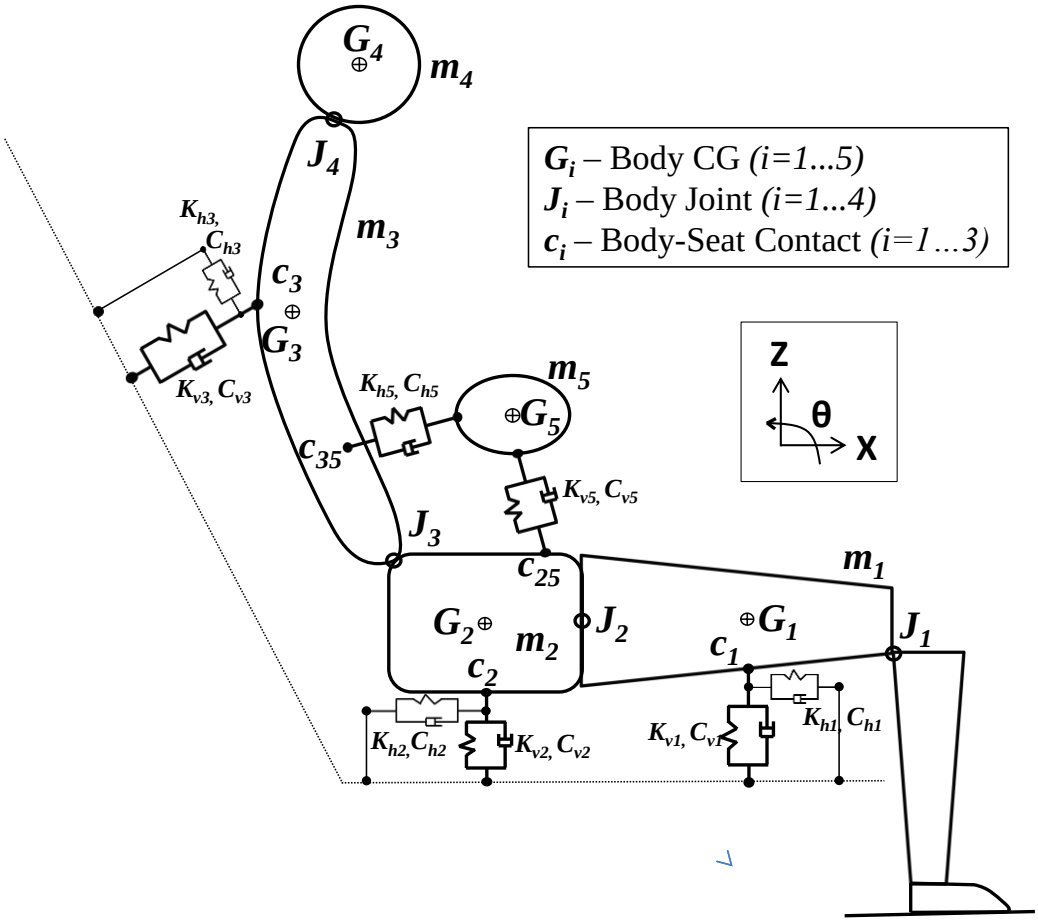

Figure 2.1 Human biodynamic model

β is the angle made by force line of K_{v5}, C_{v5} with respect to the horizontal as shown in Figure 2.2.

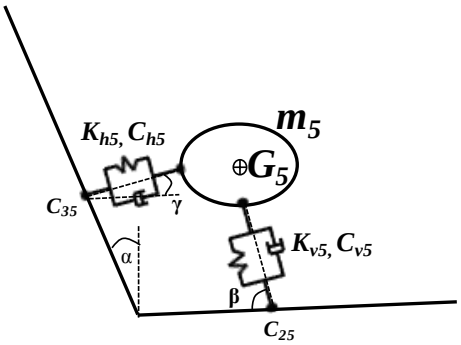

Figure 2.2 Angle made by Body 5

As shown in this figure, the human body model has 5 body elements. Mass m_1 represents the thighs with legs and feet, mass m_2 represents the pelvis, mass m_3 represents the torso, mass m_4 represents the head, and mass m_5 represents viscera of the human body. Mass and inertial properties and different center of gravity locations are summarized in Table 2.1. Points marked as G_i (i=1 to 5) are the center of gravity points of each mass. This human body model is in a seated position in which the body is in contact with the seat, and the feet are supported on the floor. The feet are supported on a vibrating vehicle floor and the vibration input thorough the feet needs to be considered. So this model considers feet support in calculation. Because a considerable amount of vibrations are transferred through the backrest support, this model considers it at a 21º angle with the vertical plane. As shown in the figure, α is the backrest support angle. So, this model considers vibrations transferred through seat, the backrest support, and the feet and this human model is clearly analogous with actual vehicle driving environment. The coordinates of each body and its important points are defined as the contact situation between the human body and the inclined backrest support at a 21º angle with the vertical plane. According to this angle and sitting position, coordinates of important points are obtained and are summarized in Table 2.1.

Each mass (from m_1 to m_4), except the mass of the viscera (m_5), has 2 translational motions (one horizontal and one vertical) and 1 rotational motion, and the mass of the viscera (m_5) has only 2 translational motions. All masses except mass m_5 are connected to each other by bushing elements. J_i (i=1 to 4) are the locations of these bushing elements representing joints in between two respective bodies. The bushing elements are represented by translational and torsional sets of springs (K_i, K_{ri}) and dampers (C_i, C_{ri}). The mass of the viscera (m_5) is connected by a horizontal and vertical translational set of springs and dampers as shown in Figure 2.1. The mass of the viscera (m_5) is tilted at an angle β with the horizontal, as shown in Figure 2.2, due to an inclined backrest. Horizontal and vertical spring and damper (K_{h5}, C_{h5} and K_{v5}, C_{h5}) are also inclined. In Figure 2.1, the contact between the seat and each body is represented by one point in each body c_i (i=1 to 3) to simplify the force calculations where c_1, and c_2 are the contact points

of Body 1 and 2 with the seat cushion, and c_3 is the contact point of Body 3 with the backrest cushion. The horizontal (K_{hi}, C_{hi}) and vertical (K_{vi}, C_{vi}) spring and damper under each mass represent the stiffness or flexibility of that respective mass. For example, the horizontal (K_{h1}, C_{h1}) and vertical (K_{v1}, C_{v1}) spring and damper represent the stiffness or flexibility of Body 1 (m_1). For Body 2 (m_2), its flexibility is represented by horizontal (K_{h2}, C_{h2}) and vertical (K_{v2}, C_{v2}) spring and damper. For Body 3 (m_3), the stiffness perpendicular to the Body 3 is marked as vertical spring and damper (K_{v3}, C_{v3}) and stiffness parallel to the Body 3 is marked as horizontal spring and damper (K_{h3}, C_{h3}). Values for all these parameters are selected from literature (Liang et al., 2008; Kim et al., 2005) and summarized in Table 2.2.

Table 2.1 Human body mass, inertial properties and geometry parameters

Body Properties				Body Locations (x, z), (mm) with 21° backrest support		
Body	Mass (Kg)	Body	Inertia ($Kg.m^2$)	C.G. location	Joint Location	Seat Contact
m_1	20.3	I_1	1.16	G_1 (133, 70)	J_1 (329, 52)	c_1 (133,0)
m_2	11	I_2	0.68	G_2 (-23, 97)	J_2 (-17, 84)	c_2 (-19,0)
m_3	19.87	I_3	1.53	G_3 (-152.3, 471.6)	J_3 (-84, 139)	c_3 (-147.3,379.3)
m_4	7.25	I_4	0.402	G_4 (-161.5, 720.9)	J_4 (-187.6, 620.9)	-
m_5	12.9	-	-	G_5 (-65.9, 250.9)	-	-

Table 2.2 Biomechanical properties of human body model

Spring Stiffness	Notations	Value	Damping Coefficient	Notations	Value
Horizontal stiffness of Body 1	K_{h1}	614	Horizontal damping of Body 1	C_{h1}	14
Vertical stiffness of Body 1	K_{v1}	16710	Vertical damping of Body 1	C_{v1}	8010
Horizontal stiffness of Body 2	K_{h2}	905	Horizontal damping of Body 2	C_{h2}	15
Vertical stiffness of Body 2	K_{v2}	121300	Vertical damping of Body 2	C_{v2}	47
Horizontal stiffness of Body 3	K_{h3}	17200	Horizontal damping of Body 3	C_{h3}	334.5
Vertical stiffness of Body 3	K_{v3}	2300	Vertical damping of Body 3	C_{v3}	154
Horizontal stiffness of Body 5	K_{h5}	1930	Horizontal damping of Body 5	C_{h5}	79
Vertical stiffness of Body 5	K_{v5}	18370	Vertical damping of Body 5	C_{v5}	197
Translational stiffness of Joint 1	K_1	23550	Translational damping of Joint 1	C_1	154
Translational stiffness of Joint 2	K_2	6400	Translational damping of Joint 2	C_2	61
Translational stiffness of Joint 3	K_3	299	Translational damping of Joint 3	C_3	1790
Translational stiffness of Joint 4	K_4	113700	Translational damping of Joint 4	C_4	66
Rotational stiffness of Joint 1	K_{r1}	220	Rotational damping of Joint 1	C_{r1}	104

Table 2.2 Continued

Spring Stiffness	Notations	Value	Damping Coefficient	Notations	Value
Rotational stiffness of Joint 2	K_{r2}	162	Rotational damping of Joint 2	C_{r2}	30
Rotational stiffness of Joint 3	K_{r3}	328	Rotational damping of Joint 3	C_{r3}	724
Rotational stiffness of Joint 4	K_{r4}	915	Rotational damping of Joint 4	C_{r4}	340
Units : Translational stiffness : N/m, Translational damping : N-s/m, Rotational stiffness : N-m/rad, Rotational damping : N-ms/rad					

2.4 Vehicle seats models

A vehicle travelling on roads vibrates due to road irregularities. These vibrations are transferred to the vehicle chassis through the tires. From the chassis, these vibrations are transferred to the vehicle body parts, including the seat. As the human body is in direct contact with the seat cushion, it is very important that the seat should provide a good vibration isolator so that a minimum amount of vibrations can be transferred to the human body. So the seat design is very crucial part in the process of vehicle design. The vibration isolation property of the seat and the cushion depends on its dynamic properties (Griffin, 1978; Kolich, 2003). Two important dynamic properties of seat design are the stiffness and mass of the seat suspension and seat cushion. The mass of the seat with cushion and suspension plays a very important role in vibration isolation. Increasing the mass will result in decreasing the absorbed power, which finally results in decreasing vibration transmission (Amirouche et al., 1997). But it is less effective compared to the reduction in absorbed power by changing the stiffness of the cushion and suspension, and in practice, there is limitation on increasing the mass of the seat. Mechanical properties of the seat cushion and suspension can vary by the changing cushion material and seat suspension linkages (Kolich, 2003). Therefore, the human body responses will be different for seats with different seat properties (Amirouche et al., 1997). So, it is

interesting to study the effect of changing seat parameters on the human body's response. In this research, three types of seat models are considered. The first seat model is with neither cushion nor seat suspension is called as a hard seat. Because there is nothing to isolate the human body from vibrations, all vibrations are directly transferred to the human body. This seat model coupled with a human body model is represented in Figure 2.3. The second type of seat model has only a cushion but no seat suspension. In this type of seat, some vibrations are isolated because of cushion stiffness. The seat model with the human body model is shown in Figure 2.4. The third seat model has both cushions and seat suspension and is called the isolated seat. This is a better seat design because maximum vibrations are isolated from the environment due to stiffness of both the seat suspension and cushion. This seat model coupled with the human body is represented in Figure 2.5.

Three different seat models with the human model are described in the following sections.

2.4.1 Case 1 - Hard seat model

In hard seat, both the seat suspension and cushion are neglected as shown in Figure 2.3. It's similar to the human body kept on only seat frame.

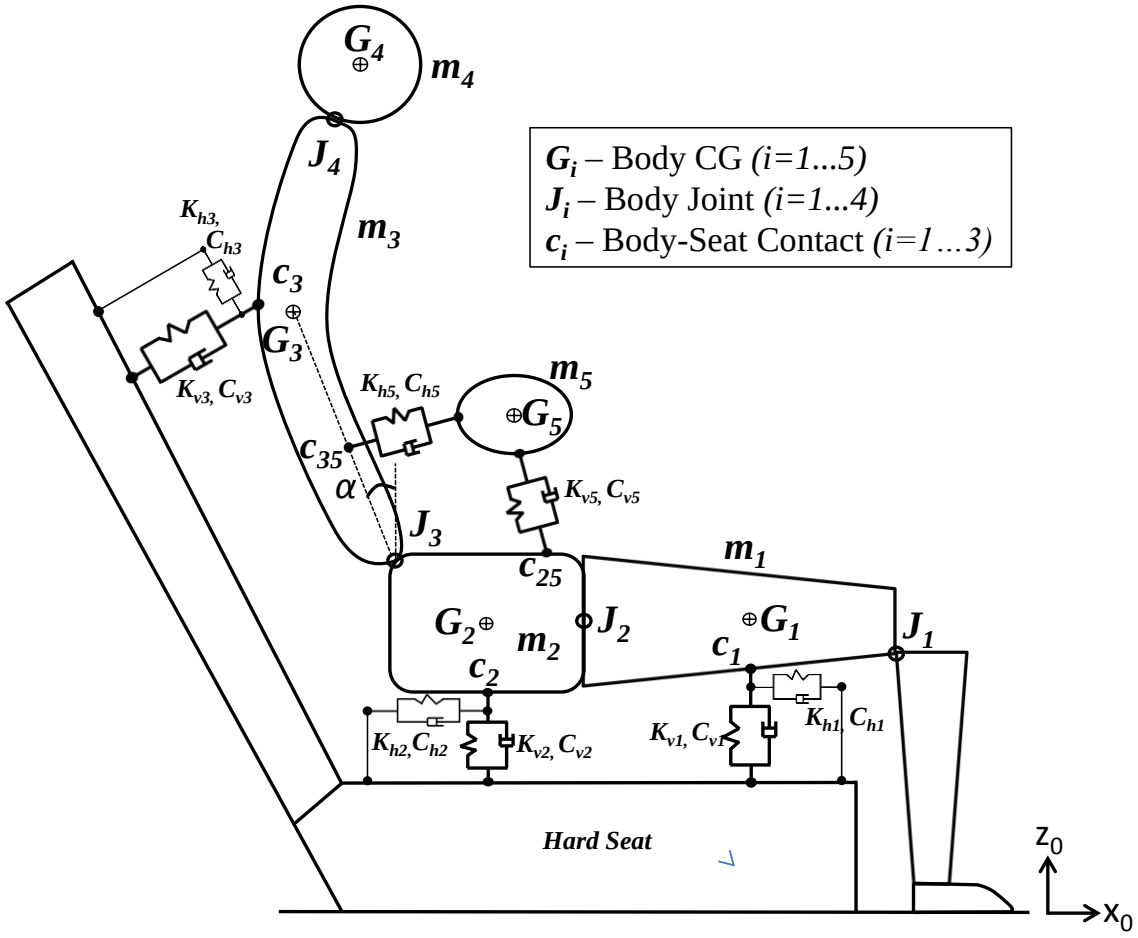

Figure 2.3 Seat model for Case 1 – Hard Seat

There is nothing to isolate the human body from vibrations in this seat. So, all the vibrations are directly transferred to the human body. As the seat directly receives inputs from the floor, the system (human model coupled with seat model) has a total of 14 DOFs. So this coupled system of human body with seat model has 14 equations of motion

2.4.2 Case 2 - Seat model with cushion but no seat suspension

A 14-DOF human model is seated on a seat model with a seat cushion and backrest cushion but without seat suspension in Figure 2.4.

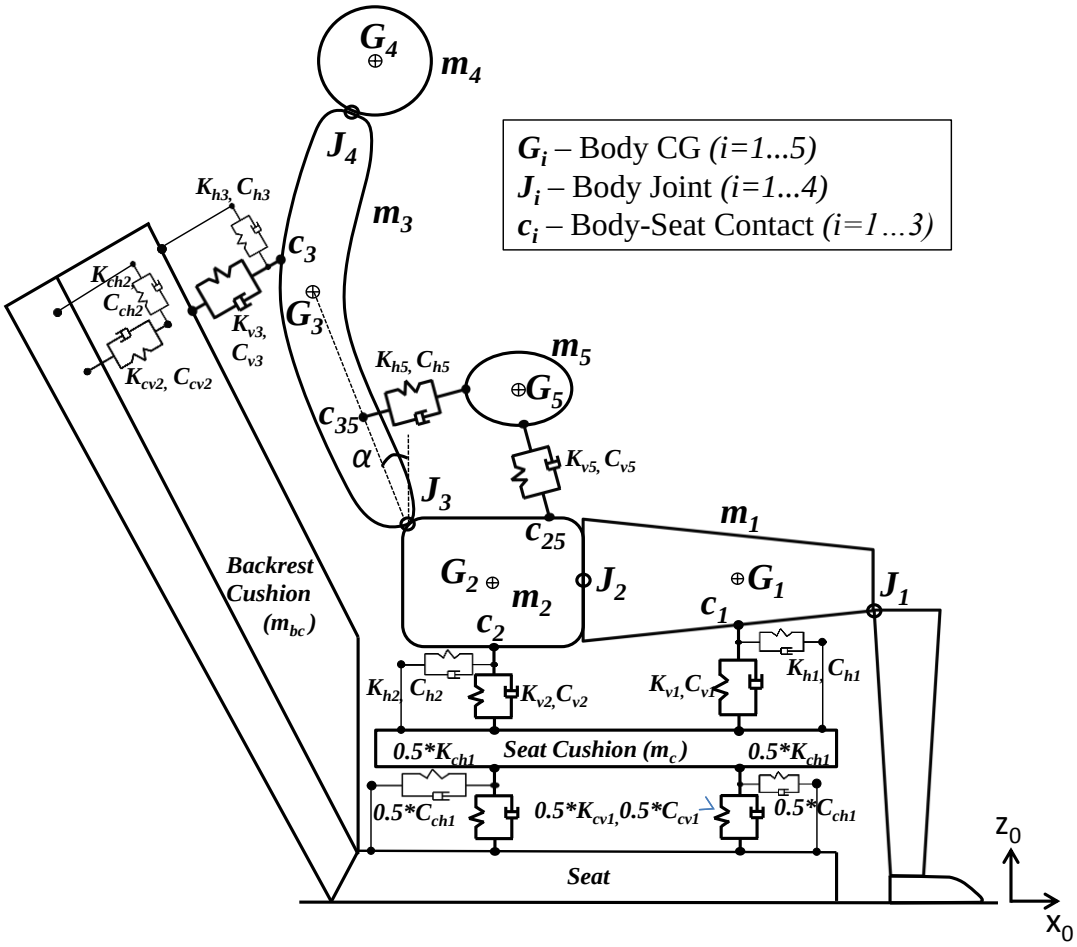

Figure 2.4 Seat model with cushion but no seat suspension – Case 2

With this seat, some vibrations are isolated as an effect of cushion stiffness. In Figure 2.4, m_c is the mass of the seat cushion, and m_{bc} is the mass of the backrest cushion. Each cushion has its own stiffness, which is highly nonlinear in its characteristics (Griffin, 1978; Leenslag et al., 1997; Griffin, 1990; Guman and Vertiz, 1997; Zhang and Yu; 2010). However, for simplicity, they are considered as linear in this study. K_{ch1} and C_{ch1} represent the horizontal stiffness, and K_{cv1} and C_{cv1} represent the vertical stiffness of the seat cushion. Similarly, K_{ch2} and K_{ch2} represent horizontal stiffness, and K_{cv2} and C_{cv2} represent the vertical stiffness of the backrest cushion. Its values are summarized in Table 2.3. Each cushion has one horizontal motion and one vertical motion with respect to its contact surface. Overall, the system for Case 2 has 18 DOFs. So this coupled system of human model with seat model will have 18 equations of motion.

2.4.3 Case 3 - Seat model with both cushion and seat suspension (Isolated Seat)

A 14-DOF model is placed on a seat model with a seat cushion, backrest cushion and seat suspension as shown in Figure 2.5.

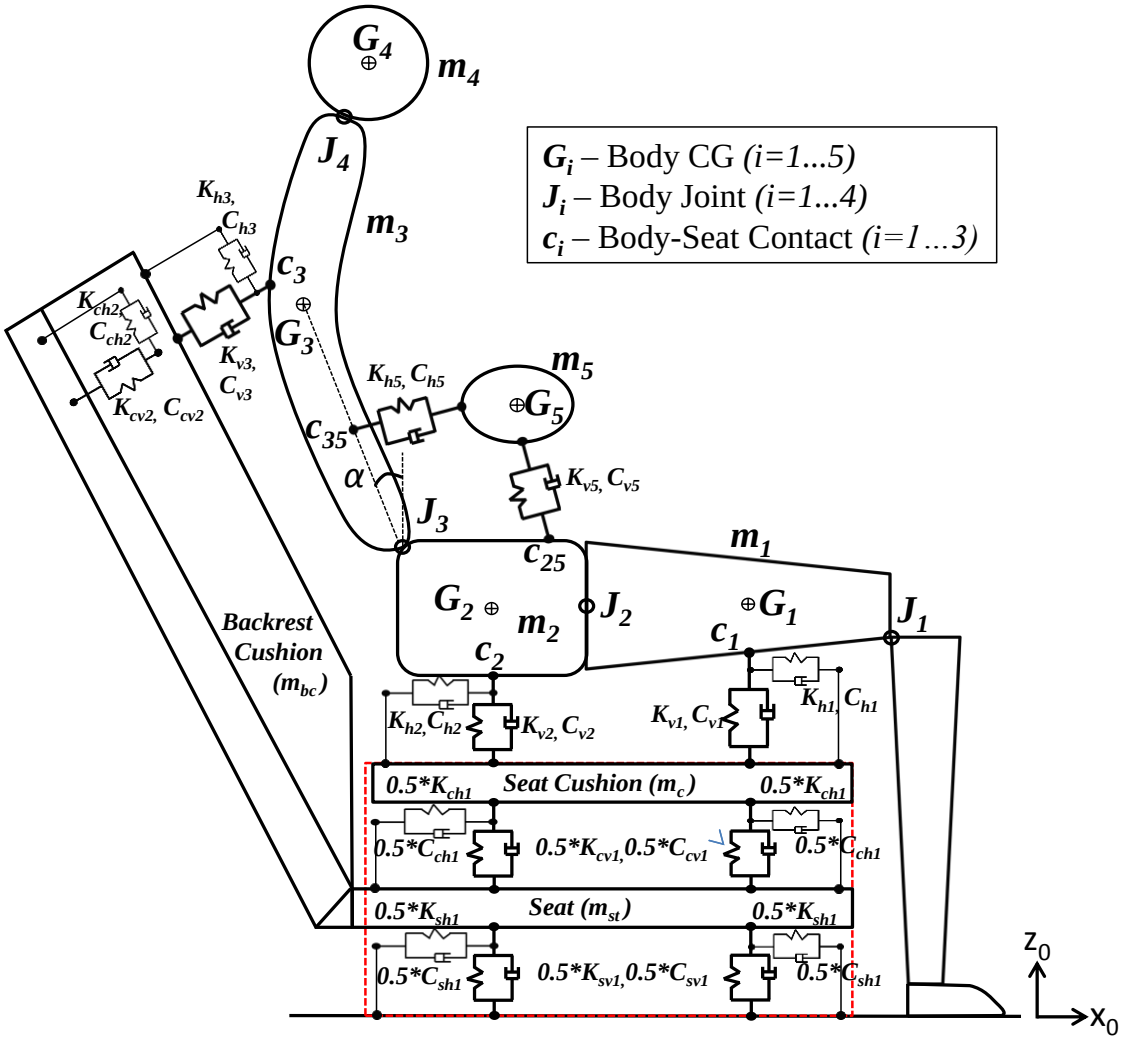

Figure 2.5 Seat model for Case 3 - Isolated Seat

In this figure, m_{st} is the mass of the seat. The seat is connected to the vehicle body floor using some linkages, which act as seat suspension. K_{sh1} and C_{sh1} represent horizontal stiffness, and K_{sv1} and C_{sv1} represent the vertical stiffness of the seat suspension. This seat has one horizontal and one vertical motion for which it receives input from a vehicle body floor. Along with this suspension, this model is having seat cushion (m_c) and backrest cushion (m_{bc}) similar to Case 2. The values of all parameters of seat suspension and cushion are summarized in Table 2.3. So, by considering 2 DOFs of the seat, 2 DOFs of the each cushion, and 14 DOFs of the human model, the total DOF of the system is 20.

So this coupled system of human model with isolated seat model is having 20 equations of motion.

Table 2.3 Seat and cushion material properties

Vehicle Seat Properties (For Case 2 and Case 3)					
Seat Components	Mass	Horizontal Stiffness	Horizontal Damping	Vertical Stiffness	Vertical Damping
Units	(Kg)	(N/m)	(N-s/m)	(N/m)	(N-s/m)
Seat	m_{st} = 4	K_{sh1} = 80000	C_{sh1} = 8000	K_{sv1} = 8000	C_{sv1} = 800
Seat Cushion	m_c = 3	K_{ch1} = 40000	C_{ch1} = 1600	K_{cv1} = 20000	C_{cv1} = 800
Backrest Cushion	m_{ci} = 3	K_{ch2} = 20000	C_{ch2} = 1500	K_{cv2} = 10000	C_{cv2} = 1000

2.5 Equations of motion

As explained in the last section, Case 1 is having 14 equations of motion, Case 2 is having 18 equations of motion and Case 3 is having 20 equations of motion. Here, the equations of motion are explained for the third case only, which is the most complicated. For other cases, the equations of motion can be derived similarly (Kumbhar et al., 2013). A Newtonian method is used to derive the equations of motion.

Define the horizontal direction as the X-direction and the vertical direction as the Z-direction as shown in Figure 2.1. So, each human body mass (from m_1 to m_4), except the mass of the viscera (m_5) has 3 displacements, including 1 rotational displacement. The mass of the viscera (m_5) has 2 translational displacements. These respective absolute displacements are shown together in vector format in equation 2.1.

$$\begin{aligned}
\mathbf{r_1} &= \begin{bmatrix} x_1, & z_1, & \theta_1 \end{bmatrix}^T \\
\mathbf{r_2} &= \begin{bmatrix} x_2, & z_2, & \theta_2 \end{bmatrix}^T \\
\mathbf{r_3} &= \begin{bmatrix} x_3, & z_3, & \theta_3 \end{bmatrix}^T \\
\mathbf{r_4} &= \begin{bmatrix} x_4, & z_4, & \theta_4 \end{bmatrix}^T \\
\mathbf{r_5} &= \begin{bmatrix} x_5, & z_5 \end{bmatrix}^T
\end{aligned} \tag{2.1}$$

Also, the seat ($\mathbf{r_{st}}$), seat cushion ($\mathbf{r_c}$) and backrest cushion ($\mathbf{r_{bc}}$) have two translational displacements in the X and Z-direction, respectively. These are represented in equation 2.2.

$$\begin{aligned}
\mathbf{r_{st}} &= \begin{bmatrix} x_{st}, & z_{st} \end{bmatrix}^T \\
\mathbf{r_c} &= \begin{bmatrix} x_c, & z_c \end{bmatrix}^T \\
\mathbf{r_{bc}} &= \begin{bmatrix} x_{bc}, & z_{bc} \end{bmatrix}^T
\end{aligned} \tag{2.2}$$

This combined system is on a vibrating floor (which is the same as the vehicle floor) with the input displacements ($\mathbf{r_0}$) as shown in equation 2.3.

$$\mathbf{r_0} = \begin{bmatrix} x_0, & z_0 \end{bmatrix}^T \tag{2.3}$$

As each body mass has a rotational motion, displacement at different points in the body is different and depends on the value of the rotational displacement, its position with respect to body's CG location, and the body's linear displacement. Therefore, it is necessary to calculate the actual displacement considering the angle of rotation. For example, in Body 1 at contact point c_1, the following are the actual displacements in X and Z directions.

$$\begin{aligned}
x_{c1} &= x_1 - (c_{1z} - G_{1z}).\theta_1 \\
z_{c1} &= z_1 + (c_{1x} - G_{1x}).\theta_1
\end{aligned}$$

Where,

x_{c1} *and* z_{c1} – Actual displacements of point c_1 in X and Z direction

x_1, z_1, θ_1 – Displacements of Body 1

(c_{1x}, c_{1z}) – Coordinates of Point c_1

(G_{1x}, G_{1z}) – Coordinates of C.G. Point G_1

Similarly, the absolute displacements are calculated at important points such as joint locations, contact locations in all body parts. For representation purpose, the actual displacement of a point in the body is represented by a subscript as that point's name after variable name. For example, x_{c1} represents the actual displacement of point c_1 of Body 1 in the X-direction. For the joint's actual displacements, two subscripts like J_{ik} are used. Where the first subscript represents the body number and the second subscript represents the joint number. For example, x_{J11} represents the actual displacement of Joint 1 in Body 1 in the X-direction. Similarly, z_{J21} represents the actual displacement of Joint 1 in Body 2 in the Z-direction.

Now equations of motions are derived for Case 3 using Newtonian method. Following are the equations of motion for all bodies including the seat and cushion.

The seat mass m_{st} gets input vibrations from vehicle body and it is allowed to move in horizontal and vertical direction. So equations of motion of seat mass are expressed in equation 2.4 and 2.5.

$$m_{st}\ddot{x}_{st} = K_{ch1}(x_c - x_{st}) + C_{ch1}(\dot{x}_c - \dot{x}_{st}) - K_{sh1}(x_{st} - x_0) - C_{sh1}(\dot{x}_{st} - \dot{x}_0) \qquad (2.4)$$

$$m_{st}\ddot{z}_{st} = K_{cv1}(z_c - z_{st}) + C_{cv1}(\dot{z}_c - \dot{z}_{st}) - K_{sv1}(z_{st} - z_0) - C_{sv1}(\dot{z}_{st} - \dot{z}_0) \qquad (2.5)$$

The mass of seat cushion m_c is also allowed to move in X and Z direction. Its equations of motion are expressed in equation 2.6 and 2.7.

$$m_c\ddot{x}_c = K_{h1}(x_{c1}-x_c)+C_{h1}(\dot{x}_{c1}-\dot{x}_c)+K_{h2}(x_{c2}-x_c)+C_{h2}(\dot{x}_{c2}-\dot{x}_c) \\ -K_{ch1}(x_c-x_{st})-C_{ch1}(\dot{x}_c-\dot{x}_{st}) \tag{2.6}$$

$$m_c\ddot{z}_c = K_{v1}(z_{c1}-z_c)+C_{v1}(\dot{z}_{c1}-\dot{z}_c)+K_{v2}(z_{c2}-z_c)+C_{v2}(\dot{z}_{c2}-\dot{z}_c) \\ -K_{cv1}(z_c-z_{st})-C_{cv1}(\dot{z}_c-\dot{z}_{st}) \tag{2.7}$$

The mass of seat backrest cushion m_{bc} is also allowed to move in X and Z direction. Its equations of motion are derived by considering seat backrest angle α and can be represented in equation 2.8 and 2.9.

$$m_{bc}\ddot{x}_{bc} = f_{c3x} - f_{bcx} \tag{2.8}$$

$$m_{bc}\ddot{z}_{bc} = f_{c3z} - f_{bcz} \tag{2.9}$$

Where,

$$\begin{pmatrix} f_{bcx} \\ f_{bcz} \end{pmatrix} = \begin{pmatrix} \cos\alpha & -\sin\alpha \\ \sin\alpha & \cos\alpha \end{pmatrix} \begin{pmatrix} K_{cv2}\cos\alpha & K_{cv2}\sin\alpha \\ -K_{ch2}\sin\alpha & K_{ch2}\cos\alpha \end{pmatrix} \begin{pmatrix} (x_{bc}-x_{st}) \\ (z_{bc}-z_{st}) \end{pmatrix} \\ + \begin{pmatrix} \cos\alpha & -\sin\alpha \\ \sin\alpha & \cos\alpha \end{pmatrix} \begin{pmatrix} C_{cv2}\cos\alpha & C_{cv2}\sin\alpha \\ -C_{ch2}\sin\alpha & C_{ch2}\cos\alpha \end{pmatrix} \begin{pmatrix} (\dot{x}_{bc}-\dot{x}_{st}) \\ (\dot{z}_{bc}-\dot{z}_{st}) \end{pmatrix}$$

$$\begin{pmatrix} f_{c3x} \\ f_{c3z} \end{pmatrix} = \begin{pmatrix} \cos\alpha & -\sin\alpha \\ \sin\alpha & \cos\alpha \end{pmatrix} \begin{pmatrix} K_{v3}\cos\alpha & K_{v3}\sin\alpha \\ -K_{h3}\sin\alpha & K_{h3}\cos\alpha \end{pmatrix} \begin{pmatrix} (x_{c3}-x_{bc}) \\ (z_{c3}-z_{bc}) \end{pmatrix} \\ + \begin{pmatrix} \cos\alpha & -\sin\alpha \\ \sin\alpha & \cos\alpha \end{pmatrix} \begin{pmatrix} C_{v3}\cos\alpha & C_{v3}\sin\alpha \\ -C_{h3}\sin\alpha & C_{h3}\cos\alpha \end{pmatrix} \begin{pmatrix} (\dot{x}_{c3}-\dot{x}_{bc}) \\ (\dot{z}_{c3}-\dot{z}_{bc}) \end{pmatrix}$$

Where α is the seat backrest angle shown in Figure 2.2. In this study, we used a 21° backrest angle (Liang and Chiang, 2008).

For all the bodies except Body 5, the equations of motion are derived by considering its motion in horizontal, vertical and rotational direction. Equations of motion of Body 1 (Thigh, Legs with Feet) are represented in equation 2.10, 2.11 and 2.12.

$$m_1\ddot{x}_1 = -f_{1x} - f_{2x} - f_{c1x} \tag{2.10}$$

$$m_1\ddot{z}_1 = -f_{1z} - f_{2z} - f_{c1z} \tag{2.11}$$

$$I_1\ddot{\theta}_1 = -f_{1x}.l_{11v} - f_{1z}.l_{11h} - f_{c1x}.l_{1c1v} - f_{c1z}.l_{1c1h} + f_{2x}.l_{12v} + f_{2x}.l_{12h} - f_{r1} - f_{r2} \tag{2.12}$$

Where,

$l_{ijv,}\ l_{ijh} -$ Respective moment arm

$f_{1x} = K_1(x_{J11} - x_0) + C_1(\dot{x}_{J11} - \dot{x}_0)$

$f_{1z} = K_1(z_{J11} - z_0) + C_1(\dot{z}_{J11} - \dot{z}_0)$

$f_{2x} = K_2(x_{J12} - x_{J22}) + C_2(\dot{x}_{J12} - \dot{x}_{J22})$

$f_{2z} = K_2(z_{J12} - z_{J22}) + C_2(\dot{z}_{J12} - \dot{z}_{J22})$

$f_{c1x} = K_{h1}(x_{c1} - x_c) + C_{h1}(\dot{x}_{c1} - \dot{x}_c)$

$f_{c1z} = K_{v1}(z_{c1} - z_c) + C_{v1}(\dot{z}_{c1} - \dot{z}_c)$

$f_{r1} = K_{r1}.\theta_1 + C_{r1}.\dot{\theta}_1$

$f_{r2} = K_{r2}(\theta_1 - \theta_2) + C_{r2}(\dot{\theta}_1 - \dot{\theta}_2)$

Similarly equations of motion of Body 2 (Pelvis) are represented in equation 2.13, 2.14 and 2.15.

$$m_2\ddot{x}_2 = f_{2x} - f_{3x} - f_{c2x} - f_{5v}\cos\beta \tag{2.13}$$

$$m_2\ddot{z}_2 = f_{2z} - f_{3z} - f_{c2z} + f_{5z}\sin\beta \tag{2.14}$$

$$\begin{aligned} I_2\ddot{\theta}_2 = {} & f_{2x}.l_{22v} + f_{2z}.l_{22h} + f_{3x}.l_{23v} + f_{3z}.l_{23h} - f_{c2x}.l_{2c2v} - f_{c2z}.l_{2c2h} \\ & + f_{5v}.\cos\beta.l_{2c25v} - f_{5v}.\sin\beta.l_{2c25h} + f_{r2} - f_{r3} \end{aligned} \tag{2.15}$$

Where,

$f_{3x} = K_3(x_{J23} - x_{J33}) + C_3(\dot{x}_{J23} - \dot{x}_{J33})$

$f_{3z} = K_3(z_{J23} - z_{J33}) + C_3(\dot{z}_{J23} - \dot{z}_{J33})$

$f_{c2x} = K_{h2}(x_{c2} - x_c) + C_{h2}(\dot{x}_{c2} - \dot{x}_c)$

$f_{c2z} = K_{v2}(z_{c2} - z_c) + C_{v2}(\dot{z}_{c2} - \dot{z}_c)$

$f_{r3} = K_{r3}(\theta_2 - \theta_3) + C_{r3}(\dot{\theta}_2 - \dot{\theta}_3)$

$f_{5v} = K_{v5}((x_{c25} - x_5)\cos\beta + (z_5 - z_{c25})\sin\beta)$

$\quad + C_{v5}((\dot{x}_{c25} - \dot{x}_5)\cos\beta + (\dot{z}_5 - \dot{z}_{c25})\sin\beta)$

Equations of motion of Body 3 (Torso) are derived in similar way as equations of seat backrest support are derived. They are expressed in equation from 2.16 to 2.18.

$$m_3\ddot{x}_3 = f_{3x} - f_{4x} + f_{5x} - f_{c3x} + f_{5h}\cos\gamma \tag{2.16}$$

$$m_3\ddot{z}_3 = f_{3z} - f_{4z} - f_{c3z} + f_{5h}\sin\gamma \tag{2.17}$$

$$\begin{aligned} I_3\ddot{\theta}_3 = {} & f_{3x}.l_{33v} + f_{3z}.l_{33h} + f_{4x}.l_{34v} + f_{4z}.l_{34h} - f_{c3x}.l_{3c3v} \\ & - f_{c3z}.l_{3c3h} + f_{5h}\cos\gamma.l_{3c3v} + f_{5h}\sin\gamma.l_{3c35h} + f_{r3} - f_{r4} \end{aligned} \tag{2.18}$$

Where,

$$\begin{aligned} f_{4x} &= K_4(x_{J34} - x_{J44}) + C_4(\dot{x}_{J34} - \dot{x}_{J44}) \\ f_{4z} &= K_4(z_{J34} - z_{J44}) + C_4(\dot{z}_{J34} - \dot{z}_{J44}) \\ f_{r4} &= K_{r4}(\theta_3 - \theta_4) + C_{r4}(\dot{\theta}_3 - \dot{\theta}_4) \\ f_{5h} &= K_{h5}((x_5 - x_{c35})\cos\gamma + (z_5 - z_{c35})\sin\gamma) \\ &\quad + C_{h5}((\dot{x}_5 - \dot{x}_{c35})\cos\gamma + (\dot{z}_5 - \dot{z}_{c35})\sin\gamma) \end{aligned}$$

Where γ is the angle made by force line of K_{h5}, C_{h5} with respect to the horizontal as shown in Figure 2.2.

Equations of motion of Body 4 (Head) are derived in simple way and are expressed in equations from 2.19 to 2.21.

$$m_4\ddot{x}_4 = f_{4x} \tag{2.19}$$

$$m_4\ddot{z}_4 = f_{4z} \tag{2.20}$$

$$I_4\ddot{\theta}_4 = f_{4x}.l_{44v} - f_{4z}.l_{44h} + f_{r4} \tag{2.21}$$

As already told Body 5 (Viscera) is allowed to move in X and Z directions only, it is having only 2 equations of motion and are represented in equation 2.22 and 2.23.

$$m_5\ddot{x}_5 = f_{5v}\cos\beta - f_{5h}\cos\gamma \tag{2.22}$$

$$m_5\ddot{z}_5 = -f_{5v}\sin\beta - f_{5h}\sin\gamma \tag{2.23}$$

These are the 20 equations of motion for the system of isolated seat model with human body model (Case 3). For the other two cases, the equations of motion can be derived in the same manner. Now these equations are in following format shown in equation 2.24.

$$\mathbf{M\ddot{X} = F(X, \dot{X}, X_0)} \tag{2.24}$$

For evaluating the transfer function, we need separate mass, spring stiffness and damping coefficient matrices. Therefore, these equations are rearranged, and terms are separated.

Now these modified equations are in the format shown in equation 2.25.

$$\mathbf{M\ddot{X} + C\dot{X} + KX = f_c X_0} \tag{2.25}$$

Where,

$\mathbf{M}$ – Mass matrix $\left(\text{For Case 3, size-20x20}\right)$

$\mathbf{C}$ – Damping coefficient matrix $\left(\text{For Case 3, size-20x20}\right)$

$\mathbf{K}$ – Spring Stiffness matrix $\left(\text{For Case 3, size-20x20}\right)$

$\mathbf{f_c}$ – Input excitation coefficient matrix $\left(\text{For Case 3, size-20x4}\right)$

$\mathbf{\ddot{X}, \dot{X}, X}$ – Output acceleration, velocity and displacement vector of each body $\left(\text{For Case 3, size-20x1}\right)$

$\mathbf{X_0}$ – Vector of the input floor displacements and velocity $\left(\text{For Case 3, size-4x1}\right)$.

$$\mathbf{M} = \begin{bmatrix} m_{st} & 0 & \cdots & \cdots & \cdots & \cdots & 0 \\ 0 & m_{st} & \ddots & & & & \vdots \\ \vdots & \ddots & m_c & \ddots & & & \vdots \\ \vdots & & \ddots & \ddots & \ddots & & \vdots \\ \vdots & & & \ddots & \ddots & \ddots & \vdots \\ \vdots & & & & \ddots & m_5 & 0 \\ 0 & \cdots & \cdots & \cdots & \cdots & 0 & m_5 \end{bmatrix}$$

$$\mathbf{C} = \begin{bmatrix} C_{11} & C_{12} & \cdots & \cdots & \cdots & \cdots & C_{120} \\ C_{21} & \ddots & & & & & C_{220} \\ \vdots & & \ddots & & & & \vdots \\ \vdots & & & \ddots & & & \vdots \\ \vdots & & & & \ddots & & \vdots \\ \vdots & & & & & \ddots & \vdots \\ C_{201} & \cdots & \cdots & \cdots & \cdots & \cdots & C_{2020} \end{bmatrix}$$

Where

$$C_{11} = C_{sh1}$$
$$C_{22} = C_{sv1} + C_{cv1}$$
$$C_{24} = -C_{cv1}$$
$$C_{31} = -C_{ch1}$$
$$C_{33} = C_{ch1}$$
$$C_{42} = -C_{cv1}$$
$$C_{44} = C_{v2} + C_{v1} + C_{cv1}$$
$$C_{48} = -C_{v1}$$
$$C_{411} = -C_{v2}$$
$$C_{412} = -0.004C_{v2}$$
$$C_{51} = -0.8716C_{ch2} - 0.1284C_{cv2}$$
$$C_{52} = -0.3346C_{ch2} + 0.3346C_{cv2}$$
$$C_{55} = 0.8716C_{h3} + 0.1284C_{v3} + 0.8716C_{ch2} + 0.1284C_{cv2}$$
$$C_{56} = 0.3346C_{ch2} - 0.3346C_{cv2} + 0.3346C_{h3} - 0.3346C_{v3}$$
$$C_{513} = -0.8716C_{h3} - 0.1284C_{v3}$$
$$C_{514} = -0.3346C_{h3} + 0.3346C_{v3}$$
$$C_{515} = -0.0805C_{h3} - 0.0119C_{v3} - 0.0017C_{h3} + 0.0017C_{v3}$$
$$C_{61} = -0.3346C_{ch2} + 0.3346C_{cv2}$$
$$C_{62} = -0.1284C_{ch2} - 0.8916C_{cv2}$$
$$C_{65} = 0.3346C_{ch2} - 0.3346C_{cv2} + 0.3346C_{h3} - 0.3346C_{v3}$$
$$C_{66} = 0.1284C_{h3} + 0.8716C_{v3} + 0.1284C_{ch2} + 0.8716C_{cv2}$$
$$C_{613} = -0.3346C_{h3} + 0.3346C_{v3}$$
$$C_{614} = -0.1284C_{h3} - 0.8716C_{v3}$$
$$C_{615} = -0.0006C_{h3} - 0.0044C_{v3} - 0.0309C_{h3} + 0.0309C_{v3}$$
$$C_{73} = -C_{h1}$$
$$C_{77} = C_2 + C_{h1} + C_1$$
$$C_{79} = -0.014C_2 + 0.07C_{h1} + 0.018C_1$$
$$C_{710} = -C_2$$
$$C_{712} = -0.013C_2$$
$$C_{84} = -C_{v1}$$
$$C_{88} = C_2 + C_1 + C_{v1}$$
$$C_{89} = -0.15C_2 + 0.196C_1$$
$$C_{811} = -C_2$$
$$C_{812} = -0.006C_2$$
$$C_{93} = -0.07C_{h1}$$

$$C_{97} = -0.014C_2 + 0.07C_{h1} + 0.018C_1$$
$$C_{98} = -0.15C_2 + 0.196C_1$$
$$C_{99} = 0.0225C_2 + 0.038416C_1 + C_{r1} + 0.000196C_2 + C_{r2} + 0.0049C_{h1} + 0.000324C_1$$
$$C_{910} = 0.014C_2$$
$$C_{911} = 0.15C_2$$
$$C_{912} = 0.0009C_2 + 0.00018C_2 - C_{r2}$$
$$C_{103} = -C_{h2}$$
$$C_{107} = -C_2$$
$$C_{109} = 0.014C_2$$
$$C_{1010} = C_{h2} + 0.1079C_{v5} + C_2 + C_3$$
$$C_{1011} = -0.3102C_{v5}$$
$$C_{1012} = 0.097C_{h2} - 0.00329C_{v5} + 0.013C_2 - 0.042C_3$$
$$C_{1013} = -C_3$$
$$C_{1015} = -0.3326C_3$$
$$C_{1019} = -0.1079C_{v5}$$
$$C_{1020} = 0.3102C_{v5}$$
$$C_{114} = -C_{v2}$$
$$C_{118} = -C_2$$
$$C_{119} = 0.15C_2$$
$$C_{1110} = -0.3102C_{v5}$$
$$C_{1111} = C_3 + 0.8923C_{v5} + C_2 + C_{v2}$$
$$C_{1112} = -0.061C_3 + 0.0095C_{v5} + 0.006C_2 + 0.004C_{v2}$$
$$C_{1114} = -C_3$$
$$C_{1115} = -0.0683C_3$$
$$C_{1119} = 0.3102C_{v5}$$
$$C_{1120} = -0.8923C_{v5}$$
$$C_{123} = -0.097C_{h2}$$
$$C_{124} = -0.004C_{v2}$$
$$C_{127} = -0.013C_2$$
$$C_{128} = -0.006C_2$$
$$C_{129} = -C_{r2} + 0.00018C_2 + 0.0009C_2$$
$$C_{1210} = 0.097C_{h2} - 0.0033C_{v5} + 0.013C_2 - 0.042C_3$$
$$C_{1211} = 0.0095C_{v5} - 0.061C_3 + 0.006C_2 + 0.004C_{v2}$$
$$C_{1212} = C_{r2} + 0.0094C_{h2} + 0.0001C_{v5} + 0.0037C_3 + 0.00017C_2 + 0.00004C_2 + C_{r3} + 0.00002C_{v2} + 0.0018C_3$$

$$C_{1213} = 0.042C_3$$
$$C_{1214} = 0.061C_3$$
$$C_{1215} = 0.0042C_3 - C_{r3} + 0.01397C_3$$
$$C_{1219} = 0.0033C_{v5}$$
$$C_{1220} = -0.0095C_{v5}$$
$$C_{135} = -0.8716C_{h3} - 0.1284C_{v3}$$
$$C_{136} = -0.3346C_{h3} + 0.3346C_{v3}$$
$$C_{1310} = -C_3$$
$$C_{1312} = 0.042C_3$$
$$C_{1313} = C_4 + 0.8719C_{h5} + 0.8716C_{h3} + 0.1284C_{v3} + C_3$$
$$C_{1314} = 0.3341C_{h5} + 0.3346C_{h3} - 0.3346C_{v3}$$
$$C_{1315} = -0.1493C_4 + 0.2213C_{h5} + 0.0805C_{h3} + 0.0119C_{v3} + 0.0017C_{h3} - 0.0017C_{v3} + 0.3326C_3$$
$$C_{1316} = -C_4$$
$$C_{1318} = -0.1C_4$$
$$C_{1319} = -0.8719C_{h5}$$
$$C_{1320} = -0.3341C_{h5}$$
$$C_{145} = -0.3346C_{h3} + 0.3346C_{v3}$$
$$C_{146} = -0.1284C_{h3} - 0.8716C_{v3}$$
$$C_{1411} = -C_3$$
$$C_{1412} = 0.061C_3$$
$$C_{1413} = 0.3341C_{h5} + 0.3346C_{h3} - 0.3346C_{v3}$$
$$C_{1414} = C_4 + 0.1284C_{h3} + 0.8716C_{v3} + 0.1280C_{h5} + C_3$$
$$C_{1415} = -0.0353C_4 + 0.0006C_{h3} + 0.0044C_{v3} + 0.0848C_{h5} + 0.0683C_3 + 0.0309C_{h3} - 0.0309C_{v3}$$
$$C_{1417} = -C_4$$
$$C_{1418} = 0.0261C_4$$
$$C_{1419} = -0.3341C_{h5}$$
$$C_{1420} = -0.1280C_{h5}$$
$$C_{155} = -0.0805C_{h3} - 0.0119C_{v3} - 0.017C_{h3} + 0.0017C_{v3}$$
$$C_{156} = -0.00064C_{h3} - 0.0044C_{v3} - 0.0309C_{h3} + 0.0309C_{v3}$$
$$C_{1510} = -0.3326C_3$$
$$C_{1511} = -0.0683C_3$$
$$C_{1512} = -C_{r3} + 0.0042C_3 + 0.0139C_3$$
$$C_{1513} = 0.2213C_{h5} + 0.0805C_{h3} + 0.01185C_{v3} + 0.0017C_{h3} - 0.0017C_{v3} - 0.1493C_4 + 0.3326C_3$$
$$C_{1514} = 0.0683C_3 + 0.00064C_{h3} + 0.0044C_{v3} + 0.0848C_{h5} - 0.0353C_4 + 0.0309C_{h3} - 0.0309C_{v3}$$

$$C_{1515} = C_{r3} + 0.0047C_3 + 0.000003C_{h3} + 0.00002C_{v3} + 0.0562C_{h5} + 0.0013C_4 + 0.0074C_{h3} + 0.0011C_{v3} + 0.00015C_{h3} - 0.00015C_{v3} + 0.00015C_{h3} - 0.00015C_{v3} + 0.0223C_4 + C_{r4} + 0.1106C_3$$

$$C_{1516} = 0.1493C_4$$

$$C_{1517} = 0.0353C_4$$

$$C_{1518} = -C_{r4} - 0.0009C_4 + 0.0149C_4$$

$$C_{1519} = -0.2213C_{h5}$$

$$C_{1520} = -0.0848C_{h5}$$

$$C_{1613} = -C_4$$

$$C_{1615} = 0.1493C_4$$

$$C_{1616} = C_4$$

$$C_{1618} = 0.1C_4$$

$$C_{1714} = -C_4$$

$$C_{1715} = 0.0353C_4$$

$$C_{1717} = C_4$$

$$C_{1718} = -0.0261C_4$$

$$C_{1813} = -0.1C_4$$

$$C_{1814} = 0.0261C_4$$

$$C_{1815} = -0.00092C_4 + 0.01493C_4 - C_{r4}$$

$$C_{1816} = 0.1C_4$$

$$C_{1817} = -0.0261C_4$$

$$C_{1818} = 0.00068C_4 + 0.01C_4 + C_{r4}$$

$$C_{1910} = -0.1079C_{v5}$$

$$C_{1911} = 0.3102C_{v5}$$

$$C_{1912} = 0.0033C_{v5}$$

$$C_{1913} = -0.8719C_{h5}$$

$$C_{1914} = -0.3341C_{h5}$$

$$C_{1915} = -0.2213C_{h5}$$

$$C_{1919} = 0.8719C_{h5} + 0.1079C_{v5}$$

$$C_{1920} = 0.3341C_{h5} - 0.3102C_{v5}$$

$$C_{2010} = 0.3102C_{v5}$$

$$C_{2011} = -0.8923C_{v5}$$

$$C_{2012} = -0.0095C_{v5}$$

$$C_{2013} = -0.3341C_{h5}$$
$$C_{2014} = -0.128C_{h5}$$
$$C_{2015} = -0.0848C_{h5}$$
$$C_{2019} = -0.3102C_{v5} + 0.3341C_{h5}$$
$$C_{2020} = 0.8923C_{v5} + 0.128C_{h5}$$

All other entries are equal to zero.

$$\mathbf{K} = \begin{bmatrix} K_{11} & K_{12} & \cdots & \cdots & \cdots & \cdots & K_{120} \\ K_{21} & \ddots & & & & & K_{220} \\ \vdots & & \ddots & & & & \vdots \\ \vdots & & & \ddots & & & \vdots \\ \vdots & & & & \ddots & & \vdots \\ \vdots & & & & & \ddots & \vdots \\ K_{201} & \cdots & \cdots & \cdots & \cdots & \cdots & K_{2020} \end{bmatrix}$$

Where

$$K_{11} = K_{sh1}$$
$$K_{22} = K_{sv1} + K_{cv1}$$
$$K_{24} = -K_{cv1}$$
$$K_{31} = -K_{ch1}$$
$$K_{33} = K_{ch1}$$
$$K_{42} = -K_{cv1}$$
$$K_{44} = K_{v2} + K_{v1} + K_{cv1}$$
$$K_{48} = -K_{v1}$$
$$K_{411} = -K_{v2}$$
$$K_{412} = -0.004K_{v2}$$
$$K_{51} = -0.8716K_{ch2} - 0.1284K_{cv2}$$
$$K_{52} = -0.3346K_{ch2} + 0.3346K_{cv2}$$
$$K_{55} = 0.8716K_{h3} + 0.1284K_{v3} + 0.8716K_{ch2} + 0.1284K_{cv2}$$
$$K_{56} = 0.3346K_{ch2} - 0.3346K_{cv2} + 0.3346K_{h3} - 0.3346K_{v3}$$
$$K_{513} = -0.8716K_{h3} - 0.1284K_{v3}$$

$$K_{514} = -0.3346K_{h3} + 0.3346K_{v3}$$
$$K_{515} = -0.0805K_{h3} - 0.0119K_{v3} - 0.0017K_{h3} + 0.0017K_{v3}$$
$$K_{61} = -0.3346K_{ch2} + 0.3346K_{cv2}$$
$$K_{62} = -0.1284K_{ch2} - 0.8916K_{cv2}$$
$$K_{65} = 0.3346K_{ch2} - 0.3346K_{cv2} + 0.3346K_{h3} - 0.3346K_{v3}$$
$$K_{66} = 0.1284K_{h3} + 0.8716K_{v3} + 0.1284K_{ch2} + 0.8716K_{cv2}$$
$$K_{613} = -0.3346K_{h3} + 0.3346K_{v3}$$
$$K_{614} = -0.1284K_{h3} - 0.8716K_{v3}$$
$$K_{615} = -0.0006K_{h3} - 0.0044K_{v3} - 0.0309K_{h3} + 0.0309K_{v3}$$
$$K_{73} = -K_{h1}$$
$$K_{77} = K_2 + K_{h1} + K_1$$
$$K_{79} = -0.014K_2 + 0.07K_{h1} + 0.018K_1$$
$$K_{710} = -K_2$$
$$K_{712} = -0.013K_2$$
$$K_{84} = -K_{v1}$$
$$K_{88} = K_2 + K_1 + K_{v1}$$
$$K_{89} = -0.15K_2 + 0.196K_1$$
$$K_{811} = -K_2$$
$$K_{812} = -0.006K_2$$
$$K_{93} = -0.07K_{h1}$$
$$K_{97} = -0.014K_2 + 0.07K_{h1} + 0.018K_1$$
$$K_{98} = -0.15K_2 + 0.196K_1$$
$$K_{99} = 0.0225K_2 + 0.038416K_1 + K_{r1} + 0.000196K_2 + K_{r2} + 0.0049K_{h1} + 0.000324K_1$$
$$K_{910} = 0.014K_2$$
$$K_{911} = 0.15K_2$$
$$K_{912} = 0.0009K_2 + 0.00018K_2 - K_{r2}$$
$$K_{103} = -K_{h2}$$
$$K_{107} = -K_2$$
$$K_{109} = 0.014K_2$$
$$K_{1010} = K_{h2} + 0.1079K_{v5} + K_2 + K_3$$
$$K_{1011} = -0.3102K_{v5}$$
$$K_{1012} = 0.097K_{h2} - 0.00329K_{v5} + 0.013K_2 - 0.042K_3$$
$$K_{1013} = -K_3$$
$$K_{1015} = -0.3326K_3$$

$$K_{1019} = -0.1079K_{v5}$$
$$K_{1020} = 0.3102K_{v5}$$
$$K_{114} = -K_{v2}$$
$$K_{118} = -K_2$$
$$K_{119} = 0.15K_2$$
$$K_{1110} = -0.3102K_{v5}$$
$$K_{1111} = K_3 + 0.8923K_{v5} + K_2 + K_{v2}$$
$$K_{1112} = -0.061K_3 + 0.0095K_{v5} + 0.006K_2 + 0.004K_{v2}$$
$$K_{1114} = -K_3$$
$$K_{1115} = -0.0683K_3$$
$$K_{1119} = 0.3102K_{v5}$$
$$K_{1120} = -0.8923K_{v5}$$
$$K_{123} = -0.097K_{h2}$$
$$K_{124} = -0.004K_{v2}$$
$$K_{127} = -0.013K_2$$
$$K_{128} = -0.006K_2$$
$$K_{129} = -K_{r2} + 0.00018K_2 + 0.0009K_2$$
$$K_{1210} = 0.097K_{h2} - 0.0033K_{v5} + 0.013K_2 - 0.042K_3$$
$$K_{1211} = 0.0095K_{v5} - 0.061K_3 + 0.006K_2 + 0.004K_{v2}$$
$$K_{1212} = K_{r2} + 0.0094K_{h2} + 0.0001K_{v5} + 0.0037K_3 + 0.00017K_2 + 0.00004K_2 + K_{r3}$$
$$+0.00002K_{v2} + 0.0018K_3$$
$$K_{1213} = 0.042K_3$$
$$K_{1214} = 0.061K_3$$
$$K_{1215} = 0.0042K_3 - K_{r3} + 0.01397K_3$$
$$K_{1219} = 0.0033K_{v5}$$
$$K_{1220} = -0.0095K_{v5}$$
$$K_{135} = -0.8716K_{h3} - 0.1284K_{v3}$$
$$K_{136} = -0.3346K_{h3} + 0.3346K_{v3}$$
$$K_{1310} = -K_3$$
$$K_{1312} = 0.042K_3$$
$$K_{1313} = K_4 + 0.8719K_{h5} + 0.8716K_{h3} + 0.1284K_{v3} + K_3$$
$$K_{1314} = 0.3341K_{h5} + 0.3346K_{h3} - 0.3346K_{v3}$$
$$K_{1315} = -0.1493K_4 + 0.2213K_{h5} + 0.0805K_{h3} + 0.0119K_{v3} + 0.0017K_{h3} - 0.0017K_{v3} + 0.3326K_3$$

$$K_{1316} = -K_4$$
$$K_{1318} = -0.1K_4$$
$$K_{1319} = -0.8719K_{h5}$$
$$K_{1320} = -0.3341K_{h5}$$
$$K_{145} = -0.3346K_{h3} + 0.3346K_{v3}$$
$$K_{146} = -0.1284K_{h3} - 0.8716K_{v3}$$
$$K_{1411} = -K_3$$
$$K_{1412} = 0.061K_3$$
$$K_{1413} = 0.3341K_{h5} + 0.3346K_{h3} - 0.3346K_{v3}$$
$$K_{1414} = K_4 + 0.1284K_{h3} + 0.8716K_{v3} + 0.1280K_{h5} + K_3$$
$$K_{1415} = -0.0353K_4 + 0.0006K_{h3} + 0.0044K_{v3} + 0.0848K_{h5} + 0.0683K_3 + 0.0309K_{h3} - 0.0309K_{v3}$$
$$K_{1417} = -K_4$$
$$K_{1418} = 0.0261K_4$$
$$K_{1419} = -0.3341K_{h5}$$
$$K_{1420} = -0.1280K_{h5}$$
$$K_{155} = -0.0805K_{h3} - 0.0119K_{v3} - 0.017K_{h3} + 0.0017K_{v3}$$
$$K_{156} = -0.00064K_{h3} - 0.0044K_{v3} - 0.0309K_{h3} + 0.0309K_{v3}$$
$$K_{1510} = -0.3326K_3$$
$$K_{1511} = -0.0683K_3$$
$$K_{1512} = -K_{r3} + 0.0042K_3 + 0.0139K_3$$
$$K_{1513} = 0.2213K_{h5} + 0.0805K_{h3} + 0.01185K_{v3} + 0.0017K_{h3} - 0.0017K_{v3} - 0.1493K_4 + 0.3326K_3$$
$$K_{1514} = 0.0683K_3 + 0.00064K_{h3} + 0.0044K_{v3} + 0.0848K_{h5} - 0.0353K_4 + 0.0309K_{h3} - 0.0309K_{v3}$$
$$K_{1515} = K_{r3} + 0.0047K_3 + 0.000003K_{h3} + 0.00002K_{v3} + 0.0562K_{h5} + 0.0013K_4 + 0.0074K_{h3} + 0.0011K_{v3} + 0.00015K_{h3} - 0.00015K_{v3} + 0.00015K_{h3} - 0.00015K_{v3} + 0.0223K_4 + K_{r4} + 0.1106K_3$$
$$K_{1516} = 0.1493K_4$$
$$K_{1517} = 0.0353K_4$$
$$K_{1518} = -K_{r4} - 0.0009K_4 + 0.0149K_4$$
$$K_{1519} = -0.2213K_{h5}$$
$$K_{1520} = -0.0848K_{h5}$$
$$K_{1613} = -K_4$$
$$K_{1615} = 0.1493K_4$$
$$K_{1616} = K_4$$
$$K_{1618} = 0.1K_4$$
$$K_{1714} = -K_4$$
$$K_{1715} = 0.0353K_4$$

$$K_{1717} = K_4$$
$$K_{1718} = -0.0261K_4$$
$$K_{1813} = -0.1K_4$$
$$K_{1814} = 0.0261K_4$$
$$K_{1815} = -0.00092K_4 + 0.01493K_4 - K_{r4}$$
$$K_{1816} = 0.1K_4$$
$$K_{1817} = -0.0261K_4$$
$$K_{1818} = 0.00068K_4 + 0.01K_4 + K_{r4}$$
$$K_{1910} = -0.1079K_{v5}$$
$$K_{1911} = 0.3102K_{v5}$$
$$K_{1912} = 0.0033K_{v5}$$
$$K_{1913} = -0.8719K_{h5}$$
$$K_{1914} = -0.3341K_{h5}$$
$$K_{1915} = -0.2213K_{h5}$$
$$K_{1919} = 0.8719K_{h5} + 0.1079K_{v5}$$
$$K_{1920} = 0.3341K_{h5} - 0.3102K_{v5}$$
$$K_{2010} = 0.3102K_{v5}$$
$$K_{2011} = -0.8923K_{v5}$$
$$K_{2012} = -0.0095K_{v5}$$
$$K_{2013} = -0.3341K_{h5}$$
$$K_{2014} = -0.128K_{h5}$$
$$K_{2015} = -0.0848K_{h5}$$
$$K_{2019} = -0.3102K_{v5} + 0.3341K_{h5}$$
$$K_{2020} = 0.8923K_{v5} + 0.128K_{h5}$$

All other entries are equal to zero.

$$\mathbf{f_c} = \begin{bmatrix} f_{c11} & f_{c12} & f_{c13} & f_{c14} \\ f_{c21} & & & \vdots \\ \vdots & \ddots & & \vdots \\ \vdots & & \ddots & \vdots \\ \vdots & & & \vdots \\ \vdots & & & \vdots \\ f_{c201} & f_{c202} & f_{c203} & f_{c204} \end{bmatrix}$$

$f_{c11} = K_{sh1}$
$f_{c13} = C_{sh1}$
$f_{c22} = K_{sv1}$
$f_{c24} = C_{sv1}$
$f_{c71} = K_1$
$f_{c73} = C_1$
$f_{c82} = K_1$
$f_{c84} = C_1$
$f_{c91} = 0.018K_1$
$f_{c92} = 0.196K_1$
$f_{c93} = 0.018C_1$
$f_{c94} = 0.196C_1$

All other entries are equal to zero.

$$\mathbf{X} = \begin{bmatrix} x_{st} & z_{st} & x_c & z_c & \cdots & \cdots & \cdots & \theta_4 & x_5 & z_5 \end{bmatrix}^T$$

and

$$\mathbf{X_0} = \begin{bmatrix} x_0 & z_0 & \dot{x}_0 & \dot{z}_0 \end{bmatrix}^T$$

These four matrices ($\mathbf{M}, \mathbf{C}, \mathbf{K}$ and $\mathbf{f_c}$) are used for evaluating different transfer functions.

2.6 Summary

In this chapter human biodynamic model and different seat models are explained in detail. First how this human model is developed is explained with its advantages. Then properties of this human model are summarized which include its mass, inertia, stiffness and geometrical properties. After the three types of seat model are explained. The first seat is called hard seat which is neither having seat suspension nor cushion. The second seat has seat and backrest cushion but not having seat suspension. The third seat has both seat suspension and cushion called as isolated seat. To get clear idea about arrangement, these three seats with human body are represented using figures.

At the end equations of motion are derived for isolated seat using Newtonian approach. These equations of motion are rearranged to get mass, damping, stiffness and input coefficient matrices. These matrices are useful for obtaining transmissibility functions.

CHAPTER 3

TRANSFER FUNCTION AND TRANSMISSIBILITY

3.1 Introduction

In this chapter, the human body response is evaluated in horizontal and vertical direction for sinusoidal displacement input. First, the expressions of transfer function are derived and transmissibility values are calculated. Then, the transmissibility plots are obtained for human model with three types of seat. Finally, the seat performances are compared.

The response of a human model under certain excitation is studied in terms of transmissibility function. Most commonly used transmissibility function is STHT which is a complex ratio of response motion of the head to the forced vibration motion at the seat-body interface. STHT signifies the extent to which the input vibration to the body is transmitted to head. But is does not give any information about response of other body parts. Therefore, in this study transmissibility values are calculated for all five body parts.

The ride comfort depends on the exposure duration, amplitude, and frequency of vibration to a human body (ISO 2631-1). The human body sensitivity to the vibration varies with respect to frequency. For same vibration input, the human body response is different at different frequencies. ISO 2631-1 defines frequency weighting factors based on human body sensitivity to vibration at different frequencies. While seated, the human body is most sensitive to the vibrations at 4-10 Hz in vertical direction and 0.5-3 Hz in horizontal direction as shown in Figure 3.1.

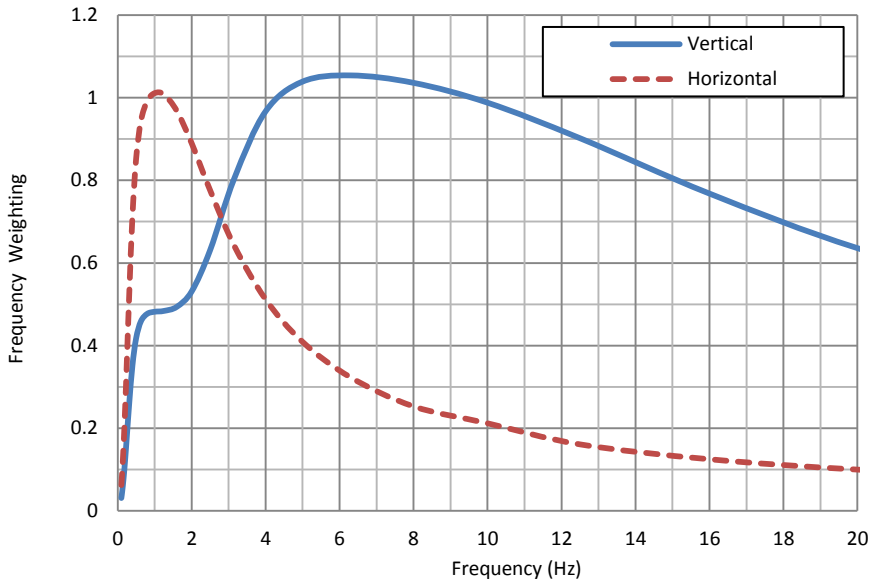

Figure 3.1 Human body vertical and horizontal frequency weighting

3.2 Derivation of transfer function and transmissibility

In previous chapter, the equations of motion are derived for human body model with three types of seats.

From equation 2.25, the equations of motion for human-seat model can be written as

$$\mathbf{M}\ddot{\mathbf{X}} + \mathbf{C}\dot{\mathbf{X}} + \mathbf{K}\mathbf{X} = \mathbf{f}_c\mathbf{X}_0 \tag{3.1}$$

This equation is a linear time invariant differential equation used to represent dynamic system of human-seat model. In linear time invariant system, the differential equation has constant coefficients.

A dynamic system with small number of mass, spring, and damper can be solved by taking Laplace transform of its equation of motion. For a system having large number of input and output, it requires taking large number of Laplace transform. So as the system become more complex it becomes more and more cumbersome and time consuming. Therefore for solving this complex system, the state space method is used. In the state

space representation, the mechanical system is represented by a mathematical model with a set of input, output and state space variables. The state space representation is a convenient and compact way for modeling and analyzing a dynamic system with multiple inputs and outputs. In this method the original input and output variables are represented by the state space variables. The system is expressed as a set of n coupled first order ordinary differential state variables where n is the order of original differential equation. As human-seat model in 2D has second order, here n is equal to two.

Defining the state equations with state variables as,

$$\begin{aligned} \mathbf{Y_1} &= \mathbf{X} \\ \mathbf{Y_2} &= \dot{\mathbf{X}} \end{aligned} \tag{3.2}$$

From these equations,

$$\dot{\mathbf{Y}}_1 = \mathbf{Y}_2 \tag{3.3}$$

Using these state space variables, equation 3.1 can be written as

$$\mathbf{M}\dot{\mathbf{Y}}_2 + \mathbf{C}\mathbf{Y}_2 + \mathbf{K}\mathbf{Y}_1 = \mathbf{f}_c\mathbf{X}_0$$

$$\dot{\mathbf{Y}}_2 = -\mathbf{M}^{-1}\mathbf{K}\mathbf{Y}_1 - \mathbf{M}^{-1}\mathbf{C}\mathbf{Y}_2 + \mathbf{M}^{-1}\mathbf{f}_c\mathbf{X}_0 \tag{3.4}$$

From equation 3.3 and 3.4,

$$\begin{Bmatrix} \dot{\mathbf{Y}}_1 \\ \dot{\mathbf{Y}}_2 \end{Bmatrix} = \begin{bmatrix} \mathbf{0} & \mathbf{I} \\ -\mathbf{M}^{-1}\mathbf{K} & -\mathbf{M}^{-1}\mathbf{C} \end{bmatrix} \begin{Bmatrix} \mathbf{Y}_1 \\ \mathbf{Y}_2 \end{Bmatrix} + \begin{bmatrix} \mathbf{0} \\ \mathbf{M}^{-1}\mathbf{f}_c \end{bmatrix} \begin{Bmatrix} \mathbf{X}_0 \\ \dot{\mathbf{X}}_0 \end{Bmatrix}$$

$$\dot{\mathbf{Y}} = \begin{bmatrix} \mathbf{0} & \mathbf{I} \\ -\mathbf{M}^{-1}\mathbf{K} & -\mathbf{M}^{-1}\mathbf{C} \end{bmatrix} \mathbf{Y} + \begin{bmatrix} \mathbf{0} \\ \mathbf{M}^{-1}\mathbf{f}_c \end{bmatrix} \mathbf{X}_0 \tag{3.5}$$

If the displacement is considered as the output, the output equations can be written as,

$$\begin{Bmatrix} \mathbf{X} \\ \dot{\mathbf{X}} \end{Bmatrix} = \begin{bmatrix} \mathbf{I} & \mathbf{0} \end{bmatrix} \begin{Bmatrix} \mathbf{Y1} \\ \mathbf{Y2} \end{Bmatrix} + \begin{bmatrix} \mathbf{0} & \mathbf{0} \end{bmatrix} \begin{Bmatrix} \mathbf{X}_0 \\ \dot{\mathbf{X}}_0 \end{Bmatrix}$$

$$\mathbf{X} = \begin{bmatrix} \mathbf{I} & \mathbf{0} \end{bmatrix} \mathbf{Y} + [\mathbf{0} \ \mathbf{0}] \mathbf{X_0} \tag{3.6}$$

Equation 3.5 and 3.6 can be written in state space representation as,

$$\begin{aligned} \dot{\mathbf{Y}} &= \mathbf{AY} + \mathbf{BX_0} \\ \mathbf{X} &= \mathbf{CY} + \mathbf{DX_0} \end{aligned} \tag{3.7}$$

Now from these equations, $\mathbf{A, B, C}$ and $\mathbf{D}$ matrices are obtained. $\mathbf{A}$ and $\mathbf{B}$ are the properties of system and determined by system elements and structure. $\mathbf{C}$ and $\mathbf{D}$ are output matrices and are determined by required output variables.

These matrices are given as input in MATLAB and this state space is converted into transfer function using MATLAB inbuilt function *ss2tf*. The transfer functions are obtained for this system for sinusoidal input excitations.

In a dynamic system expressed in terms of ordinarily differential equation, the transfer function is relation between input excitation function and output response function. This is schematically represented in Figure 3.2.

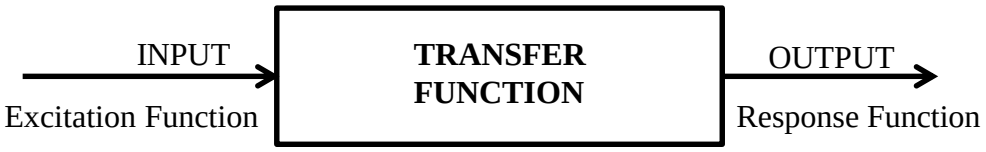

Figure 3.2 Schematic representation of transfer function

Consider the model having following equation.

$$\dot{u} + au = f(t) \tag{3.8}$$

With zero initial conditions, taking Laplace transform of equation 3.8

$$\begin{aligned} sU(s) + aU(s) &= U(s) = F(s) \\ (s+a)U(s) &= F(s) \end{aligned}$$

$$\frac{U(s)}{F(s)} = \frac{1}{(s+a)} \tag{3.9}$$

This ratio of forced output response to input excitation is called as transfer function. The transfer function expresses relation between input and output signals and can be used to study its relative magnitude and phase of that signal. The transfer function is a complex function of frequency. It can be expressed using either single complex number or both phase and magnitude together. The transfer functions can be calculated in frequency domain by considering input and output response at specific frequency as shown in equation 3.10.

$$Transfer\ Function(f) = \frac{\mathrm{Re}\,sponse\ Function(f)}{Input\ Function(f)} \tag{3.10}$$

The transfer function of a body at frequency f is calculated by considering response motion of that body and the input excitation motion. It is a complex ratio of respective output and input displacements, velocities or accelerations as shown in equation 3.11.

$$H(f) = \frac{x(f)}{x_0(f)} = \frac{v(f)}{v_0(f)} = \frac{a(f)}{a_0(f)} \tag{3.11}$$

Where $x(f), v(f)\ and\ a(f)$ are the output response displacement, velocity and acceleration of respective body at frequency f and $x_0(f), v_0(f)\ and\ a_0(f)$ are displacement, velocity and acceleration of input excitation at same frequency. This $H(f)$ is the transfer function which is a complex number and it is having real and imaginary parts.

As seen in the previous section, using MATLAB inbuilt function and state space representation, the transfer functions are obtained.

3.3 Transmissibility

As seen in the last section, the transfer function gives relationship between the input excitation and output response representing the dynamic response of the system. The transfer function is a complex number which represents both magnitude and phase of relation between input and output signals. Out of this, its magnitude is represented by

transmissibility. Thus the complex number is represented by transfer function and transmissibility is the magnitude of this complex number.

Transmissibility is a non-dimensional term and can be calculated from the transfer function. The transmissibility of body at frequency *f* is calculated by considering modulus of the transfer function as shown in equation 3.12. Also its phase angle can be calculated as shown in equation 3.13 which represents the time delay between two measurement positions.

$$\left|H(f)\right| = [(\mathrm{Re}[H(f)])^{\wedge 2} + (\mathrm{Im}[H(f)])^{\wedge 2}]^{1/2} \tag{3.12}$$

$$\phi(f) = \tan -1\left[\frac{\mathrm{Im}[H(f)]}{\mathrm{Re}[H(f)]}\right] \tag{3.13}$$

With the help of equation 3.11, the transfer functions are calculated for all five bodies in given frequency range. From these transfer functions, the transmissibility values are also calculated as shown in equation 3.12. The transmissibility plots are obtained by considering its values in given frequency range.

In this research, transmissibility plots are obtained for all five bodies in horizontal and vertical directions (Kumbhar et al., 2013). Sinusoidal displacement inputs are considered in horizontal and vertical directions and its dynamic response is analyzed.

At a specific frequency *f*, the transfer function from the vehicle floor to the human body in the horizontal direction is defined as shown in equation 3.14.

$$H(f) = \frac{x(f)}{x_0(f)} \tag{3.14}$$

Similarly at frequency *f*, the transfer function from the floor to the human body in the vertical direction is defined as shown in equation 3.15.

$$V(f) = \frac{z(f)}{z_0(f)} \tag{3.15}$$

In the human-seat model, two seat models are considered based on varying seat backrest angle in this study. The first seat model has 0º backrest angle and the second seat model

has 21º. For each seat model, there are three types of seats based on cushion and seat suspension. These three types of seat models are explained in Chapter 2. Human body response is analyzed for both of these angles using transmissibility plots.

3.3.1 Seat model with backrest angle α = 21º

Human seat model with backrest angle 21º for 3 types of seats is shown in the Figures 2.3, 2.4 and 2.5. The transmissibility values are calculated for all five bodies for three types of seat models.

Using equation 3.14, the horizontal transfer functions are calculated for all five body elements. Respective transmissibility values are obtained as shown in equation 3.12. This horizontal transmissibility's for Body 1 to 5 as shown in the Figure 3.3 to 3.7.

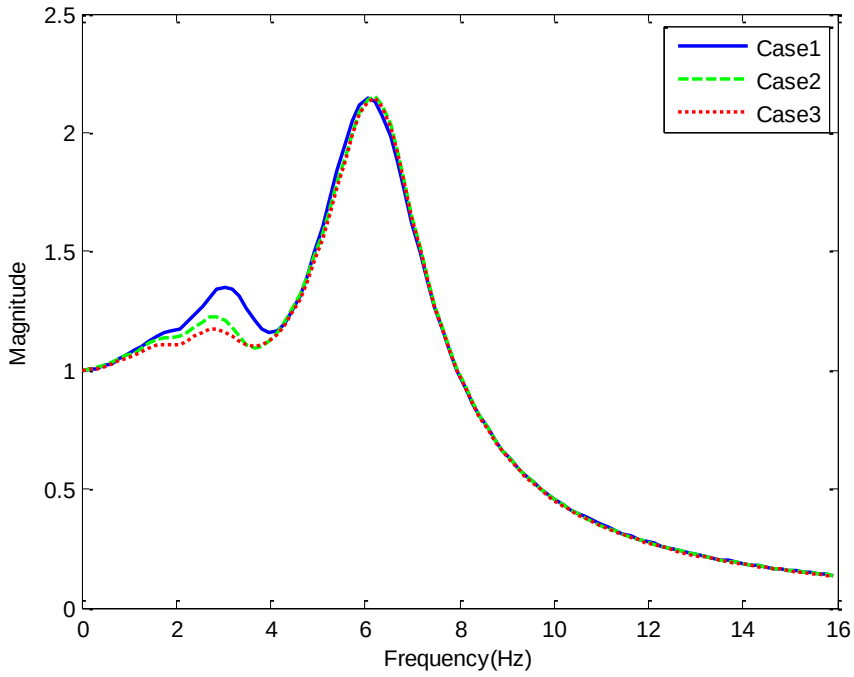

Figure 3.3 Transmissibility of Body 1 in the horizontal direction (α =21º)

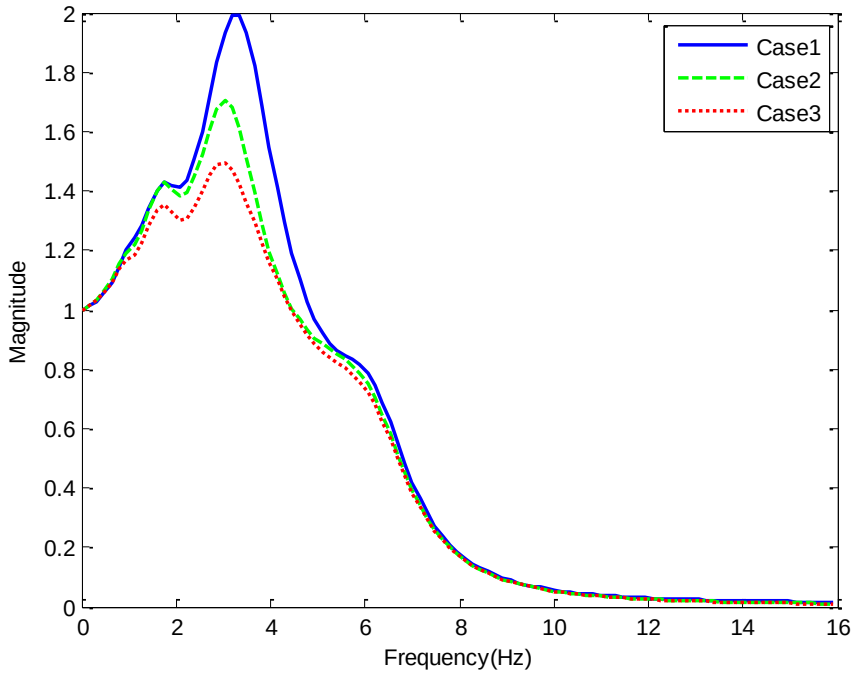

Figure 3.4 Transmissibility of Body 2 in the horizontal direction (α =21º)

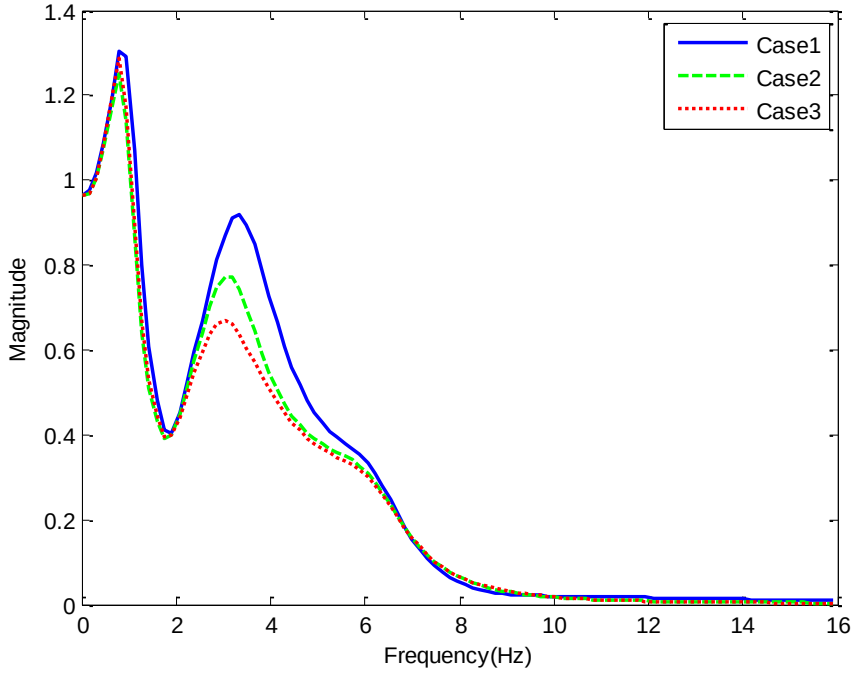

Figure 3.5 Transmissibility of Body 3 in the horizontal direction (α =21º)

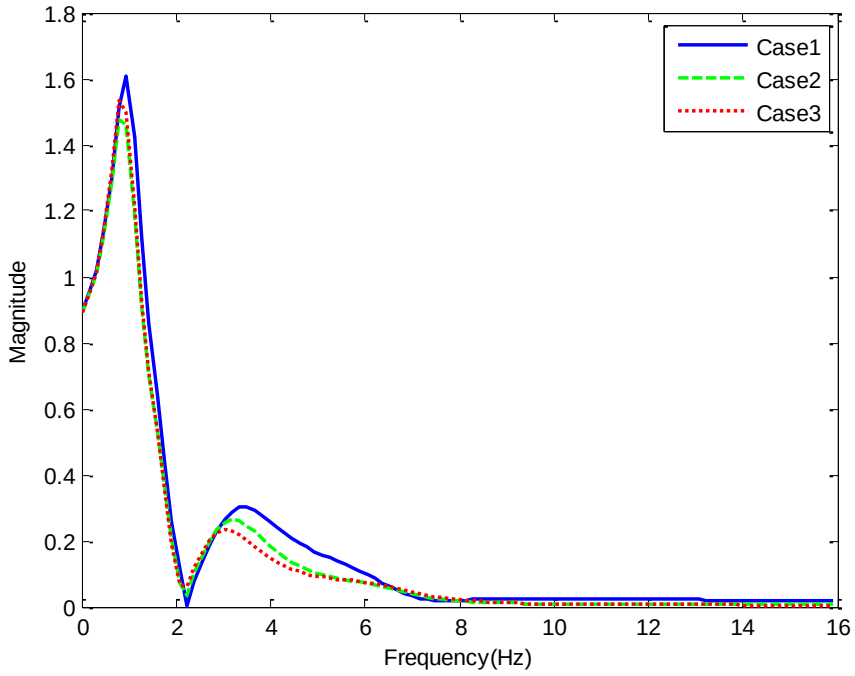

Figure 3.6 Transmissibility of Body 4 in the horizontal direction (α =21º)

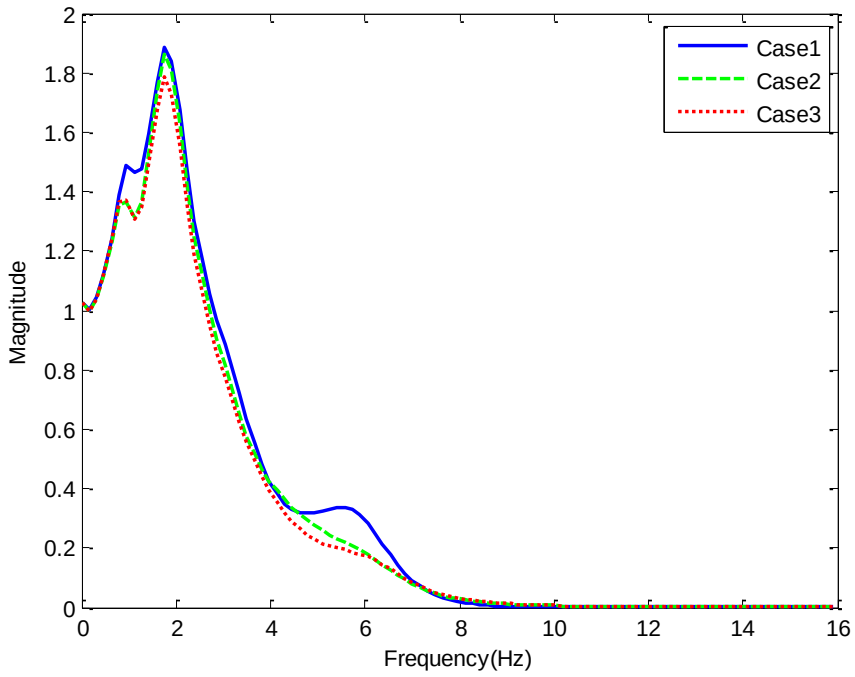

Figure 3.7 Transmissibility of Body 5 in the horizontal direction (α =21º)

Figure 3.3 to 3.7 shows transmissibility plots of Body 1 to 5 in the horizontal direction. All these figures have three plots and each one represents one type of seats. For all the body parts, the values of the horizontal transmissibility are high for the hard seat (Case 1). The transmissibility values are reduced in Case 2 and 3. Also the peak in this transmissibility plot which represents the resonance frequency of body is also reduced. It can be seen clearly that for Case 3, natural frequency is reduced in comparison with Case 1 and 2. This is because seat structure in Case 3 is softer than that in Case 1 and 2. For this reason, it will result in reduced natural frequency. As shown in Figure 3.1 and explained ISO 2631-1, the human body's horizontal comfort is highly sensitive between 0.5 and 6 Hz. This phenomenon is observed in these figures. The magnitudes can be further reduced if the cushion and seat use higher damping coefficients in horizontal direction and the backrest cushion use a higher damping coefficient in the vertical direction with respect to their contact surfaces. Therefore, the cushion and seat can improve horizontal ride comfort. A seat with both seat suspension and a cushion is the best setup for reducing vibrations transmitted to the human body.

Using equation 3.15, the vertical transfer functions are calculated for all body elements. Respective transmissibility values are obtained as shown in equation 3.12. This vertical transmissibility's for Body 1 to 5 as shown in Figure 3.8 to 3.12.

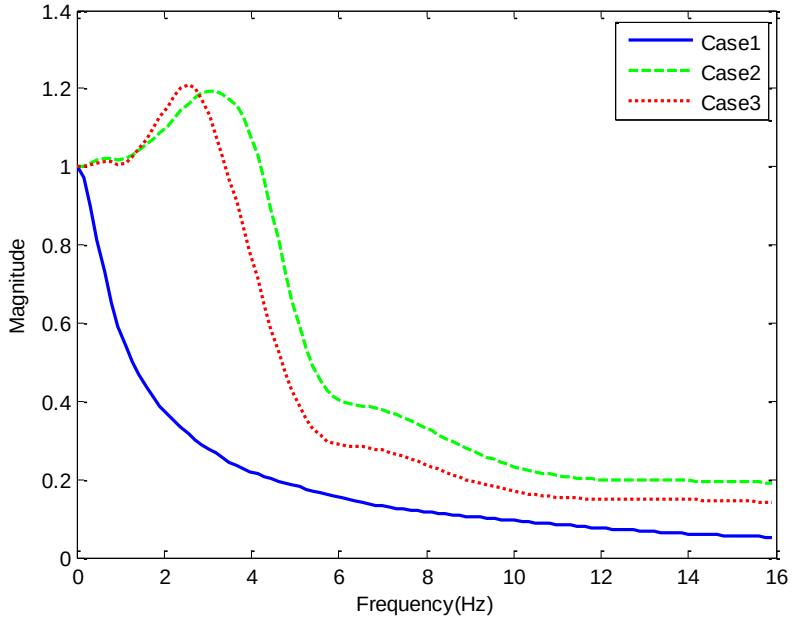

Figure 3.8 Transmissibility of Body 1 in the vertical direction (α =21º)

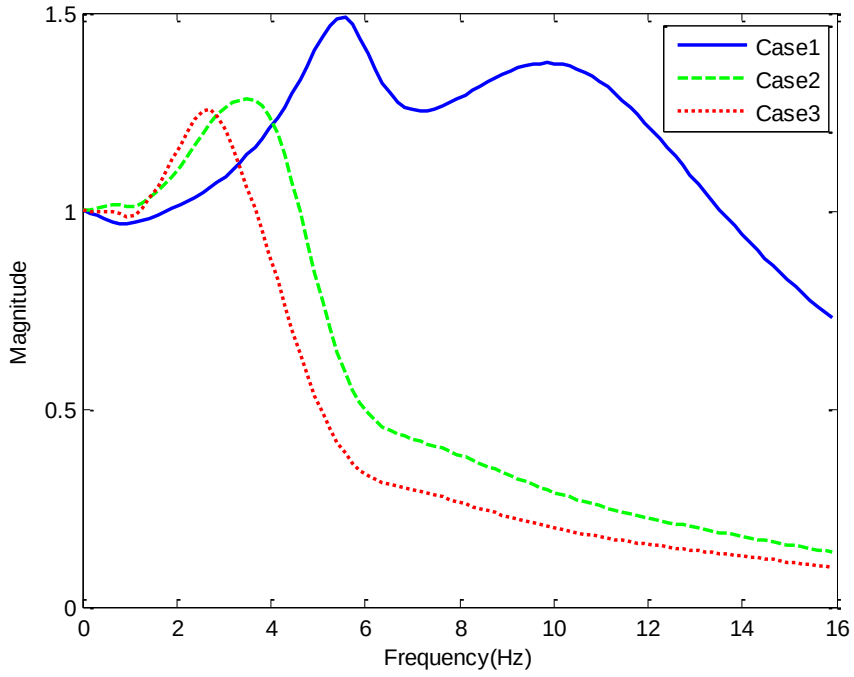

Figure 3.9 Transmissibility of Body 2 in the vertical direction (α =21º)

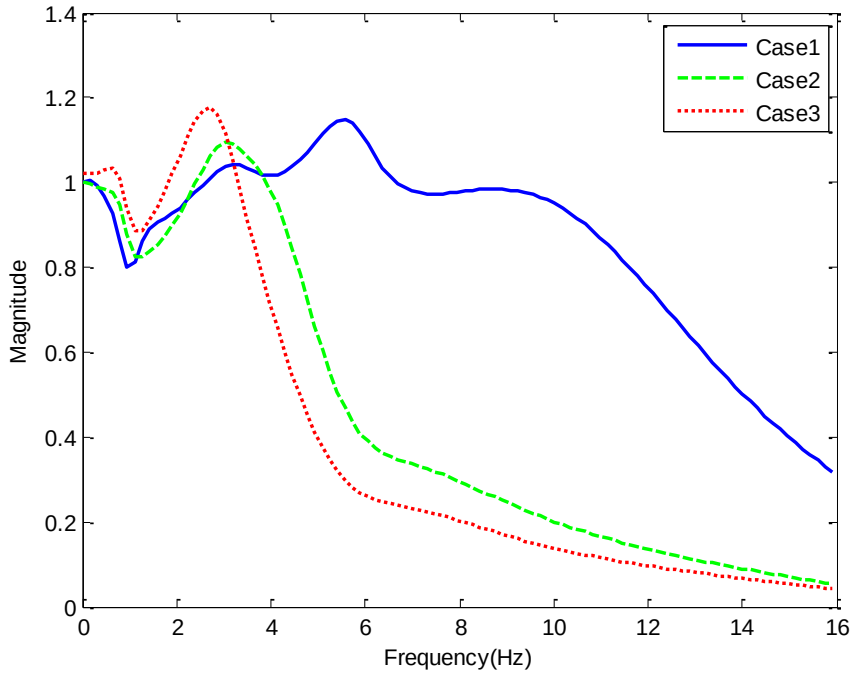

Figure 3.10 Transmissibility of Body 3 in the vertical direction (α =21º)

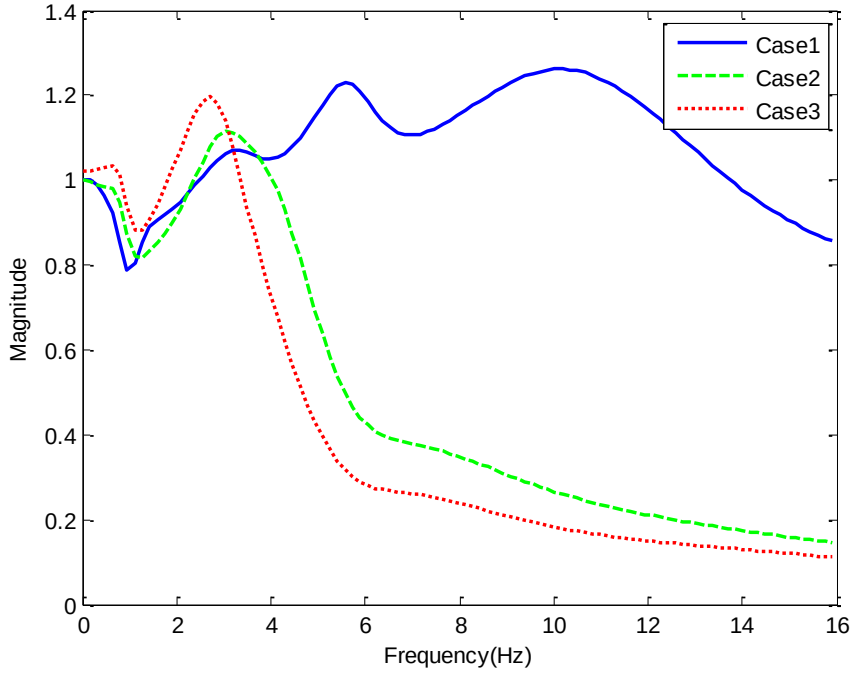

Figure 3.11 Transmissibility of Body 4 in the vertical direction (α =21º)

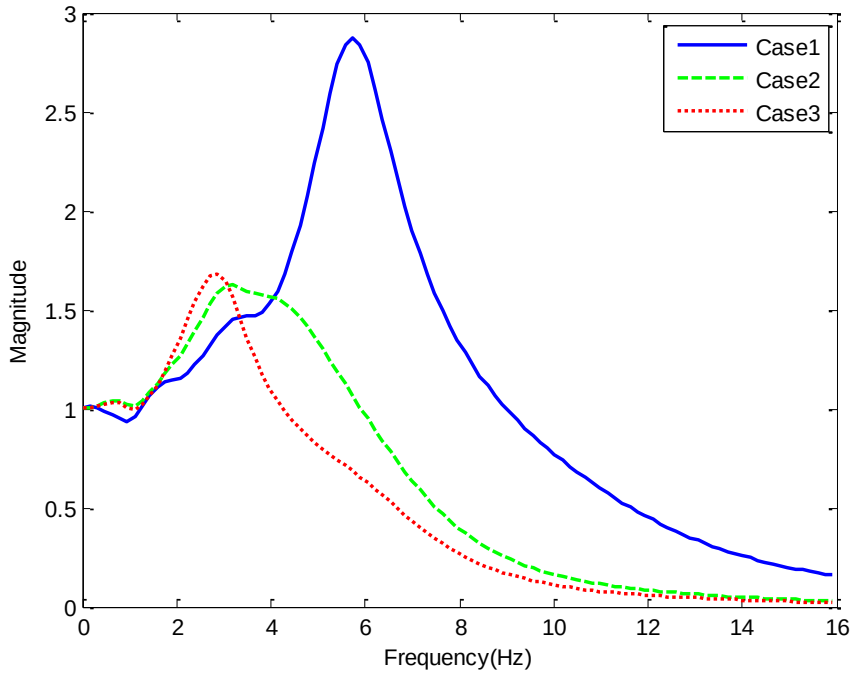

Figure 3.12 Transmissibility of Body 5 in the vertical direction (α =21º)

Figure 3.8 to 3.12 show the transmissibility's for Body 1 to 5 in the vertical direction. Each figure has three plots and each plot represents one type of seat. As shown in Figure 3.1, the vertical comfort of human body is highly sensitive between 4 and 10 Hz. This phenomenon is clearly seen in the above figures. For Case 1, the seat is a hard seat, and Body 1's vertical transfer function decreases with increasing the frequency because the vertical damping for Body 1 is very high in the human body model. Bodies 2 to 5 have high magnitudes of transfer functions and peaks in the frequency range of 4 to 10 Hz. In Case 2 and Case 3, the frequency at the transmissibility peak is reduced to lower than 4 Hz for Bodies 2 to 5. Case 3 has a lower peak-amplitude frequency. This transmissibility peak represents resonance frequency of that system and clearly it is reduced for Case 3 in comparison with Case 1 and 2. The cushion, backrest cushion, and seat suspension reduces the resonance frequencies. The transfer function peak values can be decreased by increasing the cushion and seat suspension's damping. Therefore, when the floor excitation frequency is given, a low transmissibility at this frequency can be achieved by

selecting proper stiffness and damping coefficients of the cushion and seat to minimize the vibration transmissibility to the human body and maximize the ride comfort.

3.3.2 Seat model with backrest angle α = 0º

Figure 2.1 shows the human model with backrest angle 21º. For analyzing human body response in erect position, transmissibility plots are obtained with vertical backrest support. In vertical backrest support, the backrest support angle is equal to zero. For vertical backrest support, the Body 3 (torso) is rotated 21º in clockwise direction with respect to joint J_3 as shown in Figure 2.1. Head (Body 4) is moved back to keep original posture of head and for making eye sight in straight line ahead. These changes simplify the equations of motion for all three cases. For each case, equations of motion are derived in similar fashion as did in Chapter 2. From these equations, the mass, stiffness, damping and input coefficient matrices are obtained. From this, transfer functions and transmissibility values are obtained in similar fashion as previous section.

Using equation 3.14, the horizontal transfer functions are calculated for all body elements with erect body posture. Respective transmissibility values are obtained as shown in equation 3.12. This horizontal transmissibility's for Body 1 to 5 as shown in Figure 3.13 to 3.17.

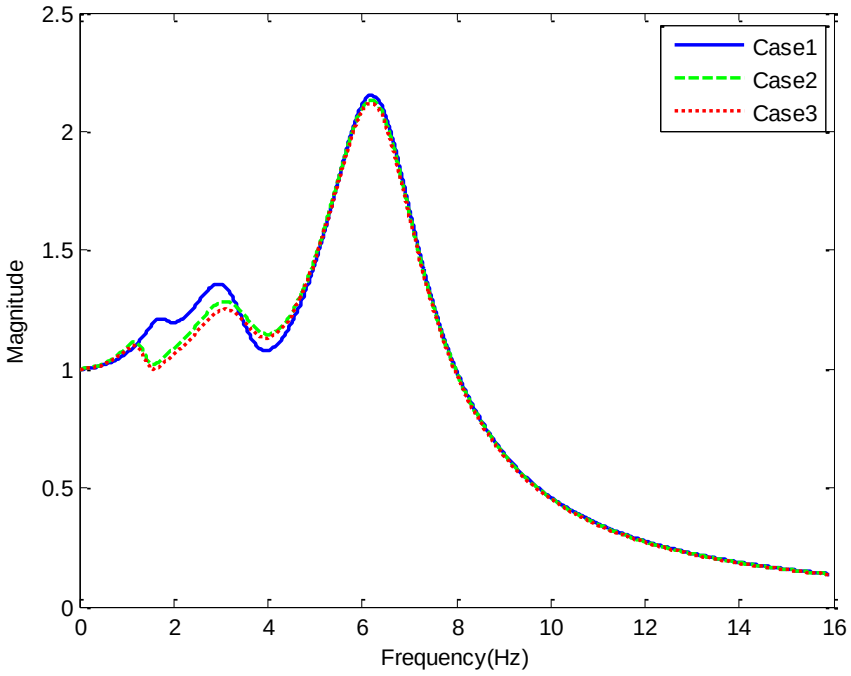

Figure 3.13 Transmissibility of Body 1 in the horizontal direction (α =0º)

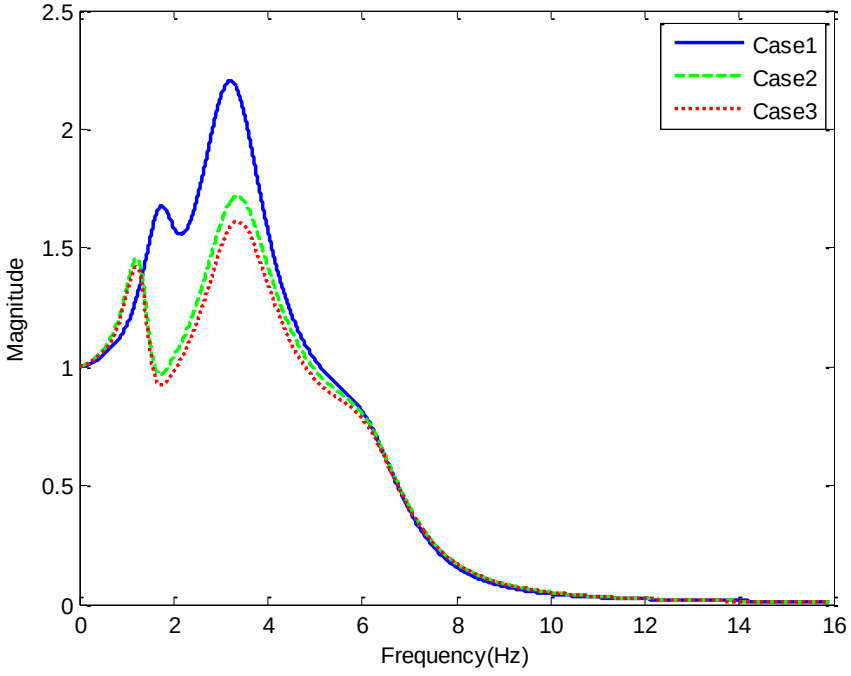

Figure 3.14 Transmissibility of Body 2 in the horizontal direction (α =0º)

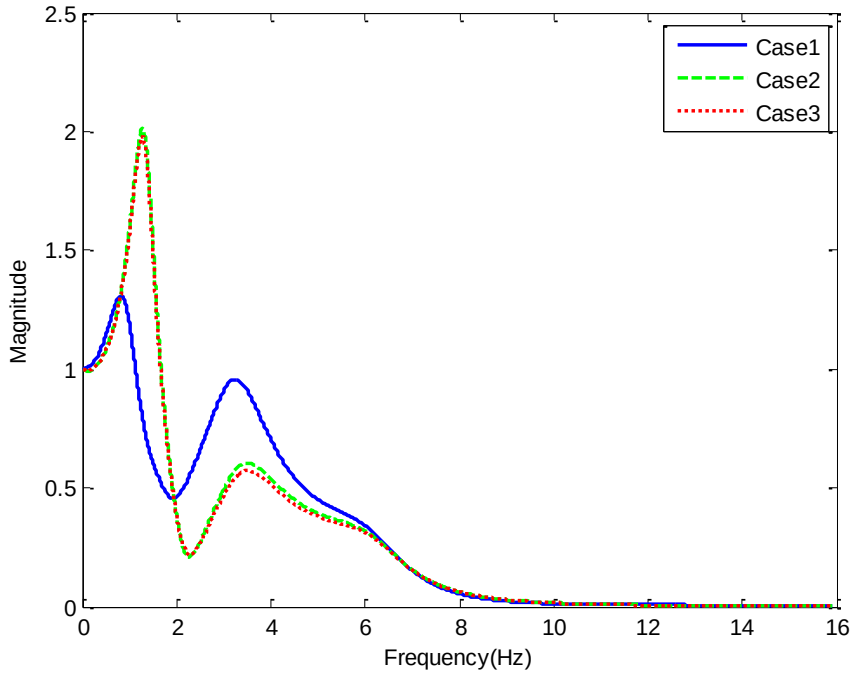

Figure 3.15 Transmissibility of Body 3 in the horizontal direction (α =0º)

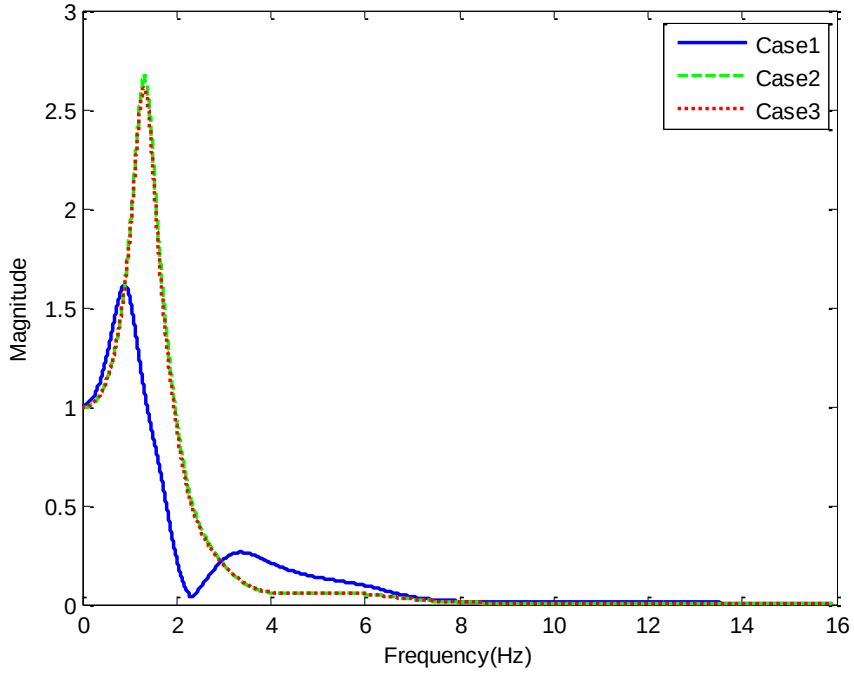

Figure 3.16 Transmissibility of Body 4 in the horizontal direction (α =0º)

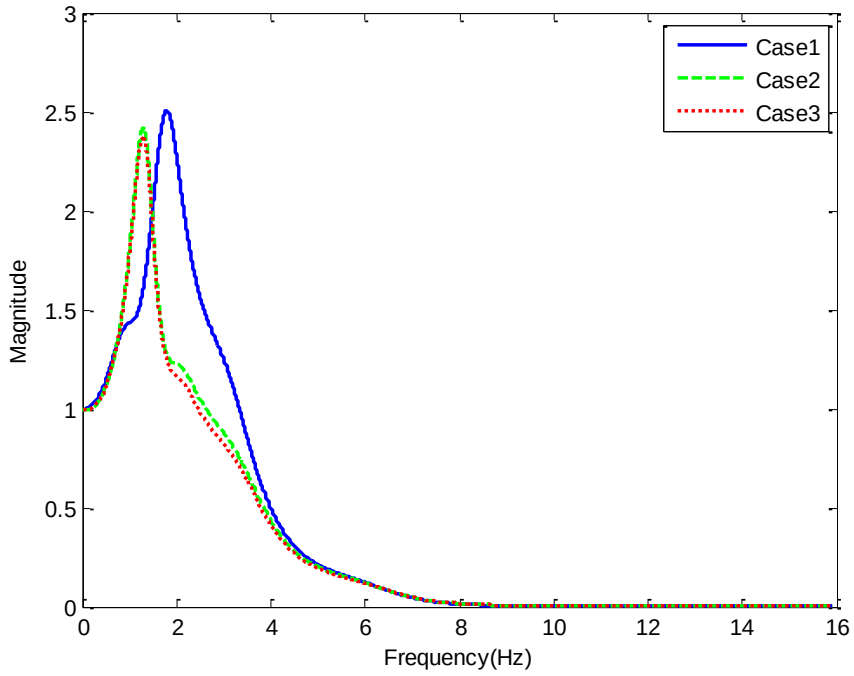

Figure 3.17 Transmissibility of Body 5 in the horizontal direction (α =0º)

Figure 3.13 to 3.17 show transmissibility's for Body 1 to 5 in the horizontal direction for erect sitting position. For Case 1, the magnitude of transmissibility is higher than those in Case 2 and 3 as there is nothing to isolate human body from input vibrations in hard seat. The magnitude is reduced in Case 2 and 3 for Body 1, 2 and 5. For Body 3 and 4, the magnitude of transmissibility is higher for Case 2 and 3 in comparison with Case 1. This is because of increase in muscle tension in Body 3 as a result of erect sitting. As explained in ISO 2631-1 and from these figures, human body horizontal response is sensitive in 0.5 to 3 Hz frequency range.

The vertical transfer functions are calculated using equation 3.15 for all body parts with erect body posture. Respective transmissibility values for erect body posture are obtained as shown in equation 3.12. The vertical transmissibility's for Body 1 to 5 are shown in Figure 3.18 to 3.22.

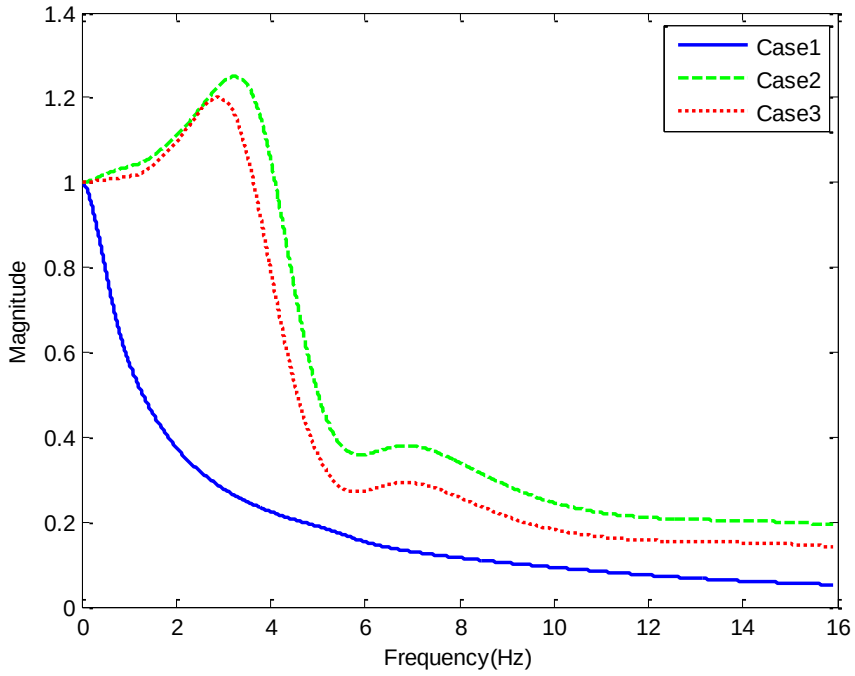

Figure 3.18 Transmissibility of Body 1 in the vertical direction (α =0º)

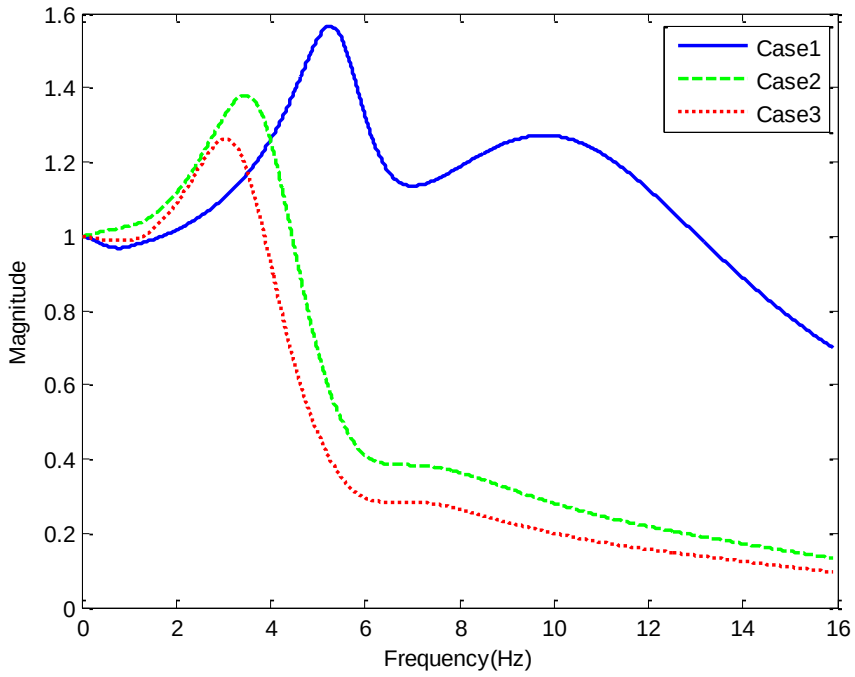

Figure 3.19 Transmissibility of Body 2 in the vertical direction (α =0º)

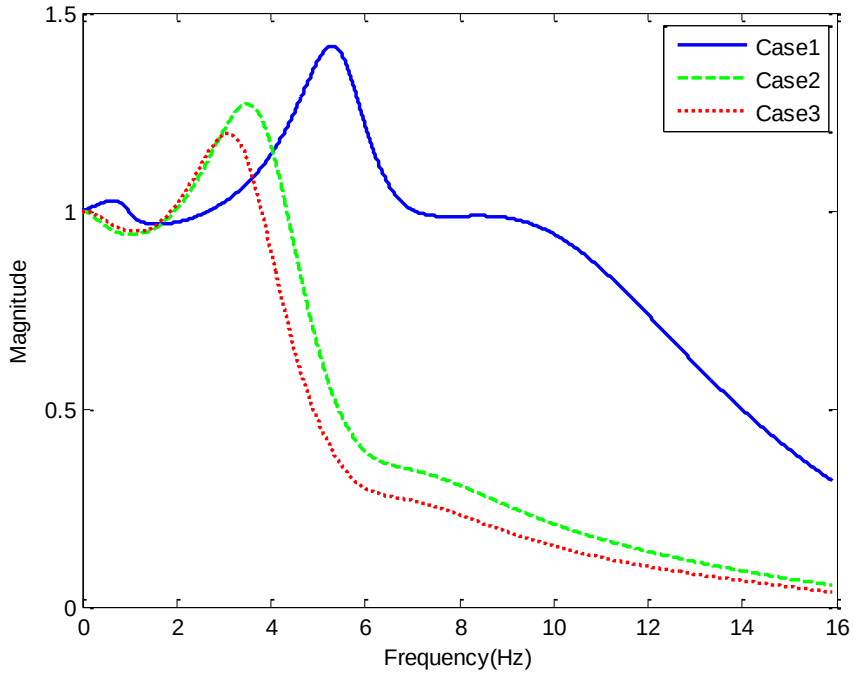

Figure 3.20 Transmissibility of Body 3 in the vertical direction (α =0º)

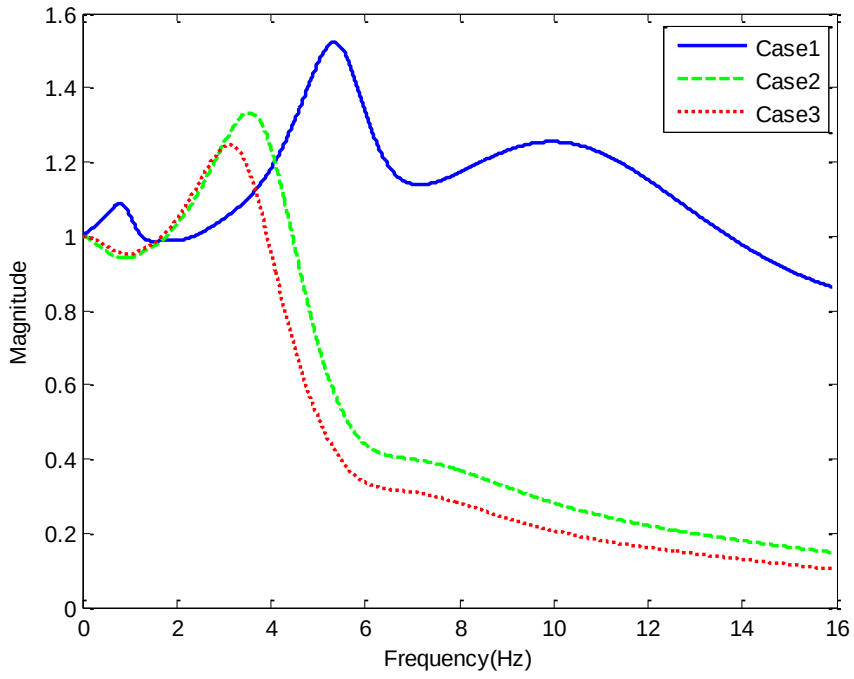

Figure 3.21 Transmissibility of Body 4 in the vertical direction (α =0º)

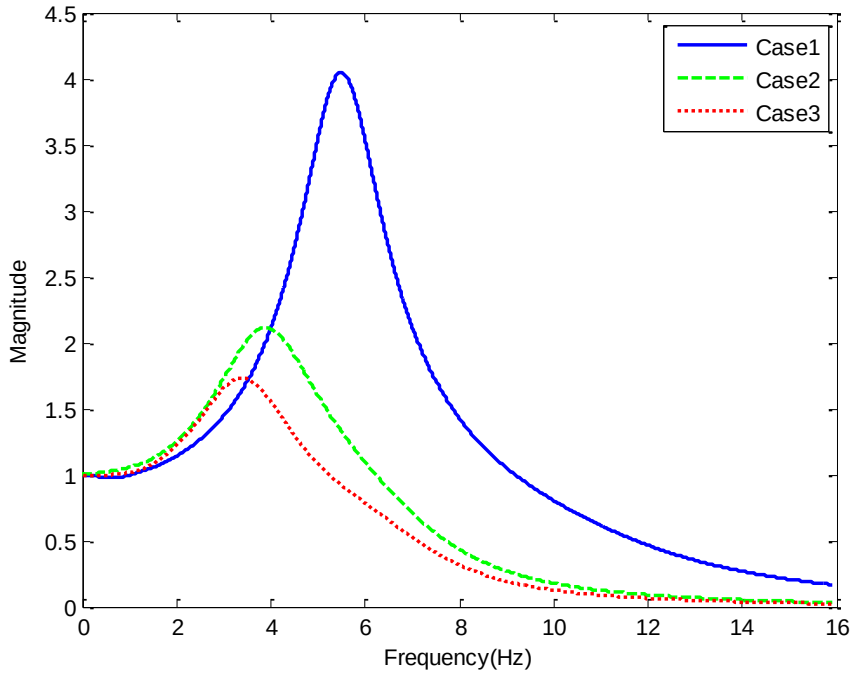

Figure 3.22 Transmissibility of Body 5 in the vertical direction (α =0º)

Figure 3.18 to 3.22 show transmissibility's for Body 1 to 5 in the vertical direction for three cases in erect sitting position. Similar to previous section, the vertical transfer function of Body 1 in Case 1 decreases with increasing the frequency. This is because the vertical damping for Body 1 is very high. Other body parts have high magnitudes of transfer functions and peaks in the frequency range of 4 to 10 Hz. This phenomenon is shown in the Figure 3.1 and explained in ISO 2631-1. For Case 2 and 3, the magnitude of transmissibility is reduced. Also the frequency of transmissibility peak value is also reduced for Case 2 and 3. This proves that resonance frequency is reduced for Case 3 in comparison with Case 1 and 2. The cushion, backrest cushion, and seat suspension reduces the transmissibility and resonance frequencies. Therefore by selecting proper stiffness and damping coefficients of the cushion and seat, minimum vibrations get transferred to the human body and this can maximize the ride comfort.

3.3.3 Comparison of two backrest angles

In previous two sections, transmissibility plots are obtained for 0º and 21º backrest angles for human model in all three cases. This transmissibility plots clearly shows that a seat with 21º backrest angle has minimum magnitude of transmissibility and resonance frequency in both horizontal and vertical direction. Also Body 3 and 4 shows some irregular behavior with backrest angle 0º. Due to erect sitting position, there is increase in muscle tension in Body 3 (Wang et al., 2004). This muscle tension result in fatigue of Body 3. This suggests that seat with backrest angle 21º gives better vibration isolation in comparison with 0 º.

3.4 Summary

In the first part of this chapter, the equations of motions are converted in state space representation and transfer functions are obtained using MATLAB. The transmissibility values are calculated for all 5 bodies. From these values, the transmissibility plots are obtained for each body in the horizontal and vertical direction. The transmissibility plots for each body are obtained for three types of seat models and comparison is made. Also in the seat model, two backrest support angles are used. Results shows that seat with backrest support angle 21º gives better results in comparison with seat having 0º backrest angle. The transmissibility plots shows that the isolated seat (Case 3) gives reduced magnitude of transmissibility than hard seat and seat with only cushion. The resonance frequency for isolated seat is also reduced. This is because the seat structure in isolated seat is softer and resulting in reducing vibration transmission.

These results shows that the magnitude of transfer function can be reduced by increasing damping coefficient of cushion and seat suspension. Therefore, a low transmissibility at excitation frequency can be achieved by selecting proper stiffness and damping coefficients of the cushion and seat. This will minimize the vibration transmission to the human body and maximize the ride comfort.

CHAPTER 4

ABSORBED POWER AND FATIGUE PREDICTION

4.1 Introduction

In this chapter, the absorbed power is calculated for three cases. Both weighted and unweighted absorbed power are calculated and based on absorbed power values, the driver's fatigue is predicted. For weighted absorbed power calculations, weighting factors are considered using ISO 2631-1.

The transfer functions allow analytical solution and transmissibility plots give graphical representation of human body response to vibration. But as it is not giving any numerical value, we cannot use these plots to understand severity of vibration. Whenever human body interacts with vibrating environment, the flow of energy takes place. After extensive study, it is seen that this rate of flow of energy can be used to study human body vibrations. The rate of flow of this energy is known as absorbed power. The absorbed power is a scalar quantity so it places vibration severity on an absolute scale and it is used in both time and frequency domain. With the help of this parameter it is possible to study variation for different seat parameters, seating arrangements and different people. Absorbed power depends upon human body type. For the same vibration input with same parameters, muscular person will get less absorbed power in comparison with obese person having same weight. It also depends upon seat contact area. Seats having larger contact area will reduce body movement which results in its elastic properties. This will produce lower absorbed power.

In literature, number of researcher used the absorbed power for analyzing human body response to the vibrations. Pradko and Lee (1965a; 1965b; 1966) introduced this concept of absorbed power in mid-1960 and they are mostly responsible for qualifying absorbed power as an indicator of human response to the vibrations. Pradko and Lee suggested that the time dependency of fatigue or discomfort can be determined from absorbed power (Lee and Pradko, 1968). Janeway (1975a; 1975b) experimented and strongly suggested

that absorbed power should be added in ISO standards. Lidstrom (1977) used this concept in the study of hand-arm vibrations. Lundstrom et al. (1998) studied relation between absorbed power and frequency, exposure level, direction, gender and body weight. There experiments showed that the absorbed power is strongly related to frequency and peak value occurs in the range of 4-6 Hz.

4.2 Power calculation in mechanical system

Power in the mechanical system is the rate of work done. Work done by a moving mechanical system calculated over a period of time *T* is given by equation 4.1,

$$W = \int_0^T F(t).x(t)dt \tag{4.1}$$

Where $F(t)$ is applied force and $x(t)$ is the resulting displacement. Both of these entities are function of time.

The power is defined as rate of work done by a system. So power of this mechanical system is the product of force and velocity as shown in equation 4.2.

$$P = F.\frac{dx}{dt} \tag{4.2}$$

When a sinusoidal force, $F_0 \sin(\omega t + \phi)$ is applied to a body and results in a displacement, $X_0 \sin(\omega t),$ the power in the body is given by

$$\begin{aligned} P &= [F_0 \sin(\omega t + \phi)].\frac{d}{dt}[X_0.\sin(\omega t)] \\ &= \frac{1}{2}\omega X_0 F_0[\sin(\phi) + \sin(2\omega t + \phi)] \end{aligned} \tag{4.3}$$

The equation 4.3 includes two parts: steady part and fluctuating part of power. The first term in this equation is constant and depends on phase angle between the force and displacement (ϕ). The second term in this equation is sine wave and it is a function of

time and it represents fluctuating part of power. The average value of fluctuating part of power is equal to zero over a complete cycle of motion. So the average power over a complete cycle of motion can be represented as shown in equation 4.4.

$$P = \frac{1}{2}\omega X_0 F_0 \sin(\phi) \tag{4.4}$$

Human body is a mechanical system having different masses interconnected by springs and dampers. So we need to consider power absorbed by three parts: mass, spring and damper.

When sinusoidal force is applied to ideal spring, phase angle between force and displacement is in phase ($\phi = 0^\circ$). There is work done by applied force in deflecting the spring followed by an equal and opposite amount of work done by the spring returning the force to its starting point. During this complete cycle, the total work done by the spring is zero. When the spring passes through equilibrium position all energy is in the form of kinetic energy and it is in the form of potential energy when spring is fully compressed or extended. So energy is converted between kinetic and potential energy and no energy is dissipated. This is also shown in equation 4.4 where the average power will be equal to zero as phase angle is zero.

When force is applied to ideal mass, the force and displacement are out of phase by 180º which results in $\sin\phi = 0.$ So from equation 4.4, the average power will be equal to zero. There is work done by applied force in accelerating and decelerating the mass but the energy is converted back and forth within kinetic and potential energies and no energy is dissipated. As a result, absorbed power over a complete cycle is equal to zero.

The scenario for ideal damper is somewhat different. The phase angle between force and displacement is 90º which results in $\sin\phi = 1.$ So for damper there is both constant and fluctuating component as shown is equation 4.3. As already explained average fluctuating component of power is equal to zero over a complete cycle. So for damper, constant component represents the absorbed power in it. It is expressed in equation 4.5.

$$P = \frac{1}{2}\omega X_0 F_0 \tag{4.5}$$

Equation 4.5 is used as basic expression for the absorbed power for a complex dynamic system containing masses, dampers and springs. Above equation can be modified to express in terms of velocity or acceleration. Therefore it is possible to determine the absorbed power by measuring complex force and either the complex displacement, velocity or acceleration.

4.3 Derivation for the absorbed power

The instantaneous power transmitted at time t can be written as,

$$P(t) = F(t).v(t)$$

This is the total power transmitted which has two parts.

$$P_{total}(t) = P_{spring}(t) + P_{damper}(t) \tag{4.6}$$

The first part of the equation 4.6 (P_{spring}) is power stored and released in the springs and the second part (P_{damper}) is the power dissipated in the dampers.

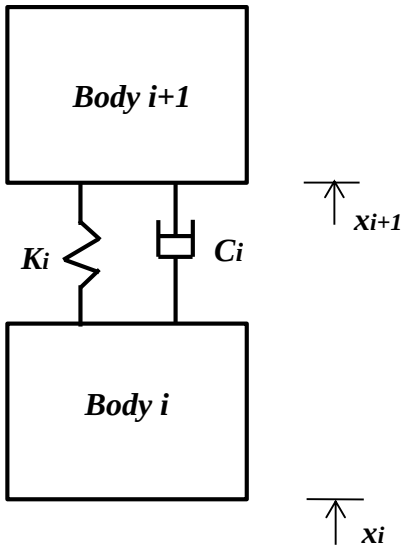

Figure 4.1 Simple dynamic system

Figure 4.1 shows simple dynamic system having two masses connected by a spring and damper. The two bodies i *and* $i+1$ are interconnected by spring K_i and damper C_i. For these two bodies, x_i and x_{i+1} are the absolute displacements respectively.

Average power stored and released in the spring over a complete cycle of time period T is calculated using equation 4.7,

$$P_{spring} = \frac{1}{T}\int_0^T K_i(x_i - x_{i+1}).(\dot{x}_i - \dot{x}_{i+1})dt \tag{4.7}$$

In the case of damper, absorbed power is calculated in the similar way by using equation 4.8,

$$P_{damper} = \frac{1}{T}\int_0^T C_i(\dot{x}_i - \dot{x}_{i+1}).(\dot{x}_i - \dot{x}_{i+1})dt$$

$$= \frac{1}{T}\int_0^T C_i(\dot{x}_i - \dot{x}_{i+1})^2 dt \tag{4.8}$$

As already explained above, the energy in the spring is converted back and forth between kinetic and potential energy and no energy is dissipated. So over a complete cycle, the power transfer through spring will be equal to zero. So over a complete cycle, the total average unweighted absorbed power of damper i will be equal to the energy dissipated in the damper.

$$P_i = \frac{1}{T}\int_0^T C_i(\dot{x}_i - \dot{x}_{i+1})^2 dt$$

When the system is subjected to sinusoidal excitation, the total unweighted absorbed power averaged over a complete time cycle can be derived as follows,

Input sinusoidal excitation: $x_i = X_i \sin(\omega t + \phi_i)$

Time period: $T = \frac{2\pi}{\omega}$

So the total unweighted absorbed power for damper C_i averaged over a complete time cycle is

$$P_i = \frac{\omega}{2\pi}\int_0^{2\pi/\omega} C_i\omega^2[X_i\cos(\omega t + \phi_i) - X_{i+1}\cos(\omega t + \phi_{i+1})]^2 dt$$

Solving this integration,

$$P_i = \frac{1}{2}C_i\omega^2[{X_i}^2 - 2X_iX_{i+1}\cos(\phi_i - \phi_{i+1}) + {X_{i+1}}^2] \tag{4.9}$$

Equation 4.9 can be written in terms of transmissibility functions:

$$P_i = \frac{1}{2}C_i\omega^2{X_0}^2\left[\left(\frac{X_i}{X_0}\right)^2 - 2\frac{X_i}{X_0}\frac{X_{i+1}}{X_0}\cos(\phi_i - \phi_{i+1}) + \left(\frac{X_{i+1}}{X_0}\right)^2\right]$$

Assume that transmissibility function at frequency *f* is

$$G_i(f) = \frac{X_i}{X_0}$$

Therefore above equation can be modified as

$$P_i = \frac{1}{2} C_i \omega^2 {X_0}^2 \left[|G_i(f)|^2 - 2|G_i(f)| \cdot |G_{i+1}(f)| \cos(\phi_i - \phi_{i+1}) + |G_{i+1}(f)|^2 \right]$$

$$= \frac{1}{2} C_i [\omega X_0]^2 |G_i(f) - G_{i+1}(f)|^2 \qquad (4.10)$$

Where $G_i(f)$ and $|G_i(f)|$ are the complex and modulus of transmissibility function of mass i whose values are already known. Equation 4.10 is used to calculate unweighted absorbed power for damper C_i. So if the transmissibility function values are known, one can calculate unweighted absorbed using equation 4.10.

Unweighted absorbed power gives power absorbed during exposure to vibration. But it does not consider effect of frequency of vibration. Effect of change in the frequency need to be considered as human body sensitivity to vibration is not fixed but it is varying with respect to frequency. Therefore, concept of weighted absorbed power is used which considers effect of frequency. Frequency weighting factors are developed by International Standards Organization (ISO) and summarized in ISO 2631-1. Frequency weighting factors compensate and normalize human body sensitivity and susceptibility at different frequencies. ISO 2631-1 standard summarizes frequency weighting factors for different direction and different comfort levels.

With the help of this weighting factors and equation 4.10, the weighted absorbed power is calculated as shown in this equation.

$$P_i^w = \frac{1}{2} C_i [W_k(f)]^2 [\omega X_0]^2 |G_i(f) - G_{i+1}(f)|^2 \qquad (4.11)$$

With the help of equation 4.11, the weighted absorbed power is calculated. Weighting factor in equation 4.11 is taken from ISO 2631-1 and it is explained in Chapter 1. By using equation 4.10 and 4.11, the unweighted and weighted absorbed power is calculated for damper C_i.

In the human model explained in Chapter 2, different dampers in horizontal and vertical direction exist. So for all dampers in horizontal and vertical direction, the absorbed power is calculated in similar fashion. Sinusoidal input displacement is given in horizontal and vertical direction independently. At the end the total absorbed power is calculated by taking summation of absorbed power of each damper that is absorbed power of different segments of the body.

For a human model having *n* body segments, initially absorbed power is calculated for individual body segment and the total unweighted absorbed power is calculated by taking summation of individual absorbed power. This is shown in equation 4.12.

$$\begin{aligned} P_{total}^{un} &= \sum_{i=1}^{n} P_i \\ &= \frac{1}{2}[\omega X_0]^2 \sum_{i=1}^{n} C_i \left| G_i(f) - G_{i+1}(f) \right|^2 \end{aligned} \tag{4.12}$$

Similarly, the total weighted absorbed power is calculated as below,

$$P_{total}^{w} = \frac{1}{2}[W_k(f)]^2[\omega X_0]^2 \sum_{i=1}^{n} C_i \left| G_i(f) - G_{i+1}(f) \right|^2 \tag{4.13}$$

Equation 4.12 and 4.13 gives the total unweighted and weighted absorbed power for complete body having *n* body elements in the given frequency range.

4.4 Derivation for Case 1 - Hard seat model

Figure 2.2 shows human model with seat model for Case 1. As shown in this figure, there are springs and dampers at each joint and contact point. First the absorbed power is calculated for these dampers one by one.

At joint J_1, there are two translational dampers, one in the horizontal direction and the other in the vertical direction. So the unweighted absorbed power due to these two dampers is

$$P_{J1\_h} = \frac{1}{2} C_1 [\omega X_0]^2 \left| H_0(f) - H_1(f) \right|^2 \tag{4.14}$$

$$P_{J1\_v} = \frac{1}{2} C_1 [\omega Z_0]^2 \left| V_0(f) - V_1(f) \right|^2 \tag{4.15}$$

Where, P_{J1_h} and P_{J1_v} are the unweighted absorbed power in horizontal (C_1) and vertical (C_1) damper at joint J_1 respectively. H_0 and V_0 are the transmissibility function of ground on which feet are rested whose values are equal to 1 as input is given through ground. H_1 and V_1 are the complex horizontal and vertical transmissibility's of body 1. X_0 and Z_0 are the magnitudes of input displacement in horizontal and vertical direction respectively as shown in Figures 2.2, 2.3 and 2.4.

At joint J_2, Body 1 is connected to Body 2 with one horizontal (C_2) and one vertical (C_2) translational damper. So the unweighted absorbed power due to these two dampers is

$$P_{J2\_h} = \frac{1}{2} C_2 [\omega X_0]^2 \left| H_1(f) - H_2(f) \right|^2 \tag{4.16}$$

$$P_{J2\_v} = \frac{1}{2} C_2 [\omega Z_0]^2 \left| V_1(f) - V_2(f) \right|^2 \tag{4.17}$$

Where, P_{J2_h} and P_{J2_v} in the equation 4.16 and 4.17 are the unweighted absorbed power in horizontal and vertical damper at joint J_2 respectively. H_2 and V_2 are the complex horizontal and vertical transmissibility's of Body 2.

At contact point c_1, there is one horizontal damper C_{h1} and one vertical damper C_{v1} which represents the flexibility of Body 1. The unweighted absorbed power due to these two dampers is shown in the equation 4.18 and 4.19.

$$P_{c1\_h} = \frac{1}{2} C_{h1} [\omega X_0]^2 \left| H_0(f) - H_1(f) \right|^2 \tag{4.18}$$

$$P_{c1\_v} = \frac{1}{2} C_{v1} [\omega Z_0]^2 \left| V_0(f) - V_1(f) \right|^2 \tag{4.19}$$

Where, P_{c1_h} and P_{c1_v} are the unweighted absorbed power due to horizontal (C_{h1}) and vertical (C_{v1}) damper at contact point c_1 respectively.

At contact point C_2, there is a horizontal damper C_{h2} and vertical damper C_{v2} which represents damping of Body 2. The unweighted absorbed power due to these two dampers is shown in equation 4.20 and 4.21.

$$P_{c2\_h} = \frac{1}{2} C_{h2} [\omega X_0]^2 \left| H_0(f) - H_2(f) \right|^2 \tag{4.20}$$

$$P_{c2\_v} = \frac{1}{2} C_{v2} [\omega Z_0]^2 \left| V_0(f) - V_2(f) \right|^2 \tag{4.21}$$

Where, P_{c2_h} and P_{c2_v} are the unweighted absorbed power due to horizontal (C_{h2}) and vertical (C_{v2}) damper at contact point c_2, respectively.

At joint J_3, there is one horizontal (C_3) and one vertical (C_3) damper connecting Body 2 with body 3. The unweighted absorbed power due to these two dampers is expressed in equation 4.22 and 4.23.

$$P_{J3\_h} = \frac{1}{2} C_3 [\omega X_0]^2 \left| H_2(f) - H_3(f) \right|^2 \tag{4.22}$$

$$P_{J3\_v} = \frac{1}{2} C_3 [\omega Z_0]^2 \left| V_2(f) - V_3(f) \right|^2 \tag{4.23}$$

Where, P_{J3_h} and P_{J3_v} are the unweighted absorbed power due to horizontal (C_3) and vertical (C_3) damper at joint J_3 respectively. H_3 and V_3 are the complex horizontal and vertical transmissibility's of body 3.

At point c_{25}, damper C_{v5} connects Body 2 with Body 5. This damper is inclined at an angle β with horizontal as shown in the figure 2.2. So the expression for unweighted absorbed power is derived separately based on previous formulation by considering displacement along inclined plane. Following equation 4.24 gives the unweighted absorbed power due to damper C_{v5}.

$$P_{c25} = \frac{1}{2} C_{v5} \omega^2 \begin{Bmatrix} [X_0 \cdot \cos\beta \cdot |H_5(f) - H_2(f)|]^2 + [Z_0 \cdot \sin\beta \cdot |V_5(f) - V_2(f)|]^2 \\ -X_0 Z_0 \sin(2\beta)[|H_5(f)||V_5(f)| + |H_2(f)||V_2(f)| \\ -(|H_5(f)||V_2(f)| + |H_2(f)||V_5(f)|)\cos(\phi_5 - \phi_2)] \end{Bmatrix} \quad (4.24)$$

Where P_{c25} is the unweighted absorbed power in damper C_{v5}. H_5 and V_5 are the complex transmissibility functions and $|H_5|$ and $|V_5|$ are modulus of transmissibility functions of Body 5 in horizontal and vertical direction respectively. In this equation, $\phi 5$ and $\phi 2$ are the phase angle of Body 5 and Body 2.

At joint J_4, there is a horizontal (C_4) and vertical (C_4) damper which connects Body 3 and Body 4. The unweighted absorbed power can be calculated in the similar fashion and shown in equation 4.25 and 4.26.

$$P_{J4\_h} = \frac{1}{2} C_4 [\omega X_0]^2 |H_3(f) - H_4(f)|^2 \quad (4.25)$$

$$P_{J4\_v} = \frac{1}{2} C_4 [\omega Z_0]^2 |V_3(f) - V_4(f)|^2 \quad (4.26)$$

Where, P_{J4_h} and P_{J4_v} are the unweighted absorbed power due to horizontal (C_4) and vertical (C_4) damper at joint J_4, respectively. H_4 and V_4 are the complex horizontal and vertical transmissibility's of Body 4.

At point c_{35} , damper C_{h5} connects Body 3 with Body 5. This damper is at an angle γ with horizontal as shown in the figure 2.2. So the expression for unweighted absorbed power is derived separately based on previous formulation by considering displacement

along inclined plane. Following equation 4.27 gives the unweighted absorbed power due to damper C_{h5}.

$$P_{c35} = \frac{1}{2} C_{h5} \omega^2 \begin{Bmatrix} [X_0 \cdot \cos\gamma \cdot |H_5(f) - H_3(f)|]^2 + [Z_0 \cdot \sin\gamma \cdot |V_5(f) - V_3(f)|]^2 \\ + X_0 Z_0 \sin(2\gamma)[|H_5(f)||V_5(f)| + |H_3(f)||V_3(f)| \\ -(|H_5(f)||V_3(f)| + |H_3(f)||V_5(f)|)\cos(\phi_5 - \phi_3)] \end{Bmatrix} \quad (4.27)$$

The contact point of human torso (Body 3) with seat backrest is c_3 . At this point, there are two dampers representing horizontal and vertical damping of human torso. Damper perpendicular to torso is C_{v3} representing vertical damping and damper parallel to torso is C_{h3} representing horizontal damping of Body 3. As backrest support is considered in this model at an angle α, we need to consider this angle during calculation of absorbed power due to damper C_{h3} and C_{v3}. For these two dampers, unweighted absorbed power is derived separately based on previous formulation by considering displacement along inclined plane and shown in equation 4.28 and 4.29.

The unweighted absorbed power due to damper C_{v3} is,

$$P_{c3\_v} = \frac{1}{2} C_{v3} \omega^2 \begin{Bmatrix} [X_0 \cdot \cos\alpha \cdot |1 - H_3(f)|]^2 + [Z_0 \cdot \sin\alpha \cdot |1 - V_3(f)|]^2 \\ + X_0 Z_0 \sin(2\alpha)[1 + |H_3(f)||V_3(f)| - (|V_3(f)| + |H_3(f)|)\cos\phi_3] \end{Bmatrix} \quad (4.28)$$

The unweighted absorbed power due to damper C_{h3} is,

$$P_{c3\_h} = \frac{1}{2} C_{h3} \omega^2 \begin{Bmatrix} [X_0 \cdot \sin\alpha \cdot |1 - H_3(f)|]^2 + [Z_0 \cdot \cos\alpha \cdot |1 - V_3(f)|]^2 \\ - X_0 Z_0 \sin(2\alpha)[1 + |H_3(f)||V_3(f)| - (|H_3(f)| + |V_3(f)|)\cos\phi_3] \end{Bmatrix} \quad (4.29)$$

The individual absorbed power is calculated for all the dampers. Equations 4.14 to 4.29 give the unweighted absorbed power due to each translational damper in human model. Using equation 4.12, the total unweighted absorbed power of human model is calculated

by taking summation of individual absorbed power of all dampers. This will give the total unweighted absorbed power (P_{total}^{un}) of human model.

$$\begin{aligned} P_{total}^{un} &= P_{J1\_h} + P_{J1\_v} + P_{J2\_h} + P_{J2\_v} + P_{J3\_h} + P_{J3\_v} + P_{J4\_h} + P_{J4\_v} \\ &+ P_{c1\_h} + P_{c1\_v} + P_{c2\_h} + P_{c2\_v} + P_{c3\_h} + P_{c3\_v} + P_{c25} + P_{c35} \end{aligned} \tag{4.30}$$

Equation 4.30 gives total unweighted absorbed power of human model due to all translational dampers transferred to human body in Case 1.

As discussed in the last section, human body response is frequency dependent. So by using frequency weighting factors, the weighted absorbed power needs to calculate. The weighted absorbed power can be calculated by multiplying above all equations by square of respective weighting factor. First individual weighted absorbed power is calculated for all dampers separately and then summation is taken.

$$P_{J1\_h}^{w} = \frac{1}{2} C_1 [W_d(f)]^2 [\omega X_0]^2 \left| H_0(f) - H_1(f) \right|^2 \tag{4.31}$$

$$P_{J1\_v}^{w} = \frac{1}{2} C_1 [W_k(f)]^2 [\omega Z_0]^2 \left| V_0(f) - V_1(f) \right|^2 \tag{4.32}$$

$$P_{J2\_h}^{w} = \frac{1}{2} C_2 [W_d(f)]^2 [\omega X_0]^2 \left| H_1(f) - H_2(f) \right|^2 \tag{4.33}$$

$$P_{J2\_v}^{w} = \frac{1}{2} C_2 [W_k(f)]^2 [\omega Z_0]^2 \left| V_1(f) - V_2(f) \right|^2 \tag{4.34}$$

$$P_{c1\_h}^{w} = \frac{1}{2} C_{h1} [W_d(f)]^2 [\omega X_0]^2 \left| H_0(f) - H_1(f) \right|^2 \tag{4.35}$$

$$P_{c1\_v}^{w} = \frac{1}{2} C_{v1} [W_k(f)]^2 [\omega Z_0]^2 \left| V_0(f) - V_1(f) \right|^2 \tag{4.36}$$

$$P_{c2\_h}^{w} = \frac{1}{2} C_{h2} [W_d(f)]^2 [\omega X_0]^2 \left| H_0(f) - H_2(f) \right|^2 \tag{4.37}$$

$$P_{c2\_v}^{w} = \frac{1}{2} C_{v2} [W_k(f)]^2 [\omega Z_0]^2 \left| V_0(f) - V_2(f) \right|^2 \tag{4.38}$$

$$P_{J3\_h}^{w} = \frac{1}{2} C_3 [W_d(f)]^2 [\omega X_0]^2 \left| H_2(f) - H_3(f) \right|^2 \tag{4.39}$$

$$P_{J3\_v}^{w} = \frac{1}{2} C_3 [W_k(f)]^2 [\omega Z_0]^2 \left| V_2(f) - V_3(f) \right|^2 \tag{4.40}$$

$$P_{c25}^{w} = \frac{1}{2} C_{v5} \omega^2 [W_k(f)]^2 \begin{Bmatrix} [X_0 \cdot \cos\beta \cdot \left| H_5(f) - H_2(f) \right|]^2 \\ +[Z_0 \cdot \sin\beta \cdot \left| V_5(f) - V_2(f) \right|]^2 \\ -X_0 Z_0 \sin(2\beta)[\left| H_5(f) \right| \left| V_5(f) \right| + \left| H_2(f) \right| \left| V_2(f) \right| \\ -(\left| H_5(f) \right| \left| V_2(f) \right| + \left| H_2(f) \right| \left| V_5(f) \right|) \cos(\phi_5 - \phi_2)] \end{Bmatrix} \tag{4.41}$$

$$P_{J4\_h}^{w} = \frac{1}{2} C_4 [W_d(f)]^2 [\omega X_0]^2 \left| H_3(f) - H_4(f) \right|^2 \tag{4.42}$$

$$P_{J4\_v}^{w} = \frac{1}{2} C_4 [W_k(f)]^2 [\omega Z_0]^2 \left| V_3(f) - V_4(f) \right|^2 \tag{4.43}$$

$$P_{c35}^{w} = \frac{1}{2} C_{h5} \omega^2 [W_d(f)]^2 \begin{Bmatrix} [X_0 \cdot \cos\gamma \cdot \left| H_5(f) - H_3(f) \right|]^2 \\ +[Z_0 \cdot \sin\gamma \cdot \left| V_5(f) - V_3(f) \right|]^2 \\ +X_0 Z_0 \sin(2\gamma)[\left| H_5(f) \right| \left| V_5(f) \right| + \left| H_3(f) \right| \left| V_3(f) \right| \\ -(\left| H_5(f) \right| \left| V_3(f) \right| + \left| H_3(f) \right| \left| V_5(f) \right|) \cos(\phi_5 - \phi_3)] \end{Bmatrix} \tag{4.44}$$

$$P_{c3\_v}^{w} = \frac{1}{2} C_{v3} \omega^2 [W_c(f)]^2 \begin{Bmatrix} [X_0 \cdot \cos\alpha \cdot \left| 1 - H_3(f) \right|]^2 \\ +[Z_0 \cdot \sin\alpha \cdot \left| 1 - V_3(f) \right|]^2 \\ +X_0 Z_0 \sin(2\alpha)[1 + \left| H_3(f) \right| \left| V_3(f) \right| \\ -(\left| V_3(f) \right| + \left| H_3(f) \right|) \cos\phi_3] \end{Bmatrix} \tag{4.45}$$

$$P_{c3\_h}^{w} = \frac{1}{2} C_{h3} \omega^2 [W_c(f)]^2 \begin{Bmatrix} [X_0 \cdot \sin\alpha \cdot |1 - H_3(f)|]^2 + [Z_0 \cdot \cos\alpha \cdot |1 - V_3(f)|]^2 \\ -X_0 Z_0 \sin(2\alpha)[1 + |H_3(f)||V_3(f)| \\ -(|H_3(f)| + |V_3(f)|)\cos\phi_3] \end{Bmatrix} \quad (4.46)$$

Where, three types of weighting factors are used. W_k is used for vibrations in Z direction, W_d is used for vibrations in X and Y direction and W_c is used for vibrations at seat-back interaction. These weighting factors are function of frequencies and it is given in the frequency range of 0.1 Hz to 400 Hz. These equations 4.31 to 4.46 gives weighted absorbed power due to each damper at each location. At each point, same notation as unweighted absorbed power is used for this power to avoid confusion except underscore w is added in front of each notation for the weighted absorbed power. In these equations frequency weighting factors are obtained from ISO 2631-1 and are summarized in Table 1.3.

The total weighted absorbed power (P_{total}^{w}) is calculated by taking summation of individual absorbed power of all dampers in equation 4.31 to 4.46 as shown in equation 4.47.

$$\begin{aligned} P_{total}^{w} = {} & P_{J1\_h}^{w} + P_{J1\_v}^{w} + P_{J2\_h}^{w} + P_{J2\_v}^{w} + P_{J3\_h}^{w} + P_{J3\_v}^{w} + P_{J4\_h}^{w} + P_{J4\_v}^{w} \\ & + P_{c1\_h}^{w} + P_{c1\_v}^{w} + P_{c2\_h}^{w} + P_{c2\_v}^{w} + P_{c3\_h}^{w} + P_{c3\_v}^{w} + P_{c25}^{w} + P_{c35}^{w} \end{aligned} \quad (4.47)$$

Equation 4.30 and 4.47 gives the total unweighted and weighted absorbed power of human model for hard seat in Case 1.

4.5 Derivation for Case 2 and Case 3

For Case 2, seat and backrest cushion is added and for Case 3, seat suspension and seat and backrest cushion are added. Due to this, expressions for the both absorbed power are changed at some locations like contact points with seat and backrest support cushion.

At contact point c_1, the unweighted absorbed power is calculated using following equation 4.48 and 4.49.

$$P_{c1\_h} = \frac{1}{2} C_{h1} [\omega X_0]^2 \left| H_C(f) - H_1(f) \right|^2 \tag{4.48}$$

$$P_{c1\_v} = \frac{1}{2} C_{v1} [\omega Z_0]^2 \left| V_C(f) - V_1(f) \right|^2 \tag{4.49}$$

Where, H_c and V_c are the complex horizontal and vertical transmissibility's of seat cushion.

In the similar ways, the weighted absorbed power at contact point c_1 is calculated using following equation 4.50 and 4.51.

$$P^w_{c1\_h} = \frac{1}{2} C_{h1} [W_k(f)]^2 [\omega X_0]^2 \left| H_C(f) - H_1(f) \right|^2 \tag{4.50}$$

$$P^w_{c1\_v} = \frac{1}{2} C_{v1} [W_d(f)]^2 [\omega Z_0]^2 \left| V_C(f) - V_1(f) \right|^2 \tag{4.51}$$

At contact point c_2, the unweighted absorbed power is calculated as shown in equation 4.52 and 4.53

$$P_{c2\_h} = \frac{1}{2} C_{h2} [\omega X_0]^2 \left| H_C(f) - H_2(f) \right|^2 \tag{4.52}$$

$$P_{c2\_v} = \frac{1}{2} C_{v2} [\omega Z_0]^2 \left| V_C(f) - V_2(f) \right|^2 \tag{4.53}$$

In the similar ways, the weighted absorbed power at contact point c_2 is calculated using following equations 4.54 and 4.55.

$$P^w_{c2\_h} = \frac{1}{2} C_{h2} [W_k(f)]^2 [\omega X_0]^2 \left| H_C(f) - H_2(f) \right|^2 \tag{4.54}$$

$$P_{c2\_v}^{w} = \frac{1}{2} C_{v2} [W_d(f)]^2 [\omega Z_0]^2 \left| V_C(f) - V_2(f) \right|^2 \tag{4.55}$$

At contact point c_3, the unweighted absorbed power is calculated as shown in equation 4.56 and 4.57.

$$P_{c3\_v} = \frac{1}{2} C_{v3} \omega^2 \begin{Bmatrix} [X_0 \cdot \cos\alpha \cdot |H_3(f) - H_{bc}(f)|]^2 + [Z_0 \cdot \sin\alpha \cdot |V_3(f) - V_{bc}(f)|]^2 \\ + X_0 Z_0 \sin(2\alpha)[|H_{bc}(f)||V_{bc}(f)| + |H_3(f)||V_3(f)| \\ -(|H_{bc}(f)||V_3(f)| + |H_3(f)||V_{bc}(f)|)\cos(\phi_3 - \phi_{bc})] \end{Bmatrix} \tag{4.56}$$

$$P_{c3\_h} = \frac{1}{2} C_{h3} \omega^2 \begin{Bmatrix} [X_0 \cdot \sin\alpha \cdot |H_{bc}(f) - H_3(f)|]^2 + [Z_0 \cdot \cos\alpha \cdot |V_{bc}(f) - V_3(f)|]^2 \\ - X_0 Z_0 \sin(2\alpha) \cdot [|H_{bc}(f)||V_{bc}(f)| + |H_3(f)||V_3(f)| \\ -(|H_3(f)||V_{bc}(f)| + |H_{bc}(f)||V_3(f)|)\cos(\phi_{bc} - \phi_3)] \end{Bmatrix} \tag{4.57}$$

In the similar ways, the weighted absorbed power at contact point c_3 is calculated using following equations 4.58 and 4.59.

$$P_{c3\_v}^{w} = \frac{1}{2} C_{v3} \omega^2 [W_c(f)]^2 \cdot \begin{Bmatrix} [X_0 \cdot \cos\alpha \cdot |H_3(f) - H_{bc}(f)|]^2 \\ + [Z_0 \cdot \sin\alpha \cdot |V_3(f) - V_{bc}(f)|]^2 \\ + X_0 Z_0 \sin(2\alpha)[|H_{bc}(f)||V_{bc}(f)| + |H_3(f)||V_3(f)| \\ -(|H_{bc}(f)||V_3(f)| + |H_3(f)||V_{bc}(f)|)\cos(\phi_3 - \phi_{bc})] \end{Bmatrix} \tag{4.58}$$

$$P_{c3\_h}^{w} = \frac{1}{2} C_{h3} \omega^2 [W_c(f)]^2 \cdot \begin{Bmatrix} [X_0 \cdot \sin\alpha \cdot |H_{bc}(f) - H_3(f)|]^2 \\ + [Z_0 \cdot \cos\alpha \cdot |V_{bc}(f) - V_3(f)|]^2 \\ - X_0 Z_0 \sin(2\alpha) \cdot [|H_{bc}(f)||V_{bc}(f)| + |H_3(f)||V_3(f)| \\ -(|H_3(f)||V_{bc}(f)| + |H_{bc}(f)||V_3(f)|)\cos(\phi_{bc} - \phi_3)] \end{Bmatrix} \tag{4.59}$$

For both Cases 2 and 3, the remaining points like C_{25}, C_{35} and joints J_1, J_2, J_3 and J_4, the expression for unweighted and weighted absorbed power are same and are calculated using same expressions as that of Case 1. After this, the total unweighted and weighted absorbed power of human model is calculated using equations 4.30 and 4.47 for Case 2 and Case 3 separately.

4.6 Plots of absorbed power under sinusoidal displacement excitation

At this stage, all expressions for the total unweighted and weighted absorbed power for all three cases are obtained. One can plot these absorbed power as a function of frequency for three cases together. There are two plots, the first is frequency verses unweighted absorbed power and the second one is frequency verses weighted absorbed power.

Assume that the system is excited by following sinusoidal excitation with constant amplitude of displacement.

$$\text{X-direction: } x_0 = X_0 \sin \omega t, \textit{ where } X_0 = 0.005\,\text{m}$$
$$\text{Z-direction : } z_o = Z_0 \sin \omega t, \textit{ where } Z_0 = 0.005\,\text{m}$$

Figure 4.2 illustrates frequency verses unweighted absorbed power for all three cases. Figure 4.3 illustrates frequency verses weighted absorbed power for three cases. Both are the results by considering constant displacement input in frequency range of 0 Hz to 20 Hz.

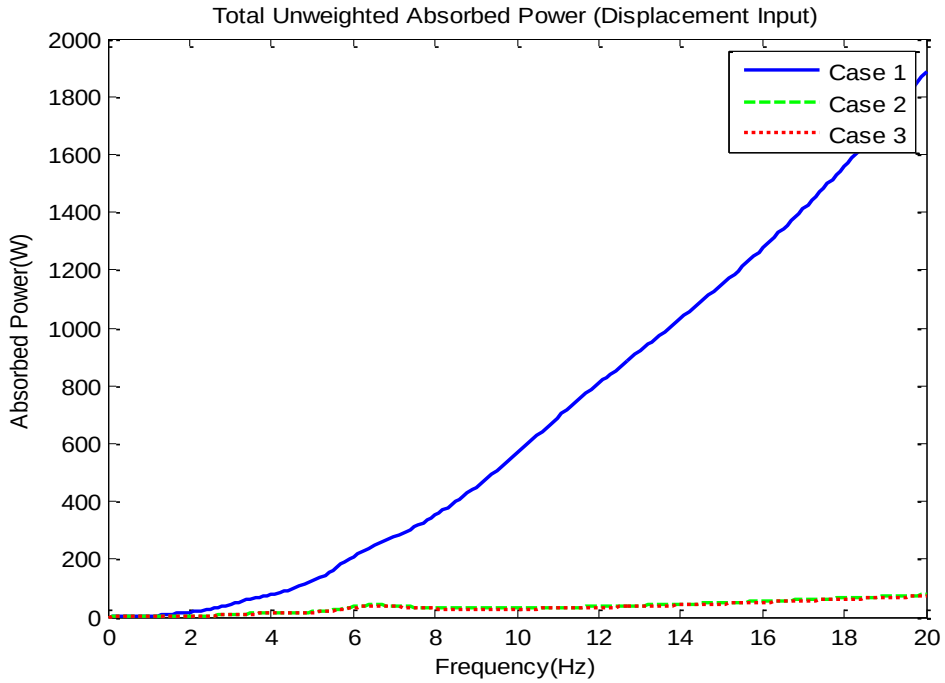

Figure 4.2 Frequency verses unweighted absorbed power (Displacement Input)

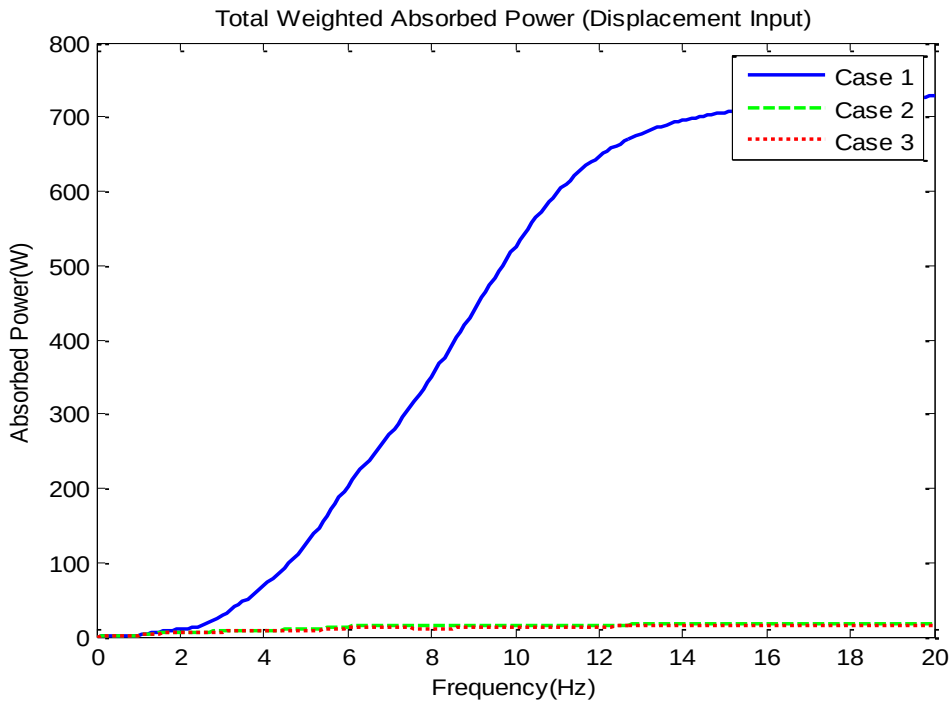

Figure 4.3 Frequency verses weighted absorbed power (Displacement Input)

For hard seat (Case 1), the magnitude of both unweighted and weighted absorbed power is very high for all frequencies in given range in comparison with Case 2 and 3. This is clearly seen in both the Figures 4.2 and 4.3. This is because there is nothing to isolate human body from input vibration and all the input vibrations get transferred to human body. This results in higher values of absorbed power which resembles to high fatigue. For Case 2, the magnitude of absorbed power is substantially reduced as shown in Figure 4.2 and 4.3. This is because the seat and backrest cushion isolates human body from vibration to some extent. So absorbed power values are reduced but still it is higher than Case 3. This absorbed power value in Case 3 is very small in comparison with Case 1 and 2. This is because in Case 3, human body is isolated using seat suspension and seat and backrest cushion. This arrangement isolates human body from input vibrations. So for isolated seat, human body will feel very less fatigue.

The plots in the Figure 4.2 and 4.3 illustrate the unweighted and weighted absorbed power over a range of frequency and compare the absorbed power for three cases. From

these plots, we know the absorbed power values for each frequency for all three cases. So as shown in the equation 4.60 and 4.61 for unweighted and weighted, if we add these values together for all the frequencies, we will get one number which will give a numerical value of total absorbed power in the given frequency range. This is similar to discretizing these plots.

$$P_{total}^{un} = \sum_{i=1}^{20} P_{total}^{un}(f_i) \tag{4.60}$$

$$P_{total}^{w} = \sum_{i=1}^{20} P_{total}^{w}(f_i) \tag{4.61}$$

The total unweighted absorbed power is calculated using equation 4.60 and the total weighted absorbed power is calculated using equation 4.61 in the given frequency range. These quantities are scalar numerical values. As suggested by Pradko and Lee (1965, 1966) we can use this total absorbed power to represent fatigue of human body. Summation is taken for all three cases and for comparing bar plots are used. Figure 4.4 and 4.5 shows bar plots comparing the total unweighted and weighted absorbed power for three cases.

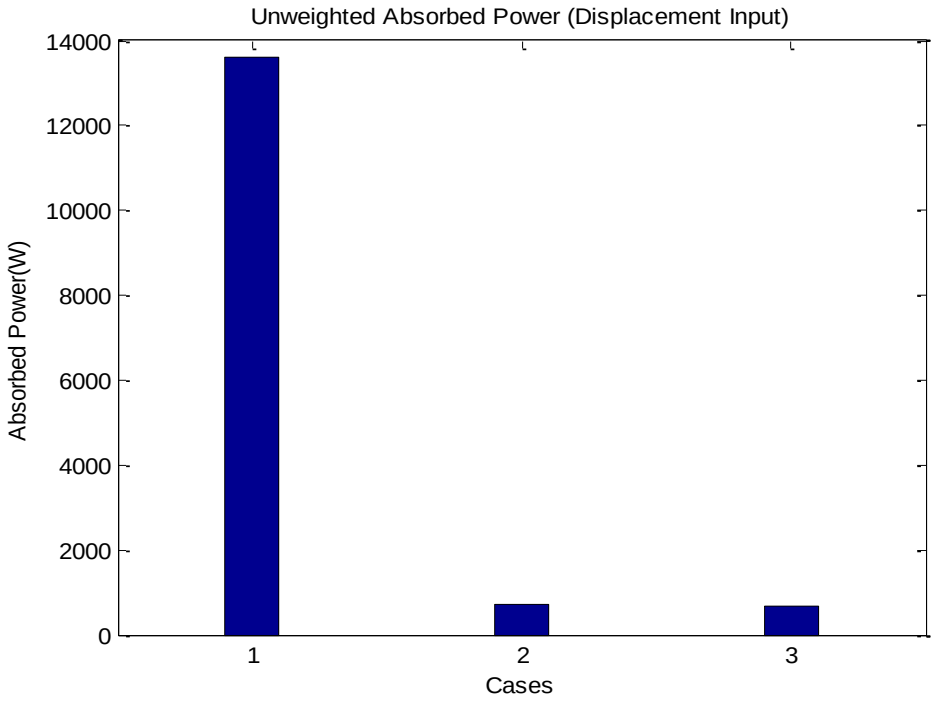

Figure 4.4 Total unweighted absorbed power for 3 cases (Displacement Input)

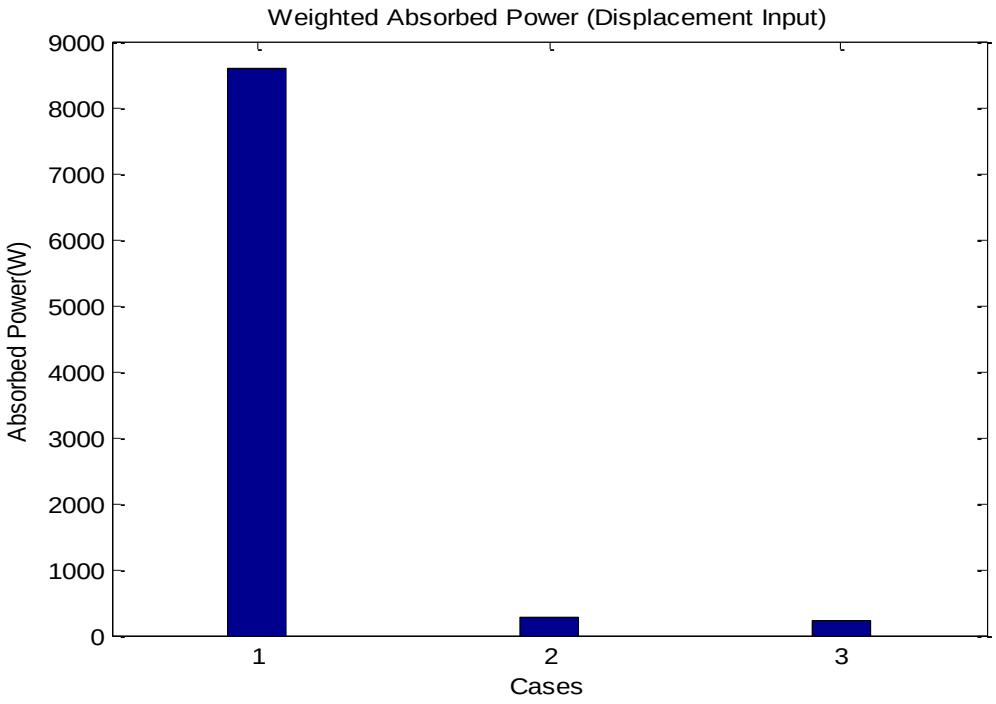

Figure 4.5 Total weighted absorbed power for 3 cases (Displacement Input)

Figure 4.4 and 4.5 compares the unweighted and weighted absorbed power for Case 1, 2 and 3. These bar plots compares respective unweighted and weighted absorbed power for these three cases. There numerical values are summarized in Table 4.1.

Table 4.1 Total unweighted and weighted absorbed power for 3 cases (Displacement)

	Displacement Input	
	Unweighted AP (W)	Weighted AP (W)
Case 1	13604	8591.4
Case 2	706.69	268.59
Case 3	655.88	234.72

From these values it is very clear that absorbed power for Case 2 is substantially reduced in comparison with Case 1. Also absorbed power in Case 3 is also reduced in comparison with Case 1 and 2. This clearly concludes that human body will get very less fatigue in Case 3 in comparison with Case 1 and 2.

4.7 Absorbed power under constant amplitude of acceleration excitation

In previous section, the absorbed power is calculated for different body parts under constant sinusoidal displacement. But it is not fully meaningful to calculate absorbed power at higher frequencies under constant sinusoidal displacement. This is because it is not realistic to have constant displacement at higher frequencies. For example, when human body is subjected to constant sinusoidal displacement of amplitude 0.005 m at excitation frequency of 20 Hz, the resultant acceleration will be $0.005x(2\pi x20)^2$ = 79 m/s^2. This value is unrealistically high and in practical life there is very less chance of getting this kind of high vibrations during vehicle driving.

So in this section absorbed power is calculated under input excitation with constant amplitude of acceleration. The relationship between amplitudes of acceleration and displacement in equation 4.62 is used.

$$A_0 = X_0(\omega)^2 \tag{4.62}$$

The left hand side of equation 4.62 (amplitude of acceleration) is constant and the right hand side quantities (that is amplitude of displacement and angular velocity) should change in such a way that their multiplication result in a constant value.

In this model, input excitations are given in X and Z directions independently. Let's assume A_{x0} and A_{z0} are the amplitudes of input accelerations in horizontal and vertical direction, respectively.

Following are the expressions derived for the unweighted absorbed power by considering constant amplitude of acceleration for Case 1. Same notations are used as previous section for absorbed power at each point and joints for avoiding confusion.

$$P_{J1\_h} = \frac{1}{2} C_1 \left[\frac{A_{x0}}{\omega} \right]^2 \left| H_0(f) - H_1(f) \right|^2 \tag{4.63}$$

$$P_{J1\_v} = \frac{1}{2} C_1 \left[\frac{A_{z0}}{\omega} \right]^2 \left| V_0(f) - V_1(f) \right|^2 \tag{4.64}$$

$$P_{J2\_h} = \frac{1}{2} C_2 \left[\frac{A_{x0}}{\omega} \right]^2 \left| H_1(f) - H_2(f) \right|^2 \tag{4.65}$$

$$P_{J2\_v} = \frac{1}{2} C_2 \left[\frac{A_{z0}}{\omega} \right]^2 \left| V_1(f) - V_2(f) \right|^2 \tag{4.66}$$

$$P_{J3\_h} = \frac{1}{2} C_3 \left[\frac{A_{x0}}{\omega} \right]^2 \left| H_2(f) - H_3(f) \right|^2 \tag{4.67}$$

$$P_{J3\_v} = \frac{1}{2} C_3 \left[\frac{A_{z0}}{\omega} \right]^2 \left| V_2(f) - V_3(f) \right|^2 \tag{4.68}$$

$$P_{J4\_h} = \frac{1}{2} C_4 \left[\frac{A_{x0}}{\omega} \right]^2 \left| H_3(f) - H_4(f) \right|^2 \tag{4.69}$$

$$P_{J4\_v} = \frac{1}{2} C_4 \left[\frac{A_{z0}}{\omega} \right]^2 \left| V_3(f) - V_4(f) \right|^2 \tag{4.70}$$

$$P_{c1\_h} = \frac{1}{2} C_{h1} \left[\frac{A_{x0}}{\omega} \right]^2 \left| H_0(f) - H_1(f) \right|^2 \tag{4.71}$$

$$P_{c1\_v} = \frac{1}{2} C_{v1} \left[\frac{A_{z0}}{\omega} \right]^2 \left| V_0(f) - V_1(f) \right|^2 \tag{4.72}$$

$$P_{c2\_h} = \frac{1}{2} C_{h2} \left[\frac{A_{x0}}{\omega} \right]^2 \left| H_0(f) - H_2(f) \right|^2 \tag{4.73}$$

$$P_{c2\_v} = \frac{1}{2} C_{v2} \left[\frac{A_{z0}}{\omega} \right]^2 \left| V_0(f) - V_2(f) \right|^2 \tag{4.74}$$

$$P_{c3\_v} = \frac{1}{2} C_{v3} \left\{ \begin{array}{l} \left[\frac{A_{x0}}{\omega} \cdot \cos\alpha \cdot \left| 1 - H_3(f) \right| \right]^2 + \left[\frac{A_{z0}}{\omega} \cdot \sin\alpha \cdot \left| 1 - V_3(f) \right| \right]^2 \\ + \left(\frac{A_{x0} A_{z0}}{\omega^2} \right) \sin(2\alpha) [1 + \left| H_3(f) \right| \left| V_3(f) \right| - (\left| V_3(f) \right| + \left| H_3(f) \right|) \cos\phi_3] \end{array} \right\} \tag{4.75}$$

$$P_{c3\_h} = \frac{1}{2} C_{h3} \left\{ \begin{array}{l} \left[\frac{A_{x0}}{\omega} \cdot \sin\alpha \cdot \left| 1 - H_3(f) \right| \right]^2 + \left[\frac{A_{z0}}{\omega} \cdot \cos\alpha \cdot \left| 1 - V_3(f) \right| \right]^2 \\ - \left(\frac{A_{x0} A_{z0}}{\omega^2} \right) \sin(2\alpha) [1 + \left| H_3(f) \right| \left| V_3(f) \right| - (\left| H_3(f) \right| + \left| V_3(f) \right|) \cos\phi_3] \end{array} \right\} \tag{4.76}$$

$$P_{c25} = \frac{1}{2} C_{v5} \left\{ \begin{array}{l} \left[\frac{A_{x0}}{\omega} \cdot \cos\beta \cdot \left| H_5(f) - H_2(f) \right| \right]^2 + \left[\frac{A_{z0}}{\omega} \cdot \sin\beta \cdot \left| V_5(f) - V_2(f) \right| \right]^2 \\ - \left(\frac{A_{x0} A_{z0}}{\omega^2} \right) \sin(2\beta) [\left| H_5(f) \right| \left| V_5(f) \right| + \left| H_2(f) \right| \left| V_2(f) \right| \\ - (\left| H_5(f) \right| \left| V_2(f) \right| + \left| H_2(f) \right| \left| V_5(f) \right|) \cos(\phi_5 - \phi_2)] \end{array} \right\} \tag{4.77}$$

$$P_{c35}=\frac{1}{2}C_{h5}\begin{Bmatrix}\left[\frac{A_{x0}}{\omega}\cdot\cos\gamma\cdot\left|H_5(f)-H_3(f)\right|\right]^2+\left[\frac{A_{z0}}{\omega}\cdot\sin\gamma\cdot\left|V_5(f)-V_3(f)\right|\right]^2\\+\left(\frac{A_{x0}A_{z0}}{\omega^2}\right)\sin(2\gamma)[\left|H_5(f)\right|\left|V_5(f)\right|+\left|H_3(f)\right|\left|V_3(f)\right|\\-(\left|H_5(f)\right|\left|V_3(f)\right|+\left|H_3(f)\right|\left|V_5(f)\right|)\cos(\phi_5-\phi_3)]\end{Bmatrix} \quad (4.78)$$

Equation 4.63 to 4.78 gives the unweighted absorbed power due to each individual translational damper considering constant amplitude of acceleration input. As shown in equation 4.79, the total unweighted absorbed power (P_{total}^{un}) is calculated by taking summation of individual absorbed power of all dampers.

$$\begin{aligned}P_{total}^{un}&=P_{J1\_h}+P_{J1\_v}+P_{J2\_h}+P_{J2\_v}+P_{J3\_h}+P_{J3\_v}+P_{J4\_h}+P_{J4\_v}\\&+P_{c1\_h}+P_{c1\_v}+P_{c2\_h}+P_{c2\_v}+P_{c3\_h}+P_{c3\_v}+P_{c25}+P_{c35}\end{aligned} \quad (4.79)$$

Equation 4.79 gives the total unweighted absorbed power of human model considering constant amplitude of acceleration input for Case 1.

Similarly expressions are obtained for the weighted absorbed power by considering constant amplitude of acceleration for Case 1. These equations are expressed from equation 4.80 to 4.95.

$$P_{J1\_h}^{w}=\frac{1}{2}C_1\left[\frac{W_d(f)A_{x0}}{\omega}\right]^2\left|H_0(f)-H_1(f)\right|^2 \quad (4.80)$$

$$P_{J1\_v}^{w}=\frac{1}{2}C_1\left[\frac{W_k(f)A_{z0}}{\omega}\right]^2\left|V_0(f)-V_1(f)\right|^2 \quad (4.81)$$

$$P_{J2\_h}^{w}=\frac{1}{2}C_2\left[\frac{W_d(f)A_{x0}}{\omega}\right]^2\left|H_1(f)-H_2(f)\right|^2 \quad (4.82)$$

$$P_{J2\_v}^{w} = \frac{1}{2} C_2 \left[\frac{W_k(f) A_{z0}}{\omega} \right]^2 \left| V_1(f) - V_2(f) \right|^2 \tag{4.83}$$

$$P_{J3\_h}^{w} = \frac{1}{2} C_3 \left[\frac{W_d(f) A_{x0}}{\omega} \right]^2 \left| H_2(f) - H_3(f) \right|^2 \tag{4.84}$$

$$P_{J3\_v}^{w} = \frac{1}{2} C_3 \left[\frac{W_k(f) A_{z0}}{\omega} \right]^2 \left| V_2(f) - V_3(f) \right|^2 \tag{4.85}$$

$$P_{J4\_h}^{w} = \frac{1}{2} C_4 \left[\frac{W_d(f) A_{x0}}{\omega} \right]^2 \left| H_3(f) - H_4(f) \right|^2 \tag{4.86}$$

$$P_{J4\_v}^{w} = \frac{1}{2} C_4 \left[\frac{W_k(f) A_{z0}}{\omega} \right]^2 \left| V_3(f) - V_4(f) \right|^2 \tag{4.87}$$

$$P_{c1\_h}^{w} = \frac{1}{2} C_{h1} \left[\frac{W_d(f) A_{x0}}{\omega} \right]^2 \left| H_0(f) - H_1(f) \right|^2 \tag{4.88}$$

$$P_{c1\_v}^{w} = \frac{1}{2} C_{v1} \left[\frac{W_k(f) A_{z0}}{\omega} \right]^2 \left| V_0(f) - V_1(f) \right|^2 \tag{4.89}$$

$$P_{c2\_h}^{w} = \frac{1}{2} C_{h2} \left[\frac{W_d(f) A_{x0}}{\omega} \right]^2 \left| H_0(f) - H_2(f) \right|^2 \tag{4.90}$$

$$P_{c2\_v}^{w} = \frac{1}{2} C_{v2} \left[\frac{W_k(f) A_{z0}}{\omega} \right]^2 \left| V_0(f) - V_2(f) \right|^2 \tag{4.91}$$

$$P_{c3\_v}^{w} = \frac{1}{2} C_{v3} [W_c(f)]^2 \begin{Bmatrix} \left[\frac{A_{x0}}{\omega} \cdot \cos\alpha \cdot |1 - H_3(f)| \right]^2 + \left[\frac{A_{z0}}{\omega} \cdot \sin\alpha \cdot |1 - V_3(f)| \right]^2 \\ + \left(\frac{A_{x0} A_{z0}}{\omega^2} \right) \sin(2\alpha) [1 + |H_3(f)||V_3(f)| \\ - (|V_3(f)| + |H_3(f)|) \cos\phi_3] \end{Bmatrix} \quad (4.92)$$

$$P_{c3\_h}^{w} = \frac{1}{2} C_{h3} [W_c(f)]^2 \begin{Bmatrix} \left[\frac{A_{x0}}{\omega} \cdot \sin\alpha \cdot |1 - H_3(f)| \right]^2 + \left[\frac{A_{z0}}{\omega} \cdot \cos\alpha \cdot |1 - V_3(f)| \right]^2 \\ - \left(\frac{A_{x0} A_{z0}}{\omega^2} \right) \sin(2\alpha) [1 + |H_3(f)||V_3(f)| \\ - (|H_3(f)| + |V_3(f)|) \cos\phi_3] \end{Bmatrix} \quad (4.93)$$

$$P_{c25}^{w} = \frac{1}{2} C_{v5} [W_k(f)]^2 \begin{Bmatrix} \left[\frac{A_{x0}}{\omega} \cdot \cos\beta \cdot |H_5(f) - H_2(f)| \right]^2 \\ + \left[\frac{A_{z0}}{\omega} \cdot \sin\beta \cdot |V_5(f) - V_2(f)| \right]^2 \\ - \left(\frac{A_{x0} A_{z0}}{\omega^2} \right) \sin(2\beta) [|H_5(f)||V_5(f)| + |H_2(f)||V_2(f)| \\ - (|H_5(f)||V_2(f)| + |H_2(f)||V_5(f)|) \cos(\phi_5 - \phi_2)] \end{Bmatrix} \quad (4.94)$$

$$P_{c35}^{w} = \frac{1}{2} C_{h5} [W_d(f)]^2 \begin{Bmatrix} \left[\frac{A_{x0}}{\omega} \cdot \cos\gamma \cdot |H_5(f) - H_3(f)| \right]^2 \\ + \left[\frac{A_{z0}}{\omega} \cdot \sin\gamma \cdot |V_5(f) - V_3(f)| \right]^2 \\ + \left(\frac{A_{x0} A_{z0}}{\omega^2} \right) \sin(2\gamma) [|H_5(f)||V_5(f)| + |H_3(f)||V_3(f)| \\ - (|H_5(f)||V_3(f)| + |H_3(f)||V_5(f)|) \cos(\phi_5 - \phi_3)] \end{Bmatrix} \quad (4.95)$$

The total weighted absorbed power (P_{total}^{w}) is calculated by taking summation of individual absorbed power of all dampers together as shown in equation 4.96.

$$P_{total}^{w} = P_{J1\_h}^{w} + P_{J1\_v}^{w} + P_{J2\_h}^{w} + P_{J2\_v}^{w} + P_{J3\_h}^{w} + P_{J3\_v}^{w} + P_{J4\_h}^{w} + P_{J4\_v}^{w} + P_{c1\_h}^{w} + P_{c1\_v}^{w} + P_{c2\_h}^{w} + P_{c2\_v}^{w} + P_{c3\_h}^{w} + P_{c3\_v}^{w} + P_{c25}^{w} + P_{c35}^{w} \quad (4.96)$$

Equation 4.96 gives total weighted absorbed power of human model considering constant amplitude of acceleration input for Case 1.

In a similar fashion, expressions for the unweighted and weighted absorbed power are obtained for Case 2 and Case 3 under constant amplitude of acceleration input excitation.

4.8 Plots of absorbed power under constant amplitude of acceleration excitation

After the formulations for unweighted and weighted absorbed power with constant amplitude of acceleration excitations are derived, one can plot these absorbed power as a function of frequency for three cases.

Assume that the system is excited by excitations with acceleration having amplitude values equal to 1 m/s^2 in both horizontal and vertical direction.

Figure 4.6 illustrates the unweighted absorbed power as a function of frequency and Figure 4.7 illustrates the weighted absorbed power verses frequency by considering constant amplitude of acceleration amplitude.

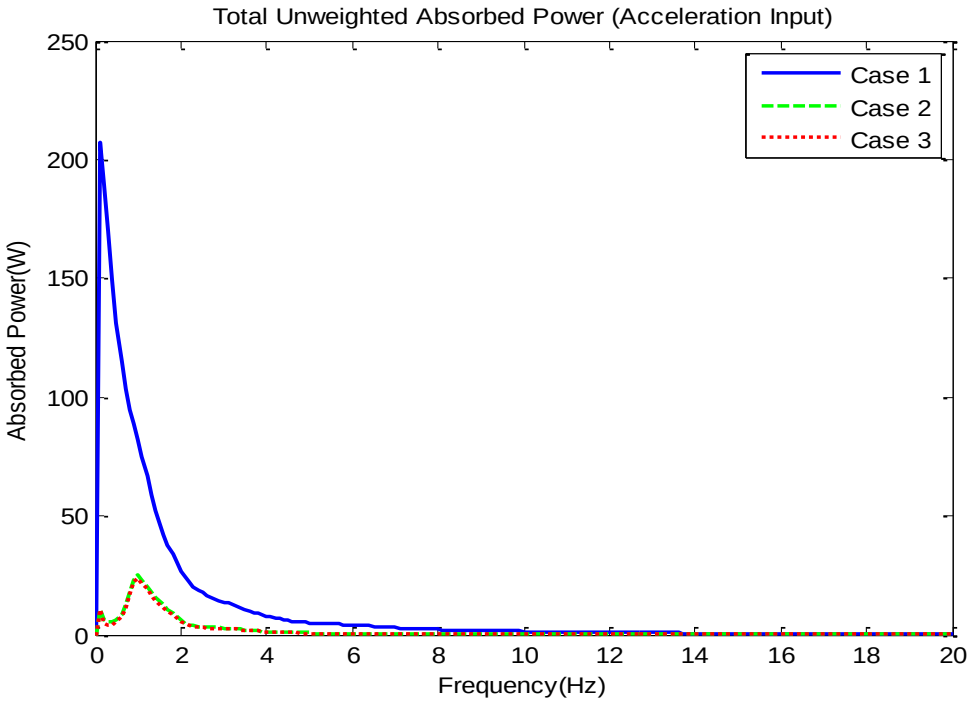

Figure 4.6 Frequency verses unweighted absorbed power (Acceleration Input)

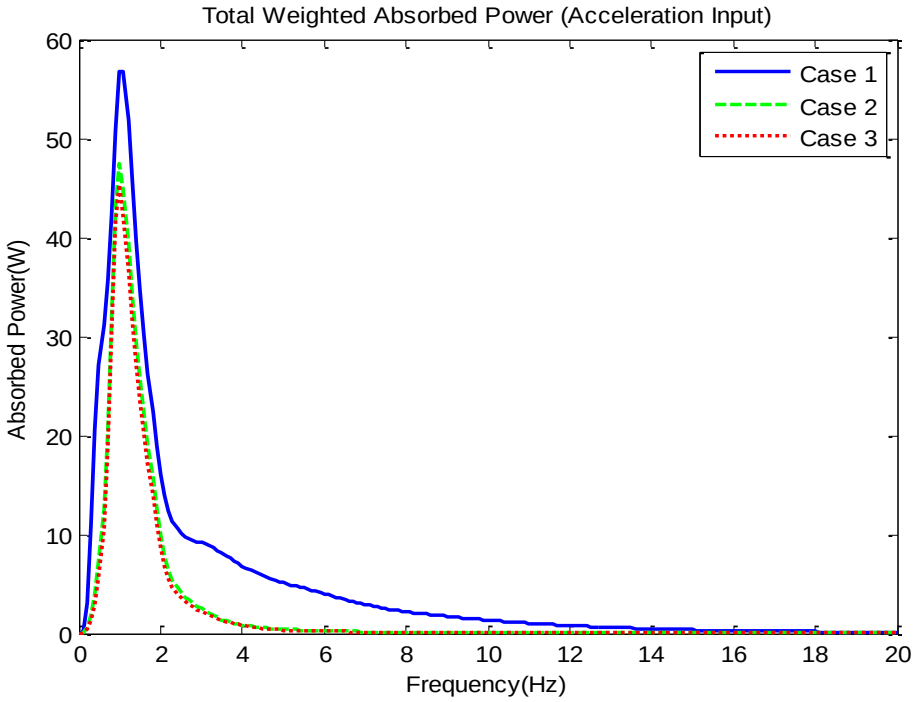

Figure 4.7 Frequency verses unweighted absorbed power (Acceleration Input)

Figures 4.6 and 4.7 gives clear idea about absorbed power in the given frequency range. For both unweighted and weighted absorbed power plots, absorbed power magnitude is higher for Case 1 in comparison with other two cases. As in Case 2 the seat and backrest cushion minimizes vibrations to human body, absorbed power values are substantially reduced. For Case 3, minimum amount of vibrations is transferred to human body as it is isolated using seat suspension and cushion. So for isolated seat, the human body will feel very less fatigue.

Similar to previous section, from these plots one can obtain absorbed power for each frequency. By taking summation of absorbed power of each frequency, the total absorbed power of human body is calculated in the given frequency range. This is expressed in the following equations 4.97 and 4.98.

$$P_{total}^{un} = \sum_{i=1}^{20} P_{total}^{un}(f_i) \tag{4.97}$$

$$P_{total}^{w} = \sum_{i=1}^{20} P_{total}^{w}(f_i) \tag{4.98}$$

As the values of total unweighted and weighted absorbed power are scalar quantities, one can use it to represent fatigue of human body. Summation is taken for all three cases separately and for comparing bar plots are used. Figure 4.8 shows bar plots comparing the total unweighted absorbed power for three cases. Figure 4.9 also shows bar plots for comparing the total weighted absorbed power for three cases.

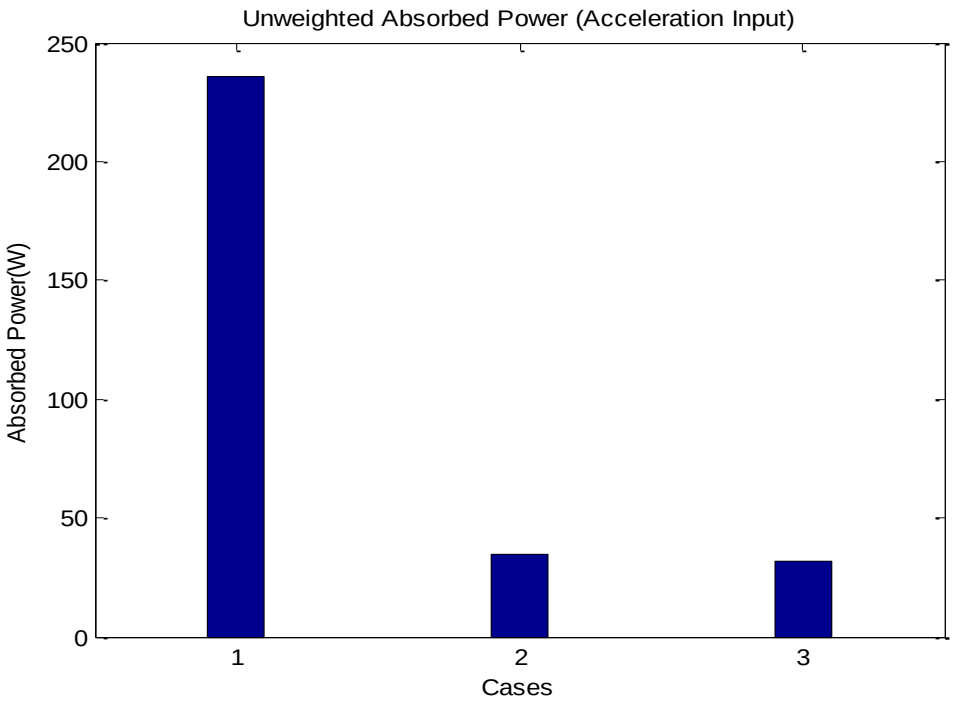

Figure 4.8 Total unweighted absorbed power for 3 cases (Acceleration Input)

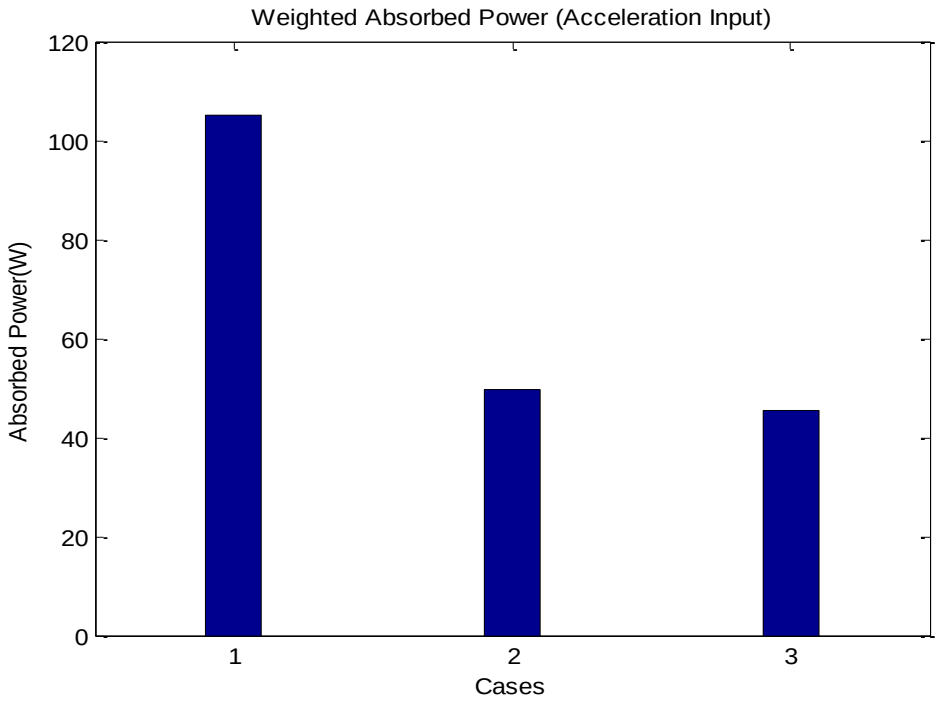

Figure 4.9 Total weighted absorbed power for 3 cases (Acceleration Input)

Figure 4.8 shows the total unweighted absorbed power and Figure 4.9 shows the total weighted absorbed power for Case 1, 2 and 3. These bar plots compares respective unweighted and weighted absorbed power for these three cases. There numerical values are summarized in Table 4.2.

Table 4.2 Total unweighted and weighted absorbed power for 3 cases (Acceleration)

	Acceleration Input	
	Unweighted AP (W)	Weighted AP (W)
Case 1	235.45	104.96
Case 2	34.41	49.51
Case 3	31.58	45.3

From these values it is very clear that absorbed power for Case 2 is substantially reduced in comparison with Case 1. Also absorbed power in Case 3 is also reduced in comparison with Case 1 and 2. This clearly concludes that human body will get very less fatigue in Case 3 in comparison with Case 1 and 2.

4.9 Summary

In this chapter, the unweighted and weighted absorbed power is calculated for the human body model for all three cases. The time dependency of fatigue or discomfort can be predicted from the absorbed power. Initially expressions are derived for unweighted absorbed power. This derived equation shows that absorbed power of each damper is not only proportional to its damping coefficient but also it depends on the square of relative transmissibility function between two connecting bodies. The transmissibility function depends on relative motion and phase of each body. This proves that these factors have significant impact on absorbed power of human body. As human body response is frequency sensitive, the weighted absorbed power is calculated by considering frequency weighting factors. These factors are obtained from ISO 2631-1. The absorbed power is calculated only for translational dampers.

Two types of input excitations are used in this chapter. First sinusoidal displacement input excitations are given in horizontal and vertical direction. Both unweighted and

weighted absorbed powers are calculated for three cases. Constant displacement amplitude input is not practical at higher frequencies. So constant amplitude of acceleration input is given and both unweighted and weighted absorbed powers are calculated for three cases. Results are compared for three types of seat models and found that seat with both seat suspension and cushion and backrest cushion works best in isolating human body from vibrations. For this seat, the absorbed power value is very less as compared with other two seats. So we can predict that for isolated seat, the human body will experience very less fatigue.

Result also shows that human body response is very sensitive to seat and cushion parameters. A small change in these parameters will result in substantial change in human body response. So for better vibration isolation, these seat and cushion parameters needs to be optimized.

CHAPTER 5

SEAT DYNAMIC PARAMETERS DETERMINATION

5.1 Introduction

The mechanical parameters of the seat include its mass, stiffness and damping coefficients. The mass of the seat suspension and cushion has significant contribution in the vibration isolation. Increasing its mass will reduce the absorbed power. But according to Amirouche et al. (1997), the effect of increasing mass is less effective comparing with effect by changing stiffness and damping coefficients of seat dynamic parameters. In the today's competitive world, the industries are trying to reduce the weight of vehicle. This puts limitation on increasing mass of seat component. The stiffness and damping values of seat component can be changed for reducing vibration transmission to human body (Kolich, 2003). Therefore in this research, the stiffness and damping coefficients of seat component are selected as design variables and their masses are kept constant.

In this chapter, an optimization problem is formulated to minimize the weighted absorbed power to determine optimal seat dynamic parameters. The optimization problem is solved in MATLAB using genetic algorithm. Based on these optimal values, human body fatigue is predicted for seat model in Case 2 and Case 3.The seat model in Case 2 have only seat and backrest cushion. Hence there are 8 cushion parameters. In Case 3, the seat model has both seat suspension and cushion. Hence there are total 12 parameters.

5.2 Optimization problem formulation

The optimization problem can be defined as follows:

$$Find: \xi$$

$$Minimize: P_{total}^{w} = \sum_{i=1}^{20} P_{total}^{w}(f_i)$$

$$Subject\ to: \xi_k^l \le \xi_k \le \xi_k^u \qquad (k = 1, \cdots, m)$$

Where, ξ is the vector having seat and cushion parameters

P_{total}^{w} is the total weighted absorbed power

ξ_k^l *and* ξ_k^u denotes the lower and upper bounds of design variables and m is the total number of design variables.

One of the important parts of this optimization problem is selection of algorithm in Matlab. For this work, genetic algorithm (*GA*) is used because it can find the global optimal solution. Genetic algorithm gives very good results for an objective function which is depending on large number of variables.

The genetic algorithm follows the principle of biological evaluation. It uses gene combination rule in biological reproduction and modifies population of individual points. This algorithm starts with creating initial population by default or based on user provided population size. For this optimization 100 is given as population size. Based on this population and number of variables, current population is calculated called as *parents*. These value are used to find minimum value of objective function and based on result, the next generation is created called as *children*. These new values are used for next iteration. The new values are found out for next subsequent iteration targeting on minimizing objective function. The algorithm runs until given function tolerance is met.

In the previous chapter, the weighted absorbed power is calculated for two types of input excitations. First one is sinusoidal displacement excitation with constant displacement amplitude of 0.005 m in X and Z-directions and second is constant acceleration amplitude excitation with amplitude 1 m/s^2 both in X and Z-directions. Therefore for each excitation, we can calculate optimized parameters for seat model in Case 2 and 3. This will result in four optimization problems as shown:

1. Case 2 seat model with sinusoidal displacement excitation
2. Case 2 seat model with constant magnitude of acceleration excitation
3. Case 3 seat model with sinusoidal displacement excitation
4. Case 3 seat model with constant magnitude of acceleration excitation

5.2.1 Case 2 seat model

The optimization problem for Case 2 is defined as:

$$Find: \xi = [K_{ch1}, C_{ch1}, \mathrm{K}_{cv1}, C_{cv1}, \mathrm{K}_{ch2}, C_{ch2}, \mathrm{K}_{cv2}, C_{cv2}]^T$$

$$Minimize: P_{total}^{w} = \sum_{i=1}^{20} P_{total}^{w}(f_i)$$

$$Subject\ to: \xi_k^l \le \xi_k \le \xi_k^u \qquad (k = 1, \cdots, 8)$$

Table 5.1 gives the values of lower and upper bounds and optimal values for Case 2 with two types of input excitations: sinusoidal displacement excitation and constant amplitude acceleration input excitation.

Table 5.1 Optimal values of seat dynamic parameters for Case 2

Value (Units: *k*: N/m *C*: N-s/m)	ξ_k^l	ξ_k^u	**Optimal value for displacement Input**	**Optimal value for acceleration Input**
k_{ch1}	1000	50000	5867.675	3007.537
C_{ch1}	100	2500	2371.013	2309.527
k_{cv1}	1000	30000	2609.49	1924.379
C_{cv1}	100	5000	4931.741	1594.685
k_{ch2}	1000	25000	1187.633	5847.221
C_{ch2}	100	3000	2368.324	2681.862
k_{cv2}	1000	50000	1579.234	1121.473
C_{cv2}	100	3000	2894.247	2744.155

Figure 5.1 shows the weighted absorbed power for seat model calculated using original and optimal seat dynamic parameters for Case 2.

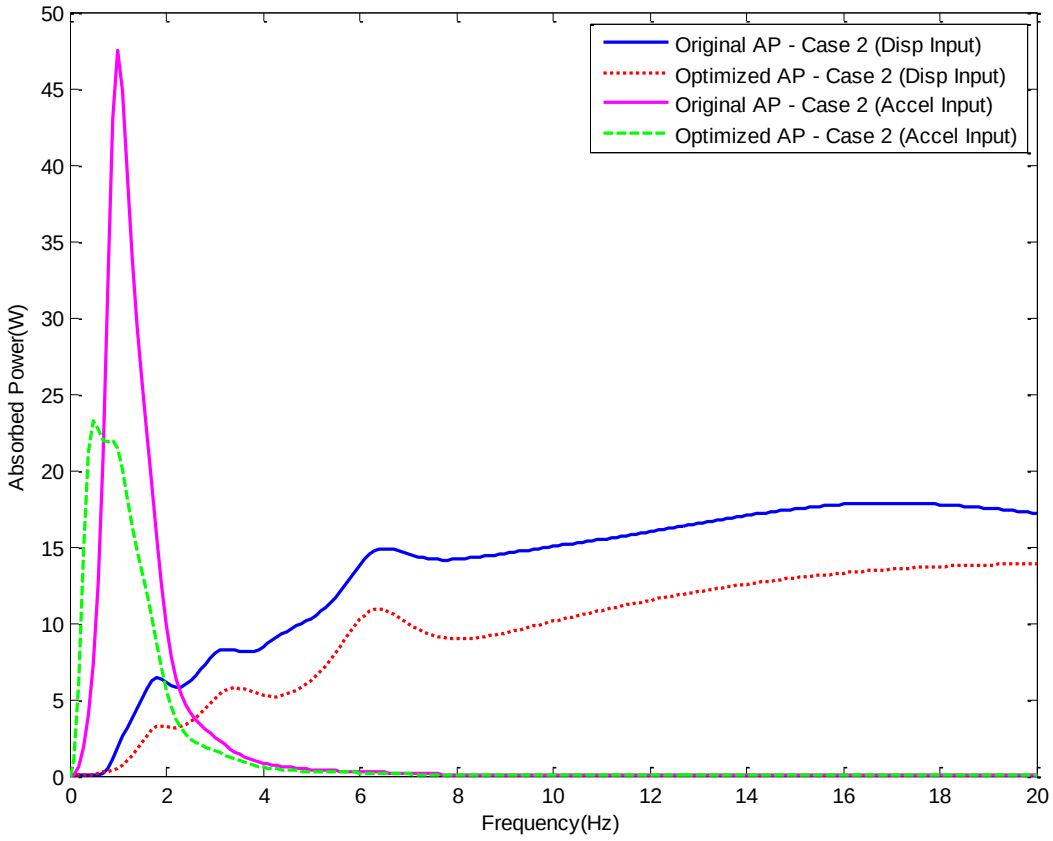

Figure 5.1 Original and optimized weighted absorbed power for Case 2

Figure 5.1 shows original and optimized weighted absorbed power for human body with seat model in Case 2. Figure shows comparison plots for two types of input as explained in the previous section. For sinusoidal input excitations, the comparison plots shows that magnitude of absorbed power is reduced for all frequencies. Also the frequency at which peak value occurs is got reduced. Same phenomenon is observed for the plots of absorbed power with constant magnitude acceleration input. In these plots also values of absorbed power are significantly decreased and peak frequency is reduced. This all shows that with optimal seat dynamic parameters, the human body fatigue is reduced. The total absorbed power is calculated for original and optimal seat dynamic parameters and is compared in Table 5.3 and Figure 5.3 and 5.4.

5.2.2 Case 3 seat model

For Case 3, the optimization problem is defined as:

$$Find: \xi = [K_{sh1}, C_{sh1}, \mathrm{K}_{sv1}, C_{sv1}, \mathrm{K}_{ch1}, C_{ch1}, \mathrm{K}_{cv1}, C_{cv1}, \mathrm{K}_{ch2}, C_{ch2}, \mathrm{K}_{cv2}, C_{cv2}]^T$$

$$Minimize: P_{total}^{w} = \sum_{i=1}^{20} P_{total}^{w}(f_i)$$

$$Subject\ to: \xi_k^l \le \xi_k \le \xi_k^u \qquad (k = 1, \cdots, 12)$$

Table 5.2 summarizes the values of lower and upper bounds and optimal values for Case 3 with sinusoidal displacement excitation and constant magnitude acceleration input excitation.

Table 5.2 Optimal values of seat dynamic parameters for Case 3

Value (Units: *k*: N/m *C*: N-s/m)	ξ_k^l	ξ_k^u	**Optimal value for displacement Input**	**Optimal value for acceleration Input**
k_{sh1}	2000	100000	2918.76	3304.444
C_{sh1}	100	10000	9607.18	9909.829
k_{sv1}	100	10000	251.068	8442.496
C_{sv1}	100	5000	4884.08	988.245
k_{ch1}	1000	50000	3089.86	8699.976
C_{ch1}	100	2500	2380.12	679.79
k_{cv1}	1000	30000	27612.2	5280.55
C_{cv1}	100	5000	4875.32	3104.676
k_{ch2}	1000	25000	13678.8	2029.023
C_{ch2}	100	3000	2213.58	296.224
k_{cv2}	1000	50000	1286.72	27627.197
C_{cv2}	100	3000	857.226	2931.248

Figure 5.2 shows comparison plots of the weighted absorbed power with original and optimal seat stiffness and damping coefficients for seat model in Case 3.

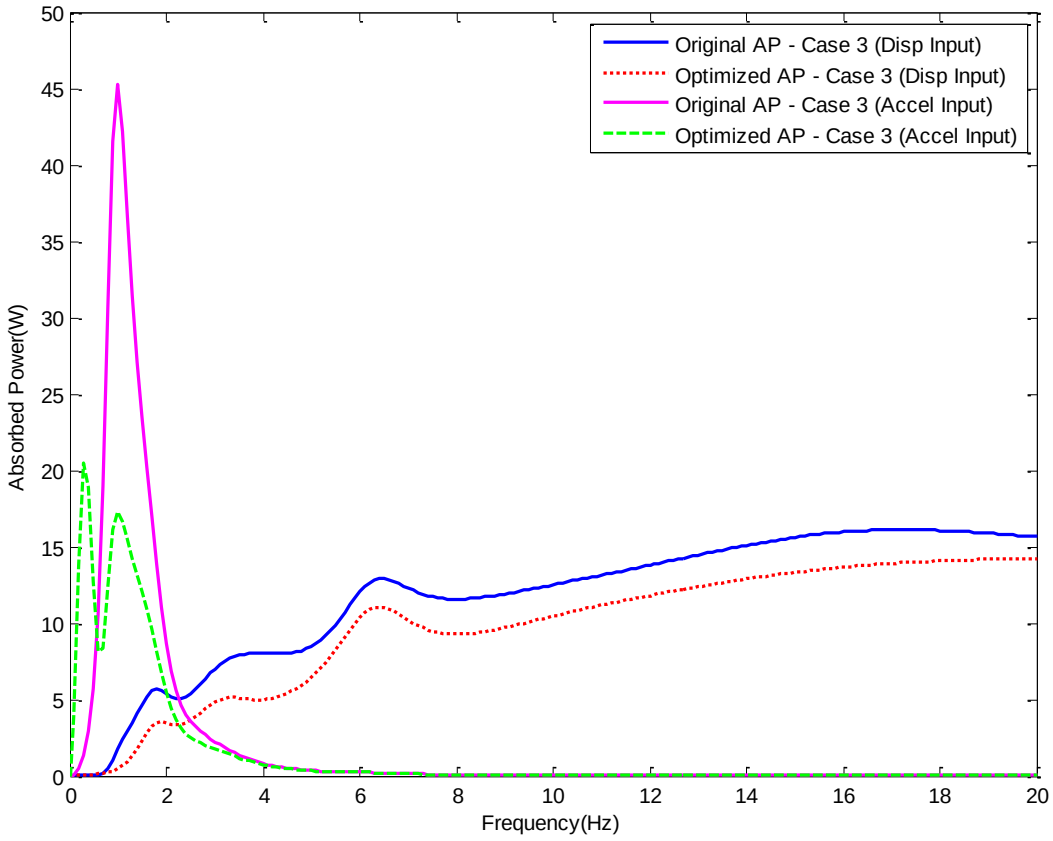

Figure 5.2 Original and optimized weighted absorbed power for Case 3

For Case 3, the original and optimized absorbed power is shown in Figure 5.2. This figure compares the weighted absorbed for original and optimized seat dynamic parameters. In first two plots, the absorbed power is calculated under sinusoidal displacement input. Constant magnitude acceleration input is considered for calculating absorbed power in last two plots. For both these inputs, original absorbed power values are high and it got reduced for optimal seat dynamic parameters. Also frequency at peak values of absorbed power is also diminished. This all proves that human body will get very less fatigue for a seat with optimal seat dynamic parameters. For original and optimal seat dynamic parameters, the total absorbed power is calculated and is compared in Table 5.3. Figure 5.3 and 5.4 shows bar plots comparing the total absorbed power for two types of input excitations.

5.3 Discussion

In the previous section, optimal seat dynamic parameters are determined for Case 2 and 3. Based on these optimal parameters, the weighted absorbed powers are calculated and compared with the weighted absorbed power with original parameters. From Figure 5.1 and 5.2, it has been seen that absorbed power values are reduced. From these values, the total absorbed power is calculated using equation 4.61 and 4.98. This total weighted absorbed power is an indication of human body fatigue over a period of time (Pradko, 1965; 1966). Table 5.3 puts together these total absorbed power values for both sinusoidal displacement input and constant magnitude acceleration input excitations calculated with original and optimized seat dynamic parameters.

Table 5.3 Original and optimal total weighted absorbed power for Case 2 and 3

	Total Weighted Absorbed Power (W)			
	Displacement Input		Acceleration Input	
	Original	**Optimal**	**Original**	**Optimal**
Case 2	268.59	190.091	49.51	34.92
Case 3	234.72	84.49	45.3	16.12

For visual comparison purpose, these total absorbed power values are plotted using bar plots. Figure 5.3 shows original and optimal total weighted absorbed power for Case 2 and 3 with sinusoidal displacement input and Figure 5.4 shows their values with constant acceleration input excitations.

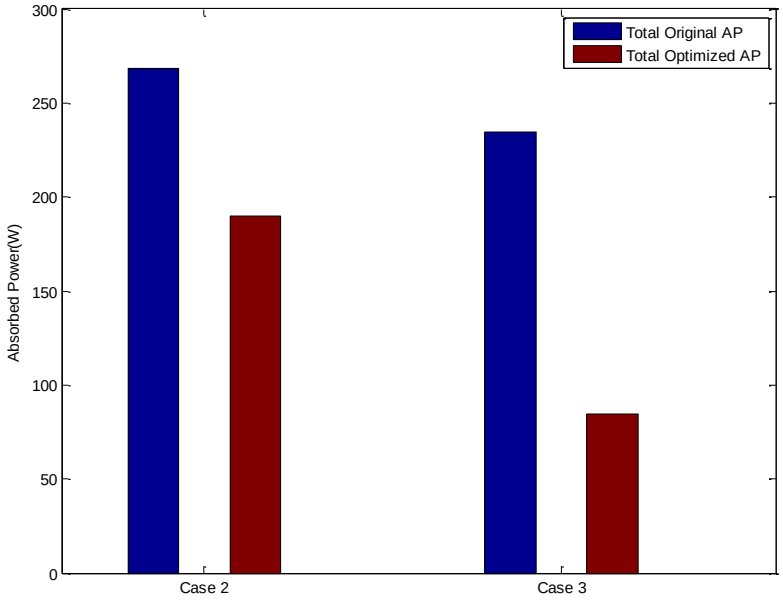

Figure 5.3 Total absorbed powers with original and optimal seat dynamic parameters for sinusoidal displacement input

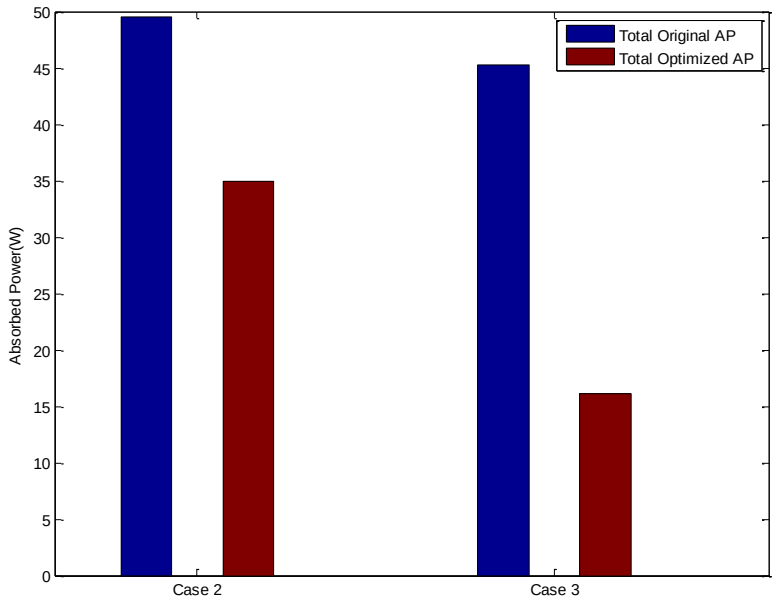

Figure 5.4 Total absorbed powers with original and optimal seat dynamic parameters for constant magnitude acceleration input

From Figure 5.3 and 5.4, it is clear that total weighted absorbed power with optimal seat dynamic parameters is reduced in comparison with its values fir original seat parameters for both types of input excitations in Case 2 and Case 3. This clearly indicates that during driving, the human body will feel less fatigue with optimal seat dynamic parameters.

5.4 Summary

In this chapter, the seat and cushion dynamic parameters are optimized for reducing human body fatigue. The genetic algorithm is used in MATLAB for optimization and optimal seat dynamic parameters are determined for Case 2 and 3. The weighted absorbed power with optimal seat parameters is compared with its value with original seat parameters. The result shows that the absorbed power value is substantially reduced for a seat with optimal seat dynamic parameters. This indicates that during driving, the human body with feel less fatigue on seat with optimal seat dynamic parameters.

CHAPTER 6

CONCLUSION AND FUTURE WORK

6.1 Conclusion

This thesis attempts to develop a simulation method to predict human body response under whole body vibration. A comprehensive literature review was conducted to have the state of the art of biodynamic models and an advance biodynamic model was chosen for this study. The selected model is a 14-DOF multibody biodynamic model in 2D sagittal plane. This human model was coupled with three types of seat models which will help in highlighting the selection of seat dynamic parameters. The first seat called hard seat which had neither cushion nor seat suspension. The second type of seat had seat and backrest cushion but did not have seat suspension. The isolated seat had seat suspension, seat and backrest cushion. For these coupled human seat models, the equations of motion were derived.

The transfer functions were calculated for sinusoidal excitations and transmissibility plots were obtained in horizontal and vertical directions. Based on these plots, performance of three seat model was compared. For predicting human body fatigue, the expressions for the absorbed power were derived for all three seat models. Based on transmissibility and absorbed power results, the isolated seat had the best performance compared to the hard seat or the seat without seat suspension.

To design a vehicle seat, one has to determine the optimal seat dynamic parameters. An optimization problem was formed and the cost function was the weighted absorbed power. GA was used to solve the optimization problem. The result shows that the seat with optimal seat parameters had better performance.

6.2 Future work

1. This simulation work considered input excitations in the form of sinusoidal displacements or constant magnitude acceleration. But in reality, the human body is exposed to complex random vibrations generating from road contours. It will be very interesting to consider real road random excitations in the future work.
2. The biodynamic human model selected in this research considered the feet were fixed on the vehicle floor. However, in real world drivers have shoes and shoes will not be fixed with the vehicle floor. In the future work, the shoes will be modeled as an elastic component and connected with the vehicle floor.
3. In this research, the absorbed power is calculated by considering only translational dampers. The results will be more accurate if absorbed power due to rotational dampers is included.
4. The biodynamic model can be made more accurate by increasing its degrees of freedom.
5. The simulation results need to be validated to crosscheck accuracy of proposed simulation method. For this experimental method on human subject can be used or Multi-body dynamic software like MSC ADAMS can be used.
6. Biodynamic model used in this research can be used to analyze human body response in horizontal and vertical direction as this model is 2-D in sagittal plane. For analyzing human body motion in other directions like fore-aft directions or role and pitch motion, this model needs to extend to 3-D.

BIBLIOGRAPHY

Allen, G., 1978, "A critical look at biomechanical modeling in relation to specifications for human tolerance of vibration and shock". *AGARD Conference Proceedings No. 253*, Paper A25-5, Paris, France, pp. 6-10.

Amirouche, F.M.L, Ider, S.K., 1988, "Simulation and analysis of a Biodynamic human model subjected to low accelerations- A correlation study". *Journal of Sound and Vibration,* 123(2), pp. 281-292.

Amirouche, F.M.L., Xu, P. and Alexa, E., 1997, "Evaluation of Dynamic Seat Comfort and Driver's Fatigue". *SAE Technical Paper* 2007-971573.

Boileau, P.E., Rakheja, S., 1998, "Whole body vertical biodynamic response characteristics of the seated vehicle driver – Measurement and model development". *International Journal of Industrial Ergonomics,* 22(1998), pp. 449-472.

Brook, S., Freman, R., Rosala, G., Dixon, N., 2009, "Ergonomic Data measuring system for driver-pedals interaction". *SAE Technical Paper* 2009-01-1164.

BS 6841, 1987, "Guide to measurement and evaluation of human exposure to whole-body mechanical vibration and repeated shock".

Coermann, R.R., 1962, "The mechanical impedance of the human body in sitting and standing positions at low frequencies". *Human Factors,* 4, pp. 227-253.

Cho, Y., Yoon, Y., 2001, "Biomechanical model of human on seat with backrest for evaluating ride quality". *International Journal of Industrial Ergonomics,* 27, pp. 331-345.

Deb, A., Joshi, D., 2012, "A Study on Ride Comfort Assessment of Multiple Occupants using Lumped Parameter Analysis". *SAE Technical Paper* 2012-01-0053.

Deusen, B.D., 1962, "Computing the ride". *Detroit Engineer,* Vol. XXVI, No. 7, March, 1962, pp.5-8.

Deusen, B.D., 1967, "Analytical Techniques for Designing Ride Quality into Automobile Vehicles". *SAE Technical Paper 670021.*

Deusen, B.D., 1967, "A statistical techniques for the Dynamic Analysis of vehicles traversing rough yielding and non-yielding surfaces". *NASA*-CR-659.

Dupuis, H., Zerlett G., 1986, "The Effects of Whole-Body Vibration". *Springer-Verlag, New York.*

El-Gindy, M., Jiang, Z., Streit, D.A., 2001, "Heavy vehicle ride comfort: literature survey". *Heavy Vehicle Systems, International Journal of Vehicle Design*, Vol. 8, No ¾, 2001.

Fairley, T.E., Griffin, M.J., 1989, "The apparent mass of the seated human body: vertical vibration". *Journal of Biomechanics,* 22(2), pp. 81-94.

Gouw, G., Rakheja, S., Sankar, S., Afework, Y., 1990, "Increased Comfort and Safety of Drivers of Off-Highway Vehicles Using Optimal Seat Suspension". *SAE Technical Paper* 901646.

Griffin, M.J., 1978, "The evaluation of vehicle vibration and seats", *Journal of Applied Ergonomics,* (1978), 9.1, pp. 15-21.

Griffin M.J., 1990, "Handbook of Human Vibration". *Academic Press Limited, 24/28 Oval Road, London, NW17 DX.*

Griffin, M., 1986, "Evaluation of vibration with respect to Human Response". *SAE Technical Paper 860047.*

Griffin, M., 1990, "Human Response to Vibration". *Journal of Sound and Vibration,* 141(3), pp. 535-538.

Griffin, M.J., 2001, "Whole Body Vibration", *Academic Press,* 10.1006/rwvb.2001.0082 pp. 1570-1578.

Guman, R., Vertiz, A.M., 1997, "The Role of Automotive Seat Cushion Deflection in Improving Ride Comfort", *SAE Technical Paper* 970596.

Hamilton, A., 1918, "Reports of physicians for the bureau of labor statistics- a study of spastic anemia in the hands of stone cutters". *Industrial Accidents and Hygiene National Technical Information Service, Bulletin* 236, pp. 53-66.

Ippili, R.K., Davies, P., Bajaj, A.K., Hagenmeyer, L., 2008, "Nonlinear multi-body dynamic modeling of seat-occupant system with polyurethane sear and H-point prediction". *International Journal of Industrial Ergonomics,* 38(2008), pp. 368-383.

ISO 5982, 2001, "Mechanical vibration and shock - Range of idealized values to characterize seated-body biodynamic response under vertical vibration".

ISO 2631-1, 1997, "Mechanical vibration and shock -Evaluation of human exposure to whole-body vibration - Part 1: General requirements".

ISO 2631-4, 2001, "Mechanical vibration and shock- Evaluation of human exposure to whole-body vibration - Part 4: Guidelines for the evaluation of the effects of vibration and rotational motion on passenger and crew comfort in fixed-guideway transport systems".

ISO 2631-5, 2004, "Mechanical vibration and shock - Evaluation of human exposure to whole-body vibration - Part 5: Method for evaluation of vibration containing multiple shocks".

Janeway R.N., 1975a, "Analysis of proposed criteria for human response to vibration". *Ride Quality Symposium, National Aeronautics and Space Administration, Williamsburg, Virginia.*

Janeway R.N., 1975b, "Human vibration tolerance criteria and application to ride evaluation". *SAE Technical paper* 750166.

Kim, T. H., Kim, Y. T., Yoon, Y.S., 2005, "Development of a biomechanical model of the human body in a sitting posture with vibration transmissibility in the vertical direction". *International Journal of Industrial Ergonomics,* 35(2005), pp. 817-829.

Kolich, M., 2003, "Automobile seat comfort: occupant preferences vs. anthropometric accommodation", *Journal of Applied Ergonomics*, 2003, pp. 177-184.

Kordestani, A., Rakheja, S., Marcotte, P., Pazooki, A., et al., 2010, "Analysis of Ride Vibration Environment of Soil Compactors". *SAE International Journal of Commercial Vehicle,* 3(1), pp. 259-272.

Kumbhar, P.B., Xu, P. and Yang, J., 2012, "A Literature Survey of Biodynamic models for whole body vibration and vehicle ride comfort", *Proceedings of the ASME 2012, International Design Engineering Technical Conference & Computers and Information in Engineering Conference*, IDETC/CIE 2012, August 12-15, 2012, Chicago, Illinois, USA.

Kumbhar, P.B., Xu, P. and Yang, J., 2013, "Evaluation of Human Body Response for Different Vehicle Seats Using a Multibody Biodynamic Model", *SAE International conference, Detroit, Michigan, USA*, 2013-01-0994.

Lee, R.A., Pradko, F., 1968, "Analytical Analysis of Human Vibration". *SAE Technical Paper* 680091.

Leenslag, J.W., Huygens E., Tan, A., 1997, "Recent Advances in the Development and Characterization of Automotive Comfort Seating Foams", *ICI Polyurethanes: Polyurethanes World Congress 97, Amsterdam, Netherland,* (1997), Vol.16, pp. 411-430.

Lewis, C.H., Griffin, M.J., 2002, "Evaluating the vibration isolation of soft seat cushions using an active anthropodynamic dummy". *Journal of Sound and Vibration,* 253(1), pp. 295-311.

Liang, C.C., Chiang, C.F., 2006, "Modeling of a Seated Human Body Exposed to Vertical Vibrations in Various Automotive Postures". *Industrial Health*, 2008, 46, pp. 125-137.

Liang, C.C., Chiang C.F., 2008, "A study on biodynamic models of seated human subjects exposed to vertical vibration". *International Journal of Industrial Ergonomics,* 36(2006), pp. 869-890.

Linder, A., 2000, "A new mathematical neck model for a low-velocity rear-end impact dummy: evaluation of components influencing head kinematics". *Accident Analysis and Prevention,* 32, pp. 261-269.

Lidstrom L.M., 1977, "Vibration injury in rock drillers, chiselers and grinders- Some views on the relationship between the quality of energy absorbed and the risk of occurrence of vibration injury". *In proceedings of the International Occupational Hand-Arm Vibration Conference, National Institute for Occupational Safety and Health, Cincinnati, OH, USA.* Publication No. 77-170, pp. 78-83.

Low, T.C., Prasad, P., 1990, "Dynamic Response and mathematical model of the side impact dummy". *Presented at the 34th Stapp Car Crash Conference, SAE Technical Paper* 902321.

Liu, X.X., Shri, J., Li, G.H., 1998, "Biodynamic response and injury estimation of ship shock motion induced by underwater explosion". *Proceeding of 69th Shock and Vibration Symposium,* Vol. 18, St. Paul, pp. 1-18.

Lundstrom R., Holmlund P., Lindberg L., 1998, "Absorption of energy during vertical whole body vibration exposure". *Journal of Biomechanics*, 31(1998), pp. 317-326.

Ma, F., Men, Y., Du, Z., 2008, "Parametric uncertainty analysis of vehicle suspension". *International Journal of Vehicle Design,* Vol. 47, Nos. 1/2/3/4, pp. 102-107.

Ma, X.Q., Rakheja, S., Su, C.Y., 2008, "Damping requirement of a suspension seat subject to low frequency vehicle vibration and shock", *International Journal of Vehicle Design,* Vol. 47, Nos. 1/2/3/4, pp. 133-156.

Magid, E.B., Coerman, R., 1960, "The reaction of the human body to extreme vibrations". *Proceedings to the Institute of Environmental Science,* pp. 135.

Mayton, A.G., DuCarme, J.P., Jobes, C.C., Matty, T.J., 2006, "Laboratory Investigation of Seat Suspension Performance during Vibration Testing". *ASME International Mechanical Engineering Congress and Exposition, Chicago, USA.*

Montazeri, G.H., Jazayeri, M., Soleymani, M., 2008, "Vehicle ride evaluation based on a time-domain variable speed driving pattern". *International Journal of Vehicle Design,* Vol. 47, Nos. 1/2/3/4, pp. 81-101.

Muksian, R., Nash, C.D., 1974, "A model for the response of seated human to sinusoidal displacement of seat". *Journal of Biomechanics,* 7, pp. 209-215.

Muksian, R., Nash, C.D., 1976, "On frequency dependent damping coefficients in lumped parameter models of human beings". *Journal of Biomechanics,* 9, pp. 339-342.

Nigam, S.P., Malik, M., 1987, "A study on a vibratory model of a human body". *Journal of Biomechanical Engineering,* 109(2), pp. 148-153.

Pang, J., Qatu, M., Dukkipati, R., Sheng, G., Patten, W.N., 2004, "Model identification for nonlinear automotive seat cushion structure". *International Journal of Noise and Vibration,* Vol. 1, Nos.1/2, pp. 142-157.

Pang, J., Qatu, M., 2005, "Nonlinear seat cushion and human body model". *International Journal of Noise and Vibration,* Vol. 1, Nos. ¾, pp. 194-206.

Patil, M., Palanichamy, M.S., Ghista, D.N., 1977, "Dynamic response of human body seated on a tractor and effectiveness of suspension systems". *SAE Technical Paper 770932,* pp. 755-792.

Patil, M., Palanichamy, M.S., 1988, "A mathematical model of tractor-occupant system with a new seat suspension for minimization of vibration response". *Applied Mathematical Modeling,* Vol. 12, pp. 63-71.

Pennestri, E., Valentini, P.P., Vita, L., 2005, "Comfort analysis of car occupants: comparison between multibody and finite element models". *International Journal of Vehicle Systems Modeling and Testing,* Vol. 1, Nos. 1/2/3.

Pradko F., Lee R.A., Greene J.D., 1965a, "Human vibration response theory". *International Winter Annual Meeting of the Human Factors Division, Chicago.*

Pradko F., Orr T.R., Lee R.A., 1965b, "Human vibration analysis". *SAE Technical Paper* 650426.

Pradko, F., Lee, R.A., 1966, "Vibration Comfort criteria". *SAE Technical Paper* 660139.

Qassem, W., Othman, M., Abdul-Majeed, S., 1994, "The effects of vertical and horizontal vibrations on the human body". *Medical Engineering Physics,* 16, pp. 151-161.

Qassem, W., Othman, M., 1996, "Vibration effect on sitting pregnant women-subjects of various masses". *Journal of Biomechanics,* 29(4), 493-501.

Shurpali, M., Mullinix, L., 2011, "An Approach for Validation of Suspension Seat for Ride Comfort using Multi-Body Dynamics". *SAE Technical Paper* 2011-01-0434.

Soliman, A., 2011, "Adaptive LQR Control Strategy for Suspension System". *SAE Technical Paper* 10-4271/2011-01-0430.

Suggs, C.W., Abrams, C.F., Stikeleather, L.F., 1969, "Application of a damped spring-mass human vibration simulator in vibration testing of vehicle seats", *Applied Ergonomics,* 12, pp. 79-90.

Tang, C., Chan, W., Tsui, C., 2010, "Finite Element Analysis of contact pressures between seat cushion and human buttock-thigh tissue". *Scientific Research Journal,* 2, 720-726.

Wan, Y., Schimmels, J., 1995, "A simple model that captures the essential dynamics of a seated human exposed to whole body vibration". *Advances in Bioengineering, ASME, BED*, 31, pp. 333-334.

Wang, W., Rakheja S. and Boileau P.E., 2004, "Effects of sitting postures on biodynamic response of seated occupants under vertical vibration", *International Journal of Industrial Ergonomics,* 34, 289–306.

Wagner, J., Liu, X., 2000, "An active vibration isolation system for vehicle seats". *SAE Technical Paper* 2000-01-0275, pp. 7-18.

Wei, L., Griffin, J., 1998, "Mathematical models for the Apparent Mass of the seated Human body exposed to vertical vibration". *Journal of Sound and Vibration*, 212(5), pp. 855-874.

Wei, L., Griffin, J., 1998, "The prediction of seat transmissibility from measures of seat impedance". *Journal of Sound and Vibration*, 214(1), pp. 121-137.

Wong, J.Y., 2008, "Theory of Ground Vehicle". 4th edition, *John Wiley & Sons*.

Xu, P., Wong, D., LeBlanc, P., Peticca, G., 2005, "Road Test Simulation Technology in Light Vehicle Development and Durability Evaluation". *SAE Technical Paper* 2005-01-0854.

Xu, P., LeBlanc, P., Peticca, G., Wong, D., 2006, "Steering Measurement, Analysis and Simulation on 6DOF Road Test Simulator". *SAE Technical Paper* 2006-01-0733.

Xu, P., Peticca, G., Wong, D., 2008, "A technique for developing a high accuracy durability test for a Light Truck on a Six Degree-of-Freedom Road Test Simulator". *International Journal of Vehicle Design*, Vol. 47, Nos. 1/2/3/4, pp. 290–304.

Xu, P., Bernardo, B., Tan, K., 2011, "Optimal mounting design for cab vibration isolation". *International Journal of Vehicle Design*, Vol. 57, Nos. 2/3, pp. 292–304.

Zhang, X., Yu, J., 2010, "A Computer Simulation Study of Seating Comfort of Air-Inflated Seat Cushion", *2nd International Conference on Future Computer and Communication.*

Zong, Z., Lam, K.Y., 2002, "Biodynamic response of shipboard sitting subject to ship shock motion". *Journal of Biomechnics,* 35, pp. 35-43.